

การเหนี่ยวนำโปรตีนพี 21^{วฟ1/ชิป1} ในวิถีอีอาร์บีบี 1 ริเซฟเตอร์ทรานส์แอกติเวชัน
ในเซลล์เพาะเลี้ยงจากเยื่อหลอดเลือดดำที่สายสะดือโดยไซโตเคียมอาซีไนท์



นาง นพรัตน์ นันทรัตนพงศ์

สถาบันวิทยบริการ จุฬาลงกรณ์มหาวิทยาลัย

วิทยานิพนธ์นี้เป็นส่วนหนึ่งของการศึกษาตามหลักสูตรปริญญาวิทยาศาสตรดุษฎีบัณฑิต

สาขาวิชาเภสัชศาสตร์ชีวภาพ

คณะเภสัชศาสตร์ จุฬาลงกรณ์มหาวิทยาลัย

ปีการศึกษา 2547

ISBN 974-17-6368-9

ลิขสิทธิ์ของจุฬาลงกรณ์มหาวิทยาลัย

**INDUCTION OF p21^{WAF1/CIP1} THROUGH ERBB1 RECEPTOR
TRANSACTIVATION IN HUMAN UMBILICAL VEIN
ENDOTHELIAL CELL BY SODIUM ARSENITE**

Mrs. Nopparat Nuntharatanapong

สถาบันวิทยบริการ
จุฬาลงกรณ์มหาวิทยาลัย

A Dissertation Submitted in Partial Fulfilment of the Requirements
for the Degree of Doctor of Philosophy in Biopharmaceutical Sciences

Faculty of Pharmaceutical Sciences

Chulalongkorn University

Academic Year 2004

ISBN 974-17-6368-9

Thesis Title Induction of p21^{Waf1/Cip1} through ErbB1 receptor
transactivation in human umbilical vein endothelial
cell by sodium arsenite

By Mrs. Nopparat Nuntharatanapong

Field of Study Biopharmaceutical Sciences

Thesis Advisor Associate Professor Palarp Sinhaseni, Ph.D.

Thesis Co-advisor Professor John F. Keaney Jr., M.D.

Accepted by the Faculty of Pharmaceutical Sciences, Chulalongkorn
University in Partial Fulfillment of the Requirements for the Doctor's Degree

.....Dean of the Faculty of
Pharmaceutical Sciences
(Associate professor Boonyong Tuntisira, Ph.D.)

THESIS COMMITTEE

.....Chairman
(Assistant Professor Niyada Kiatying-Angsulee, Ph.D.)

.....Thesis Advisor
(Associate Professor Palarp Sinhaseni, Ph.D.)

.....Thesis Co-advisor
(Professor John F. Keaney Jr., M.D.)

.....Member
(Associate Professor Duangdeun Meksuriyen, Ph.D.)

.....Member
(Kai Chen, M.D, Ph.D.)

นาง นพรัตน์ นันทรัตนพงษ์ : การเหนี่ยวนำโปรตีนพี 21^{Waf1/Cip1} ในวิถีอีอาร์บีบี 1 รีเซพเตอร์ทรานส์ แอกติเวชัน ในเซลล์เพาะเลี้ยงเยื่อบุหลอดเลือดดำที่สายสะดือโดยโซเดียมอาร์ซีไนท์ (Induction of p21^{Waf1/Cip1} through ErbB1 receptor transactivation in human umbilical vein endothelial cell by sodium arsenite) อาจารย์ที่ปรึกษา: รศ.ดร.พาลาภ ลิงหเสนี, อาจารย์ที่ปรึกษาร่วม: Professor Dr. John F. Keaney Jr., 155 หน้า ISBN 974-17-63-68-9

การปนเปื้อนของสารหนู ในน้ำดื่มก่อให้เกิดปัญหาในหลายประเทศทั่วโลกรวมถึงในประเทศไทย การศึกษาทางระบาดวิทยาพบว่า การได้รับสารหนูเป็นเวลานาน มีความสัมพันธ์กับการเกิดโรคของระบบหัวใจ และหลอดเลือด เช่น ภาวะหลอดเลือดแดงแข็ง เส้นเลือดโป่งพอง ความดันโลหิตสูง และอื่นๆ และมีรายงานว่า เซลล์เยื่อบุผนังหลอดเลือดเป็นเป้าหมายสำคัญของการเกิดพิษของสารหนู ซึ่งความผิดปกติในการทำงานหรือ การตายของเซลล์เยื่อบุผนังหลอดเลือดเป็นปัจจัยหนึ่งของการเกิดโรค อย่างไรก็ตามการเกิดพิษของสารหนูต่อ เซลล์เยื่อบุผนังหลอดเลือดยังไม่ทราบแน่ชัด

ผู้วิจัยได้ทำการศึกษาการเกิดพิษของสารหนูอนินทรีย์ (โซเดียมอาร์ซีไนท์) ต่อการนำส่งสัญญาณภายใน เซลล์และความเปลี่ยนแปลงที่เกิดขึ้นในเซลล์เพาะเลี้ยงจากเยื่อบุหลอดเลือดดำที่สายสะดือ ผู้วิจัยพบว่าผล ยับยั้งการเจริญเติบโตของเซลล์ ขึ้นกับขนาดและระยะเวลาที่เซลล์สัมผัสกับสารโซเดียมอาร์ซีไนท์ และผลนี้มีความสัมพันธ์กับ การเหนี่ยวนำโปรตีน พี 21^{Waf1/Cip1} ซึ่งเป็นโปรตีนที่เกี่ยวข้องกับวิถีการแบ่งตัวของเซลล์และการ ตายแบบอะพอพโตซิส โซเดียมอาร์ซีไนท์มีผลกระตุ้นการทำงานของตัวรับ อีอาร์บีบี 1 และ 2 ที่ผิวเซลล์ โดยพบ การเพิ่มขึ้นของ ปริมาณฟอสฟอริเซชันของ กรดอะมิโนไทโรซีน การยับยั้งการทำงานของ ตัวรับ อีอาร์บีบี โดย การใช้สารยับยั้งเฉพาะ หรือ โดยการใช้เทคโนโลยี siRNA เพื่อลดปริมาณตัวรับ ส่งผลให้การเหนี่ยวนำ โปรตีน พี 21^{Waf1/Cip1} จากผลของโซเดียมอาร์ซีไนท์ลดลงอย่างชัดเจน จึงอาจกล่าวได้ว่า ตัวรับ อีอาร์บีบี เป็นตัวควบคุม การเหนี่ยวนำ โปรตีน พี 21^{Waf1/Cip1} ในรูปแบบการทดลองนี้

นอกจากนี้ยังพบว่าโซเดียมอาร์ซีไนท์กระตุ้นการทำงานของเอนไซม์ p38 และ JNK ในวิถีที่แตกต่างกัน โดย JNK เป็นตัวเชื่อมสัญญาณจากตัวรับ อีอาร์บีบี1 สู่การเหนี่ยวนำ โปรตีน พี 21^{Waf1/Cip1} ในนิวเคลียส ซึ่งไม่พบ การเชื่อมโยงนี้ในวิถีของ p38 การใช้สารยับยั้งการทำงานของเอนไซม์ p38 และ JNK หรือการใช้ negative dominant DNA ต่อ MKK4 หรือ MKK7 ซึ่งเป็นควบคุมการทำงานของ p38 และ JNK ส่งผลต่อการเหนี่ยวนำ โปรตีนพี 21^{Waf1/Cip1} และโปรตีนพี 53 แตกต่างกัน

จากผลการทดลอง การยับยั้งการเหนี่ยวนำ โปรตีน พี 21^{Waf1/Cip1} สามารถลดการตายของเซลล์เยื่อ บผนังหลอดเลือดจากผลของโซเดียมอาร์ซีไนท์ ได้ ดังนั้นผู้วิจัยจึงนำเสนอว่า การควบคุมการ เหนี่ยวนำโปรตีน พี 21^{Waf1/Cip1} ผ่านทางตัวรับอีอาร์บีบี 1 เป็นกลไกสำคัญของการเกิดพิษของสารหนูต่อเซลล์เยื่อบุผนังหลอดเลือด ซึ่งอาจส่งผลต่อเนื่องต่อการเกิดภาวะของโรคหัวใจและหลอดเลือด จากการสัมผัสกับสารหนูในระยะยาวได้

สาขาวิชา วิทยาศาสตร์ชีวภาพ

ปีการศึกษา 2547

ลายมือชื่อนิสิต

ลายมือชื่ออาจารย์ที่ปรึกษา

ลายมือชื่ออาจารย์ที่ปรึกษาร่วม

4376954733 MAJOR BIOPHARMACEUTICAL SCIENCES

KEY WORD: ARSENIC, p21^{Waf1/Cip1}, ERBB1 RECEPTOR, HUVEC

NOPPARAT NUNTHARATANAPONG: INDUCTION OF P21^{WAF1/CIP1} THROUGH ERBB1 RECEPTOR TRANSACTIVATION IN HUMAN UMBILICAL VEIN ENDOTHELIAL CELLS BY SODIUM ARSENITE. THESIS ADVISOR: ASSOC. PROF. PALARP SINHASANI PH.D., THESIS CO-ADVISOR: PROF. JOHN F. KEANEY JR., M.D., 155 PP. ISBN 974-17

Arsenic exposure is associated with an increased risk of atherosclerosis and vascular diseases. While endothelial cells have long been considered to be the primary targets of arsenic toxicity, the underlying molecular mechanism remain largely unknown. This study was conducted to examine the signaling pathway triggered by sodium arsenite and its implication(s) on endothelial phenotype change. Human umbilical vein endothelial cell (HUVEC) was used as a model system for this study. We found that sodium arsenite produced time- and dose-dependent on viability of HUVECs. This effect correlated with an induction of p21^{Waf1/Cip1}, a regulatory protein of cell cycle and apoptosis. Sodium arsenite-stimulated ErbB1 and ErbB2 receptor transactivation manifested as receptor tyrosine phosphorylation appeared to be a proximal signaling event leading to p21^{Waf1/Cip1} induction. Since both pharmacological receptor kinase inhibitors (AG1478 and AG825) as well as knockdown of the receptors by SiRNA blocked arsenite-induced the p21^{Waf1/Cip1} upregulation. The activation of these receptors culminated in a specific activation of the JNK pathway. Although arsenite increased both JNK and p38 MAPK phosphorylation, the activation of these two stress kinases was distinct, with only JNK as a downstream target of the ErbB1 receptor. Moreover, inhibition of JNK with SP600125 or dominant-negative MKK7 inhibited only p21^{Waf1/Cip1} induction, whereas the p38 MAPK inhibitor SB203580 or dominant-negative MKK4 inhibited both p21^{Waf1/Cip1} and p53 induction. Functionally, inhibition of p21^{Waf1/Cip1} induction prevented endothelial death due to arsenite treatment. Insofar as endothelial dysfunction promotes vascular diseases, these data provide a mechanism of sodium arsenite-mediated the diseases and p21^{Waf1/Cip1} may represent an attractive target to ameliorate endothelial dysfunction in vascular diseases.

Field of study Biopharmaceutical sciences
Academic year 2004

Student's signature
Advisor's signature
Co-advisor's signature

ACKNOWLEDGEMENTS

This dissertation could not have been completed without funding from Thailand Research Fund and the help of a number of individuals.

First and foremost I would like to thank my advisor, Associate Professor Dr. Palarp Sinhaseni, for her enthusiastic support, and encouragement in the development of this work during my years at Chulalongkorn University, and for providing me with an independent environment in which to cultivate and sharpen my scientific skills. I am extremely thankful for her endless effort to provide invaluable guidance and inspired ideas.

I would like to give a very special thank you to Professor Dr. John F Keaney Jr., my thesis co-advisor in Whitaker Cardiovascular Institute, Boston University School of Medicine, Boston, Massachusetts, U.S.A. for his kindness, support and good advice and for providing me with wonderful facilities in his laboratory and supporting my living cost during my extension time in U.S.A. This dissertation would not be successful without his guidance and assistance from him.

I am deeply grateful to Dr. Kai Chen, Whitaker Cardiovascular Institute, Boston University, School of Medicine, Boston, Massachusetts, U.S.A. who provided a continued source of encouragement and support, great help and good advice during my stay in U.S.A.

I also wish to express my thank you to W632, Keaney's Laboratory members, Dr. Annong Huang, Dr. Eisabella Lapinska, Dr. Eberhard Schulz, Dr. Elad Anter, Dr. Shane R. Thomas, Tina Wu, Hui Xiao, Adam Albano, Yu Yang, Ana Sharma, and Nikheil Rau, for their helps in laboratory and their friendship. I had a very great time with them during my stay there.

I would like to acknowledge the contributions of the members of my committee: Assistant Professor Niyada Kiatying-Angsulee, Associate Professor Duangdeun Meksuriyen for their advice, criticism, and support are very helpful and greatly appreciated.

I would like to thank the Institute of Health Research, and Department of Pharmacology, Faculty of Pharmaceutical Sciences, Chulalongkorn University, and all staffs, for providing me good facilities in the institute and Department.

I would like to acknowledge the help of my lovely colleagues at the Faculty of Pharmaceutical Sciences, Chulalongkorn University: Dr. Teeradach Suramana, Dr. Tipicha Posayanonda, Mr. Veerakit Taechakitiroj, and Miss Nuttiya Veerawattanachai.

I would like to express my love and deep gratitude to my husband, Mr. Wichit Nuntharatanapong. His love, understanding, guidance, encouragement, and support allow me to complete my Ph.D.

Finally, I would like to dedicate this thesis to my loving mother, Mrs. Kanlaya Thitiwatanakarn.

I also would like to share my success to my father, Mr. Tanit Thitiwatanakarn, who passed away. I would like give a big thanks to him for his love and teaching.

TABLE OF CONTENTS

| | Page |
|--|-------------|
| THAI ABSTRACT..... | iv |
| ENGLISH ABSTRACT..... | v |
| ACKNOWLEDGEMENTS..... | vi |
| TABLE OF CONTENTS..... | vii |
| LIST OF TABLES..... | ix |
| LIST OF FIGURES..... | x |
| LIST OF ABBREVIATION..... | xiii |
| CHAPTER | |
| I INTRODUCTION..... | 1 |
| Problem Statement..... | 1 |
| Objectives..... | 4 |
| Hypothesis..... | 4 |
| Contributions of the Study..... | 4 |
| II LITERATURE REVIEW | |
| Arsenic..... | 5 |
| Sources of arsenic..... | 6 |
| Guideline value for arsenic in drinking-water..... | 9 |
| Toxicokinetics..... | 11 |
| Effect of arsenic on human health..... | 12 |
| Arsenic and carcinogenesis..... | 13 |
| Arsenic and cardiovascular diseases..... | 14 |
| Mechanism of toxicity..... | 15 |
| Molecular mechanism of arsenic in relation to signaling.... | 16 |
| Cell signaling..... | 21 |
| Tyrosine kinase receptor..... | 22 |
| Epidermal growth factor receptor (EGFR/ErbB1)..... | 24 |
| EGFR transactivation..... | 29 |
| Non receptor tyrosine kinase..... | 30 |

TABLE OF CONTENTS (Continued)

| | Page |
|--|-------------|
| Mitogen activated protein kinases (MAPKs)..... | 30 |
| Regulation of the Cell Division Cycle..... | 32 |
| Cell cycle..... | 33 |
| p21 ^{waf1/cip1} | 40 |
| Cell Death..... | 43 |
| Reactive Oxygen Species..... | 50 |
| III MATERIALS AND METHODS | |
| Cells..... | 54 |
| Chemicals..... | 54 |
| Cell culture condition..... | 55 |
| Experimental procedures..... | 55 |
| Data Analysis..... | 58 |
| IV RESULTS..... | 59 |
| V DISCUSSION..... | 95 |
| REFERENCES..... | 99 |
| APPENDICES | |
| APPENDIX A..... | 110 |
| APPENDIX B..... | 115 |
| APPENDIX C..... | 125 |
| APPENDIX D..... | 128 |
| APPENDIX E..... | 134 |
| APPENDIX F..... | 139 |
| APPENDIX G..... | 145 |
| CURRICULUM VITAE..... | 155 |

LIST OF TABLES

| | Page |
|---|-------------|
| Table 1 The valence states of arsenic..... | 8 |
| Table 2 EGFR family of receptor tyrosine kinases and their ligands..... | 26 |
| Table 3 Cdk Inhibitors..... | 39 |
| Table 4 Apoptosis VS Necrosis..... | 46 |
| Table 5 Chemical identity of arsenic..... | 112 |
| Table 6 Physical and chemical properties of arsenic..... | 113 |



สถาบันวิทยบริการ
จุฬาลงกรณ์มหาวิทยาลัย

LIST OF FIGURES

| | | | Page |
|--------|----|---|-------------|
| Figure | 1 | Arsenic..... | 1 |
| Figure | 2 | Toxicity of arsenic species..... | 9 |
| Figure | 3 | World map of documented arsenic problems in groundwater and the environment..... | 10 |
| Figure | 4 | The receptor tyrosine kinase signal transduction pathway... | 23 |
| Figure | 5 | Structure of EGFR (ErbB-1)..... | 25 |
| Figure | 6 | EGFR signal transduction pathway..... | 28 |
| Figure | 7 | EGFR transactivation..... | 29 |
| Figure | 8 | Mitogen activated protein kinase module..... | 31 |
| Figure | 9 | Cell division cycle..... | 34 |
| Figure | 10 | Determination of cellular DNA content..... | 34 |
| Figure | 11 | Cell cycle check points..... | 36 |
| Figure | 12 | Complexes of cyclines and cyclin-dependent kinases..... | 37 |
| Figure | 13 | The cycling of the different cyclins..... | 37 |
| Figure | 14 | Map of p21 ^{Waf1/Cip1} and its direct protein-protein interactions..... | 41 |
| Figure | 15 | Role of p53 in G1 arrest induced by DNA damage..... | 42 |
| Figure | 16 | Balance between cell growth and cell death..... | 44 |
| Figure | 17 | Cell death..... | 45 |
| Figure | 18 | Caspase activation and apoptosis..... | 48 |
| Figure | 19 | Role of oxygen in cell injury..... | 50 |
| Figure | 20 | Formation of ROSs and antioxidant mechanisms in biological systems..... | 51 |
| Figure | 21 | Oxidative stress..... | 52 |
| Figure | 22 | Cell viability after treated with 50 μ M sodium arsenite at various time points (MTT assay)..... | 60 |
| Figure | 23 | Cell viability after treated with 50 μ M sodium arsenite at various time points (trypan blue exclusion)..... | 61 |

LIST OF FIGURES (Continued)

| | | | Page |
|---------------|-----------|--|-------------|
| Figure | 24 | Cell viability after treated with increasing concentrations of sodium arsenite for 24 h (MTT assay)..... | 62 |
| Figure | 25 | Cell viability after treated with with increasing concentrations of sodium arsenite for 24 h (trypan blue exclusion)..... | 63 |
| Figure | 26 | Western Blot for p21 and p53 induction in HUVECs after treated with sodium arsenite various concentration for 4 h..... | 65 |
| Figure | 27 | Western Blot for p21 and p53 induction in HUVECs after treated with sodium arsenite various concentration for 16 h..... | 66 |
| Figure | 28 | Western Blot for p21 and p53 induction in HUVECs after treated with 50 μM sodium arsenite at various time points..... | 67 |
| Figure | 29 | RT-PCR for p21 and p53 mRNA expression in HUVECs after treated with 50 μM sodium arsenite for 4 h..... | 68 |
| Figure | 30 | Western Blot for p21 induction in HUVECs after treated with 50 μM sodium arsenite for 4 h, pretreated with Cycloheximide or Actinomycin D..... | 69 |
| Figure | 31 | Half-life of p21 in HUVECs, measured by Cycloheximide chase assay..... | 70 |
| Figure | 32 | Western Blot for p21 and p53 induction, pretreated with AG1478, AG825, AG1295 or AG1433..... | 72 |
| Figure | 33 | Western Blot for p21 and p53 induction, pretreated with AG1478 at various concentration..... | 73 |
| Figure | 34 | Western Blot for p21 and p53 induction, pretreated with AG825 at various concentration..... | 74 |

LIST OF FIGURES (Continued)

| | | | Page |
|---------------|-----------|---|-------------|
| Figure | 35 | Phosphorylation of ErbB1 by sodium arsenite (dose-dependence)..... | 75 |
| Figure | 36 | Phosphorylation of ErbB1 by sodium arsenite (time-dependence)..... | 76 |
| Figure | 37 | Phosphorylation of ErbB2 by sodium arsenite (time-dependence)..... | 77 |
| Figure | 38 | Inhibition of Phosphorylation of ErbB1 by AG1478, AG825 or PP2..... | 78 |
| Figure | 39 | Inhibition of Phosphorylation of ErbB2 by AG1478, AG825 or PP2..... | 79 |
| Figure | 40 | SiRNA transfection experiment for ErbB1..... | 80 |
| Figure | 41 | SiRNA transfection experiment for ErbB2..... | 81 |
| Figure | 42 | Induction of MAPKs after sodium arsenite treatment..... | 83 |
| Figure | 43 | Inhibition of p21- and p53-induction by SB203580..... | 84 |
| Figure | 44 | Inhibition of p21- and p53-induction by SP600125..... | 85 |
| Figure | 45 | Induction of p21 and p53 in COS-7 cells transfected with dominant negative MKK7 or MKK4..... | 86 |
| Figure | 46 | Effect of inhibitors on phospho-MKK4, phospho-p38 and phospho-JNK1/2..... | 87 |
| Figure | 47 | Inhibition of p21- and p53-induction by several kinase inhibitors..... | 88 |
| Figure | 48 | HUVECs morphology after treated with sodium arsenite..... | 90 |
| Figure | 49 | Pyknotic nuclei in HUVECs after treated with sodium arsenite in the presence or absence of inhibitors..... | 91 |
| Figure | 50 | Pyknotic nuclei in ErbB1-transfected HUVECs after treated with sodium arsenite..... | 92 |

LIST OF FIGURES (Continued)

| | | | Page |
|---------------|-----------|--|-------------|
| Figure | 51 | HUVEC viability by MTT assay after treated with sodium arsenite in the presence or absence of inhibitors... | 93 |
| Figure | 52 | Schematic model depicting the signaling pathways involved in arsenite-induced p21^{Waf1/Cip1} | 94 |
| Figure | 53 | Diagram of transfection procedure with Lipofectamine Reagent..... | 128 |
| Figure | 54 | SiRNA-mediated mRNA degradation pathway..... | 137 |
| Figure | 55 | HUVEC photograph from phase contrast microscopy..... | 140 |



 สถาบันวิทยบริการ
 จุฬาลงกรณ์มหาวิทยาลัย

LIST OF ABBREVIATIONS

| | |
|-----------------------------------|--|
| % | Percentage |
| °C | Degree Celsius |
| As | Sodium arsenite |
| CDK | Cyclin-dependent Kinase |
| CKI | Cyclin-dependent Kinase Inhibitor |
| DMA | Dimethyl arsinic acid |
| MMA | Monomethyl arsonic acid |
| DNA | Deoxy-ribonucleic acid |
| ECL | Enhanced chemiluminescence |
| EGF | Epidermal growth factor |
| EGFR | Epidermal growth factor receptor |
| EGM-2 | Endothelial growth medium-2 |
| ERK | Extracellular signal-regulated kinase |
| FBS | Fetal bovine serum |
| g | Gram |
| h | Hour |
| H₂O₂ | Hydrogen peroxide |
| HUVEC | Human umbilical vein endothelial cell |
| JNK | c-Jun N-terminal kinase |
| MAPK | Mitogen activated protein kinase |
| mg | Miligram |
| min | Minute |
| MKK | Mitogen activated protein kinase kinase |
| ml | Mililiter |
| mM | Microliter |
| MTT | Tetrazolium salt 3,[4,5-dimethylthiazol-2-yl]-2,5-diphenyltetrazolium bromide |
| PBS | Phosphate buffer saline |
| PDGF | Platelet-derived growth factor |
| PDGFR | Platelet-derived growth factor receptor |

| | |
|-----------------|--|
| PP2 | 4-amino-5-(4-chlorophenyl)-7- (<i>t</i>-butyl)pyrazolo[3,4-D] pyrimidine, |
| PI | Propidium iodide |
| PTPase | Protein tyrosine phosphatase |
| RNA | Ribonucleic acid |
| ROS | Reactive oxygen species |
| RT-PCR | Reverse transcription and polymerase chain reaction |
| SDS-PAGE | Sodium dodecyl-poly acrylamide gel electrophoresis |
| sec | Second |
| SiRNA | Small interference RNA |
| SAPK | Stress-activated protein kinases |
| μg | Microgram |
| μl | Microliter |
| μM | Micromolar |



สถาบันวิทยบริการ
จุฬาลงกรณ์มหาวิทยาลัย

CHAPTER I

INTRODUCTION

Problem Statement

Arsenic is a naturally occurring element in the earth's crust. Environmental exposure to arsenic is primarily from consumption of contaminated drinking water and food in certain regions of the world including areas of the southwestern United States Europe and Asia for example Taiwan, India, Bangladesh, and Thailand. On the basis of numerous epidemiological studies, arsenic has been classified as a potent human carcinogen (Gosselin *et al.*, 1984) and chronic arsenic intake has been associated with other adverse effects such as cardiovascular disease, peripheral vascular disease, hypertension, diabetes mellitus, and neurological effects (Smith *et al.*, 2000). Emerging evidence indicates that endothelial cell dysfunction is an early, perhaps causal, component of both chronic vascular (Ross, 1999) and neurologic diseases (De La Torre, 2004).

Arsenic apparently affects numerous intracellular signal transduction pathways and causes many alterations in cellular function. Arsenic has been reported to activate or inhibit a number of cellular signaling pathways leading to alterations in cell growth, differentiation and apoptosis. Numerous reports have shown that arsenite treatment induces DNA strand breaks and DNA-protein crosslinks in a variety of cell types. Damage to DNA results in increased abundance of tumor suppressor p53 protein through *de novo* protein synthesis and stabilization of existing protein. When p53 protein is modified by phosphorylation and acetylation, it has increased stability and becomes an active transcription factor, transactivating several key proteins regulating DNA repair processes, apoptosis and cell proliferation. The most important of these in term of cell cycle arrest is p21^{Waf1/Cip1}. Although p21^{Waf1/Cip1} has been shown to play an important role in cell cycle regulation, it also acts as a modulator of apoptosis (Chopin, 2004). Evidence of several studies has been shown that overexpression of p21^{Waf1/Cip1} increases apoptosis (Fotedar 1999; Shibata 2001, Kondo 1996, Kang 1999, Hsu 1999, Li 1999) whereas disruption of p21^{Waf1/Cip1}

function lead to a decrease in apoptosis (Chinery 1997, Seoane 2002, Detjen 2003, Chopin 2004).

Endothelial cells have long been suspected as primary targets of arsenic toxicity. However, the evidences supported the role of arsenic-induced toxicity in endothelial cells and underlying mechanisms are still unclear.

The MAP kinase (MAPK) pathway has been implicated in a number of phenomena associated with cardiovascular disease. Several studies have been suggested that arsenic activates gene expression by modulation of intracellular phosphorylation events and MAPK cascades. Arsenite was reported to induce ERKs, JNKs and p38 kinases activation in a time-dependent manner in a variety of human cell lines. In one study, arsenite treatment of human bronchial epithelial cells resulting in direct ErbB1 receptor (EGFR: epidermal growth factor receptor) tyrosine phosphorylation and activation of MEK1/2, increased phosphorylation of ERKs and enhanced transcription factor, Elk-1 activity (Wu *et al.*, 1999). Simeonova *et al.* (2002) demonstrated that the activity of non-receptor tyrosine kinase, pp60c-src, was induced by arsenite treatment in epithelial cell and involved in ErbB1 receptor transactivation and ERK activation. Tanaka-Kagawa *et al.* (2003) also showed that arsenite and arsenate activate ERK in normal human keratinocytes involved ErbB1 receptor-mediated pathway and induced the assembly of ErbB1R-Shc-Grb2 complexes. Arsenite, a well-recognized sulfhydryl binding agent, exerts its toxic effects by reacting with thiol of many cellular proteins in cells. ErbB1 receptor contains extracellular cysteine-rich domain that are important for ligand trigger dimerization. Some researchers suggested that arsenite may alter the conformation of ErbB1 receptor, resulting in an increase of its intrinsic tyrosine kinase activity by reacting with vicinal dithiols of ErbB1 receptor (Tanaka-Kagawa *et al.*, 2003). More recently, p38 and JNK are shown to be involved in cell cycle regulation under certain circumstances (Daly *et al.*, 1999; Lee *et al.* 1999; Wang *et al.*, 1999; Chen *et al.*, 2001). There are several reports on p38 and JNK in relation to cell growth and apoptosis respond to a variety of external cellular stresses. Kim *et al.*, 2002, reported the involvement of p38-mediated cell growth inhibition by sodium arsenite in NIH3T3 and a link between the activation of p38 and induction of p21^{Waf1/Cip1}. However, the precise mechanisms of the MAPKs-mediated cell growth regulation and the

involvement of membrane receptor kinase in responses to stress stimuli have not yet been clearly elucidated.

Understanding how arsenite enhances p21^{Waf1/Cip1} induction may help unveil cellular responses to arsenite toxicity in endothelial cells and could provide an important knowledge on the vascular dysfunction caused by arsenite. The goal of this study is to examine the implications of arsenite-induced toxicity for endothelial cells and to identify the underlying signaling mechanisms involved in the expression of p21^{Waf1/Cip1} by sodium arsenite. We focus on the role of the membrane receptor, ErbB1 family, and MAPKs in the expression of p21^{Waf1/Cip1} induction by sodium arsenite.



สถาบันวิทยบริการ
จุฬาลงกรณ์มหาวิทยาลัย

Objectives

1. To examine the role of arsenite for endothelial cell growth.
2. To investigate the mechanism that mediates sodium arsenite-induced p21^{Waf1/Cip1} upregulation and the role of ErbB1 receptor and MAPKs in this effect in endothelial cells.

Hypothesis

p21^{Waf1/Cip1} upregulation by sodium arsenite-induced toxicity may exert its effects through MAPK pathway which relates to the ErbB1 receptor transactivation.

Contributions of the Study

1. To understand the roles of arsenite-induced toxicity in endothelial cells
2. To understand the molecular mechanism that mediates sodium arsenite-induced p21^{Waf1/Cip1} upregulation and the role of ErbB-1 receptor and MAPK in this effect. This will provide important knowledge on the vascular dysfunction caused by arsenite.

สถาบันวิทยบริการ
จุฬาลงกรณ์มหาวิทยาลัย

CHAPTER II

LITERATURE REVIEW

ARSENIC (ATSDR, 2000)

Arsenic is an element that is widely distributed in the earth's crust. Elemental arsenic is ordinarily a steel grey metal-like material that sometimes occurs naturally. However, arsenic is usually found in the environment combined with other elements such as oxygen, chlorine, and sulfur (Merck 1989). Arsenic combined with these elements is called inorganic arsenic. Arsenic combined with carbon and hydrogen is referred to as organic arsenic. The organic forms are usually less harmful than the inorganic forms.



Figure 1. Arsenic is grayish metal (elemental form), which is rarely found under natural conditions.

The factors that determine whether human will be harmed when they are exposed to arsenic include the dose (how much), the duration (how long), and how come in contact with it.

Inorganic arsenic has been recognized as a human poison since ancient times, large oral doses (above 60,000 ppb in food or water) can produce death. Ingestion

lower levels of inorganic arsenic (ranging from about 300 to 30,000 ppb in food or water), may cause an irritation of stomach and intestines, with symptoms such as stomach ache, nausea, vomiting, and diarrhea (Marcus and Rispin, 1998). Other effects from swallowing inorganic arsenic include decreased production of red and white blood cells which may cause fatigue, abnormal heart rhythm, blood-vessel damage resulting in bruising, and impaired nerve function causing a "pins and needles" sensation in hands and feet (Gosselin et al., 1984).

Perhaps the single most characteristic effect of long-term oral exposure to inorganic arsenic is a pattern of skin changes. These include a darkening of the skin and the appearance of small "corns" or "warts" on the palms, soles, and torso. A small number of the corns may ultimately develop into skin cancer. Swallowing arsenic has also been reported to increase the risk of cancer in the liver, bladder, kidneys, prostate, and lungs (Gosselin et al., 1984). The European Protection Agency (EPA) has determined that inorganic arsenic is a human carcinogen and has assigned it the cancer classification, Group 1 (ATSDR 2000).

Since arsenic is found naturally in the environment, people can be exposed to arsenic by eating food, drinking water, or breathing air and by skin contact with soil or water that contains arsenic. Children may also be exposed to arsenic by eating dirt.

Most inorganic and organic arsenic compounds are white or colorless powders that do not evaporate. They have no smell, and most have no special taste. Thus, we usually cannot tell if arsenic is present in our food, water, or air.

Source of arsenic

Inorganic arsenic occurs naturally in soil and in many kinds of rock, especially in minerals and ores that contain copper or lead. When these ores are heated in smelters, most of the arsenic goes up the stack and enters the air as a fine dust. Smelters may collect this dust and take out the arsenic as arsenic trioxide. Volcanic eruptions are another source of arsenic. Small amounts of arsenic also may be released into the atmosphere from coal-fired power plants and incinerators because coal and waste products often contain some arsenic. About 90% of all arsenic produced is used as a preservative for wood to make it resistant to rotting and decay (chromated copper arsenate (CCA)). In the past, arsenic was primarily used as a

pesticide, e.g. on cotton fields, potato, apple and fruit orchards. Organic arsenicals, cacodylic acid, disodium methylarsenate (DSMA), and monosodium methylarsenate (MSMA), are used in agriculture as pesticides, principally on cotton fields and in orchards. However, most agricultural uses of arsenic were banned because of concerns about human health risk during production and application or accidental poisoning at the point of use (EPA 1998). Small quantities of arsenic metal are added to other metals forming metal mixtures or alloys with improved properties. The greatest use of arsenic in alloys is in lead-acid batteries used in automobiles. Another important use of arsenic compounds is in semiconductors and light-emitting diodes (Carapella, 1992).

Arsenic compounds have a long history of use in medicine. Inorganic arsenic was used as a therapeutic agent through the mid twentieth century, primarily for the treatment of leukemia, psoriasis, and chronic bronchial asthma. Organic arsenic antibiotics were extensively used in the treatment of spirochetal and protozoal disease (National Research Council 1999). Recently, there has been renewed interest in arsenic trioxide as a therapeutic agent for the treatment of acute promyelocytic leukemia (APL) (Gallagher 1998).

Arsenic cannot be destroyed in the environment. It can only change its form, or become attached or separated, from particles. It may change its form by reacting with oxygen or other molecules present in air, water, or soil, or by the action of bacteria that live in soil or sediment. Many common arsenic compounds can dissolve in water. Thus, arsenic can get into lakes, rivers, or underground water by dissolving in rain or snow or through the discharge of industrial wastes. Some fish and shellfish take in arsenic which may build up in tissues. However, most of this arsenic is in a form (often called "fish arsenic") that is less harmful.

The concentration of arsenic in soil varies widely, generally ranging from about 1 to 40 parts of arsenic to a million parts of soil (ppm) with an average level of 5 ppm. However soils in the vicinity of arsenic-rich geological deposits, some mining and smelting sites, or agricultural areas where arsenic pesticides had been applied in the past may contain much higher levels of arsenic. The concentration of arsenic in natural surface and groundwater is generally about 1 part in a billion parts of water (1

ppb) but may exceed 1,000 ppb in mining areas or where arsenic levels in soil are high. Groundwater is more likely to contain high levels of arsenic than surface water. Levels of arsenic in food range from about 20 to 140 ppb. Levels of arsenic in the air generally range from less than 1 to about 2,000 nanograms of arsenic per cubic meter of air (less than 1–2,000 ng/m³), depending on location, weather conditions, and the level of industrial activity in the area. Concentrations in air in remote locations range from 1 to 3 ng/m³, while concentrations in urban areas may range from 20 to 100 ng/m³.

Arsenic episodes all over the world are divided into three categories.

1. Natural groundwater arsenic contamination
2. Arsenic contamination from industrial source
3. Arsenic contamination from food and beverage

Chemical Forms of concern

The amounts of arsenic required to cause adverse health effects depend on the chemical and physical form of the arsenic. Analysis of the toxic effects of arsenic is complicated by the fact that arsenic can exist in several different valence states (Table 1) and many different inorganic and organic compounds.

Table 1. The valence (oxidation) states of arsenic.

| | |
|------------------|-------------------|
| As ⁻³ | arsin |
| As ⁰ | elemental arsenic |
| As ⁺¹ | arsonium metal |
| As ⁺³ | arsenite |
| As ⁺⁵ | arsenate |

Inorganic forms are generally more acutely toxic than organic forms (Figure 2). Most cases of human toxicity from arsenic have been associated with exposure to inorganic arsenic. The common inorganic arsenical in air is arsenic trioxide (As_2O_3), while a variety of inorganic arsenates (AsO_4^{3-}) or arsenites (AsO_2^-) occur in water, soil, or food. A number of studies have noted differences in the relative toxicity of these compounds, with trivalent arsenites (As^{3+}) tending to be more toxic than pentavalent arsenates (As^{5+}) (Sardana et al. 1981; Willhite 1981). The duration of arsenic exposure appears to be a key factor in determining the toxic effects.

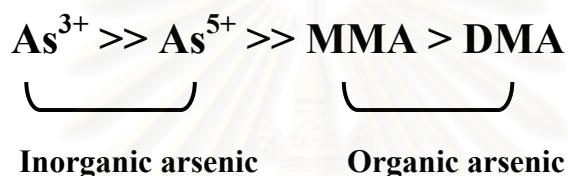


Figure 2. Toxicity of arsenic species. Inorganic arsenic compounds are about 100 times more toxic than organic arsenic compounds.

Guideline value for arsenic in drinking-water

In 1958, the International Standards for Drinking-water established 0.02 mg/L as an allowable concentration for arsenic. In 1963 the standard was re-evaluated and reduced to 0.05 mg/L. In 1984, this was maintained as WHO's "Guideline Value", and many countries have kept this as the national standard or as an interim target. However increased risks of arsenic-related diseases have been observed at arsenic concentration in drinking-water less than 0.05 mg/L. The Safe Drinking Water Act requires U.S. EPA to revise the existing this value standard for arsenic in drinking-water. Based on health criteria, EPA (January, 2001) established a Minimum concentration level (MCL) for arsenic in drinking-water of 0.01 mg/L. This standard must become fully effective in all water systems covered in January, 2006.

Reliable data on exposure and health effects are rarely available, but it is clear that there are many countries in the world where arsenic in drinking-water has been detected at concentration greater than the Guideline Value, 0.01 mg/L. These include

Argentina, Australia, Bangladesh, Chili, China, Hungary, India, Mexico, Peru, Thailand, and the United States of America.



Figure 2. World map of documented arsenic problems in groundwater and the environment.

สถาบันวิทยบริการ
จุฬาลงกรณ์มหาวิทยาลัย

Toxicokinetics

Absorption, Distribution, Metabolism, and Excretion.

Available data from toxicokinetic studies in humans reveal that arsenates and arsenites are well absorbed following both oral and inhalation exposure. Arsenic absorption depends on its chemical form. In humans, As^{+3} , As^{+5} , MMA, and DMA are orally absorbed 80%. Absorption appears to be by passive diffusion in humans and mice, although there is evidence for a saturable carrier-mediated transport process for arsenate in rats (Gonzalez et al. 1995). Csanaky and Gregus (2001) demonstrated that arsenate appears to employ phosphate transporters for uptake into cells since fosfarnet (phosphonoformic acid), a phosphate antagonist, blocked arsenate uptake in rats but was ineffective on arsenite. Dermal absorption appears to be much less than by the oral or inhalation routes. The rate of absorption of arsenic in highly insoluble forms (e.g., arsenic sulfide, lead arsenate) is much lower than that of more soluble forms via both oral and inhalation routes. Once absorbed, arsenites are partially oxidized to arsenates and arsenates are partially reduced to arsenites, yielding a mixture of As^{+3} and As^{+5} in the blood. Data on distribution are limited, but it appears that arsenic and its metabolites distribute to all organs in the body. Metabolism involves mainly reduction-oxidation reactions that interconvert As^{+5} and As^{+3} and methylation of As^{+3} to yield MMA and DMA. The rate and relative proportion of methylation production varies among species and also vary among tissues. Since the liver is a major site for the methylation of inorganic arsenic, a “first-pass” effect is possible after gastrointestinal absorption; however, this has not been investigated in animal models. Most arsenic is rapidly excreted in the urine as a mixture of inorganic arsenics, MMA, and DMA, although some may remain bound in tissues (especially skin, hair, and fingernails). Excretion can also occur via feces after oral exposure; a minor excretion pathway is nails and hair. The methylation of inorganic arsenic is the major detoxification pathway.

Studies in mice and rats have shown that arsenic compounds induce metallothionein, a metal-binding protein thought to detoxify cadmium and other heavy metals, *in vivo* (Albores et al. 1992; Hochadel and Waalkes 1997; Kreppel et al. 1993; Maitani et al. 1987a). The potency of arsenic compounds in inducing metallothionein parallels their toxicity (i.e., $\text{As}^{+3} > \text{As}^{+5} > \text{MMA} > \text{DMA}$). For

cadmium or zinc, it is thought that metallothionein binds these metal, making their biologically inactive. However, only a small percentage of arsenic is actually bound to metallothionein (Albores et al. 1992; Kreppel et al. 1994; Maitani et al. 1987a). *In vitro* studies have shown that affinity of arsenic for metallothionein is much lower than that of cadmium or zinc (Waalkes et al. 1984). It has been proposed that metallothionein might protect against arsenic toxicity by acting as an antioxidant against oxidative injury produced by arsenic.

Arsenic and health problems

The manifestation of arsenic toxicity depends on dose and duration of exposure.

Acute Toxicity

Single oral doses in the range of 20 mg As/kg and higher have caused death in humans. Signs of acute poisoning in humans include intense abdominal pains, weakness, trembling, salivation, gastrointestinal effects such as vomiting and diarrhea, fast feeble pulse, prostration, hypothermia, collapse and death (Marcus and Rispin, 1988). Early symptoms in most human cases are those of severe gastritis or gastroenteritis. A violent hemorrhagic gastroenteritis leads to loss of fluids and electrolytes, resulting in collapse, shock, and death (Gosselin et al., 1984).

Arsenite has been shown to induce oxidative DNA damage in human vascular smooth muscle cells *in vitro* (Lynn et al., 2000). Therefore, it appears to be a plausible mechanism for vascular cell damage following acute *in vivo* exposures.

Subchronic Toxicity

Subacute and subchronic arsenic exposures generally affect many of the same organs or systems as those affected by acute arsenic exposure. Doses as low as 0.05 mg As/kg/day over longer periods (weeks to months) have also caused gastrointestinal, hematological, hepatic, dermal, and neurological effects. These effects appear to be a result of direct cytotoxicity. Feinglass (1973) reported the acute gastrointestinal effects of acute and subacute exposure to well water in the United States contaminated with 11,800 to 21,000 ppb of arsenic.

Chronic Toxicity

Long-term exposure (years) to arsenic via drinking-water causes cancer of the skin, lungs, urinary bladder, and kidney, as well as other skin changes such as pigmentation changes and thickening (hyperkeratosis). Following long-term exposure, the first changes are usually observed in the skin. Cancer is a late phenomenon, and usually takes more than 10 years to develop. In addition to cancer development, chronic oral exposure to arsenic has also resulted in serious damage to the vascular system in humans, including Blackfoot disease (a progressive loss of circulation in the fingers and toes that may lead to gangrene), Raynaud's disease, and cyanosis of fingers and toes. The intima of the blood vessels appeared to have thickened (ATSDR 2000). Arsenic has caused anemia in humans exposed by the oral route. Increased hemolysis and a toxic effect on the erythropoietic cells of bone marrow may be factors in the development of anemia. Wood and Fowler (1997) have identified arsenic-induced disturbances of the heme biosynthetic pathway.

Signs of renal damage generally are not seen or are mild in humans exposed to arsenic by the oral route. Signs of peripheral and/or central neuropathy are commonly seen in humans exposed to arsenic orally, with high-dose exposure producing central nervous system effects and low-dose exposure producing peripheral nervous system effects (ATSDR 2000).

Arsenic and Carcinogenesis

The EPA and the International Agency for Research on Cancer (IARC) classify arsenic as a carcinogen. Several mechanisms for genotoxicity caused by arsenic have been proposed. The genotoxicity database for arsenic indicates that it does not induce point mutations or DNA adducts, but chromosomal aberrations and sister chromatid exchanges have been reported. Arsenic can potentiate mutagenicity observed with other chemicals. This potentiation may be the result of direct interference by arsenic with DNA repair processes, perhaps by inhibiting DNA ligase (Li and Rossman 1989). Arsenic can also induce DNA amplification (Lee et al. 1988). It has been hypothesized that methylation changes in genes or their control regions can lead to altered gene expression, and potentially, carcinogenesis.

U.S. EPA, 1997, considered the potential modes of action for arsenic-induced carcinogenicity, as follow:

- Chromosomal Abnormalities.
- DNA repair
- DNA methylation
- Oxidative stress
- Cell proliferation
- Co-carcinogenicity

Arsenic and Cardiovascular Effects

The cardiovascular system is a very sensitive target of arsenic toxicity. A number of studies in humans indicate that arsenic ingestion may lead to serious effects on the cardiovascular system. Characteristic effects on the heart from both acute and long-term exposure include altered myocardial depolarization (prolonged Q-T interval, nonspecific S-T segment changes) and cardiac arrhythmias. Long-term low-level exposures may also lead to damage to the vascular system. The most dramatic example of this is "Blackfoot disease," a condition that is endemic in an area of Taiwan where average drinking water levels of arsenic range from 0.17 to 0.80 ppm (Tseng 1977), corresponding to doses of about 0.014–0.065 mg As/kg/day (Abernathy et al. 1989). Arsenic exposure in Taiwan has also been associated with an increased incidence of cerebrovascular disease (Chiou et al. 1997) and ischemic heart disease (Chen et al. 1996; Hsueh et al. 1998b). Increased arsenic exposure has been associated with an increase in hypertension in Bangladesh (Rahman et al. 1999).

Studies in Chile indicate that ingestion of 0.6–0.8 ppm arsenic in drinking water (corresponding to doses of 0.02–0.06 mg As/kg/day, depending on age) increase the incidence of Raynaud's disease and of cyanosis of fingers and toes (Zaldivar and Guillier 1977). Thickening and vascular occlusion of blood vessels were noted in German vintners exposed to arsenical pesticides in wine and in adults who drank arsenic-contaminated drinking water (Roth 1957). Epidemiological studies from the United States have also suggested correlations between standard

mortality ratios for cardiovascular diseases and arsenic levels in drinking water (Engel and Smith, 1994; Engel et al., 1994 and Lewis et al., 1999).

Mechanisms of Toxicity

At relatively high oral exposure, methylation capacity may not be adequate to prevent cytotoxic levels of arsenic from reaching tissues. Some of the effects of higher-dose oral exposure to arsenic are result of direct cytotoxicity. It is believed that the toxicity of trivalent arsenic (As^{+3}) results primarily from its inhibition of critical sulfhydryl-containing enzymes. As^{+3} reacts with the sulfhydryl groups of proteins, inactivates enzymes, and interferes with mitochondrial function by inhibiting succinic dehydrogenase activity (ATSDR, 2000).

Pentavalent arsenic is recognized as an uncouple of mitochondrial oxidative phosphorylation. It can competitively substitute for phosphate in many biochemical reactions. Replacing the stable anion with the less stable arsenate anion lead to rapid hydrolysis of high energy bonds in compounds such as ATP. Loss of these bonds results in the loss of energy needed for critical steps in cellular metabolism (ATSDR, 2000).

Mechanism of Arsenic in Relation to Cell Signaling

Arsenic acts on cells through a variety of mechanisms, influencing numerous signal transduction pathways and resulting in a vast range of cellular effects that include apoptosis induction, growth inhibition, promotion or inhibition of differentiation, and angiogenesis inhibition. Responses vary depending on cell type and the form of arsenic.

The cellular response to arsenic shares many features with the heat shock response as well as oxidative stress. This includes the differential sensitivity of the stress signal pathway elements to the magnitude of the stress, stressor-specific activation of the response elements, and the protective role of the heat shock response. Oxidative stress, the central component of heat shock response, is typical of arsenic-related effects that are, in fact, regarded as the chemical paradigm of heat stress. Similar to heat stress, arsenite induces heat shock proteins (HSPs) of various sizes. The signal cascade triggered by arsenite like heat stress induces the activities of the mitogen-activated protein (MAP) kinases, extracellular regulated kinase (ERK), c-jun terminal kinase (JNK), and p38. Through the JNK and p38 pathways, arsenite activates the immediate early genes c-fos, c-jun, and egr-1, usually activated by various growth factors, cytokines, differentiation signals, and DNA-damaging agents. Like other oxygen radical-producing stressors, arsenic induces nitric oxide production at the level of transcriptional activation along with induction of poly(ADP)-ribosylation, NAD depletion, DNA strandbreak, and formation of micronuclei (Bernstam and Nriagu, 2000). Porter et al. (1999) also reported that arsenate and arsenite activate JNK, however, the mechanism by which this occurs is not known.

In vitro studies with endothelial cell cultures suggested that arsenic can cause cellular redox modulation, transcription factor activation, and gene expression relevant to endothelial dysfunction. For example, it has been demonstrated that exposure of endothelial cells to arsenite induces NF- κ B activation and DNA synthesis through reactive oxygen species (Barchowsky et al., 1996 and Barchowsky et al., 1999). Hirano et al. (2003) have demonstrated an uptake of arsenic into endothelial cells and concomitant induction of antioxidative enzymes, including heme oxygenase-1 (HO-1), thioredoxin peroxidase-2, NADPH dehydrogenase, and glutathione S-

transferase P subunit, which suggests arsenic-induced oxidative stress. Chen and coworkers, 1990 have demonstrated that arsenic disrupts cell proliferation in endothelial cell cultures.

Recently, it has been reported that arsenic increases the expression of cyclooxygenase-2 in bovine aortic endothelial cells as well as human umbilical vein endothelial cells (HUVEC) through peroxynitrite formation and NF-kB activation, respectively (Bunderson et al., 2002 and Tsai et al., 2002). Simeonova et al. (2003) found that arsenic induces expression of genes coding for inflammatory mediators including IL-8 in human aortic endothelial cells (HAEC).

Previous studies demonstrated that arsenic is a potent activator of AP-1 and NF-kB DNA binding activity in different type of cells including porcine aortic endothelial cells, keratinocytes, and urinary bladder cells (Barchowsky et al., 1996; Simeonova et al., 2000). AP-1 and NF-kB can regulate inflammatory gene expression and the transcription factors are subject to redox-dependent regulation (Simeonova et al., 1999). The effects induced by arsenic, including transcription factor activation, gene expression, or an impaired NO homeostasis, might be mediated indirectly by induction of oxidative stress or directly through arsenic reactivity to vicinal sulfhydryl groups. Macromolecules involved in cell signaling, such as receptors, integrins, or protein phosphatases contain high numbers of vicinal sulfhydryls and are capable of reacting with arsenic (Simeonova and Luster, 2002).

Emerging data indicate that receptor tyrosine kinases (RTKs) are targets of ROS signaling through a process known as “receptor transactivation” that involves ligand-independent stimulation of receptor kinase activity. For example, H₂O₂ stimulates JNK activation through a pathway involving EGF receptor transactivation (Chen K., et al., 2001). Similarly, arsenite mediated-ERK pathway involved activation of Src kinase-dependent EGF receptor transactivation (Simeonova et al., 2002).

Huang et al., (1999) reported that arsenite inhibited EGF-induced cell transformation in JB6 cells and induced apoptosis. In this study, arsenic-induced apoptosis was almost totally blocked by expression of a dominant-negative mutant of JNK1 (DN-JNK1). The results of these studies support the hypothesis that the

induction of ERKs by arsenic may promote arsenic's carcinogenic effects whereas induction of JNKs may enhance its apoptotic activity and therefore its anti-carcinogenic effects.

Evidence continues to accumulate suggesting that MAPKs are important in mediating the effects of arsenic. Many studies indicate that arsenite is more effective than arsenate in producing immediate and potent effects. That observation may be due to differences in cell permeability between arsenite and arsenate, endogenous GSH levels or to the time required to metabolize arsenate to arsenite. Most reports indicate that ERKs, JNKs, and p38 kinases are differentially activated by arsenic. Arsenic-induced activation of ERKs seems to consistently lead to proliferative responses whereas activation of JNKs appears to be associated with induction of apoptosis and inhibition of cell transformation. Some studies suggest that the effects of arsenic may be mediated through tyrosine kinase receptors, and in particular the EGF receptor. In almost every case, the effects of arsenic appear to be a time- and dose-dependent.

Bode and Dong (2002) suggests that chronic exposure to low levels of arsenic may eventually result in effects similar to those induced by acute exposure to higher concentrations of arsenic.

Recently arsenic trioxide (As_2O_3) has demonstrated a specific beneficial effect in the treatment of acute promyelocytic leukemia (APL) (Chen *et al.*, 1996b). Zhang *et al.* (1998) studied the *in vitro* effects of arsenic trioxide on seven lymphoid lineage cell lines. They demonstrated that arsenic trioxide inhibited the proliferation of myeloid and lymphoid cultured cell lines. Apoptosis was induced at 1 μM arsenic trioxide in cell lines such as NB4, NKM-1, and NOP-1 but not in Raji, Daudi and HL-60 cells. The induction of apoptosis was associated with the downregulation of bcl-2 protein.

Chen *et al.* (1998) propose a mechanism of arsenite-induced apoptosis involving the following sequential steps: (1) initial activation of flavoprotein-containing superoxide production enzyme such as NADPH-oxidase and an increase in cellular superoxide levels; (2) conversion of superoxide to hydrogen peroxide; (3) release of cytochrome c (from mitochondria) to the cytosol, activation of CPP32 protease, and PARP (a DNA repair enzyme) degradation. Action of arsenite on Bcl-2

gene expression (Bcl-2 protein can attenuate As-induced apoptosis) also seems to occur between steps (1) and (3) above.

Inorganic arsenic induces apoptosis, or programmed cell death, in CHO cells (Wang et al., 1996), immature rat thymocytes (Bustamante et al., 1997) and human HL-60 cells (Ochi et al., 1996). A characteristic marker of apoptosis is internucleosomal DNA cleavage, which was observed in all cell types after exposure to inorganic arsenic. In the HL-60 cells, sodium arsenite (0.05 μM) produced a greater response than sodium arsenate (0.1 μM). The apoptotic response by both arsenicals was increased when the cells were depleted of GSH by buthione sulfoximine (BSO). The mechanism of apoptosis in the thymocytes is unknown, but Wang *et al.* (1996) observed that in CHO cells, arsenite induces a cascade of events that leads to apoptosis. This cascade involves the generation of reactive oxygen species, production of hydroxyl radicals via a metal-catalyzed Fenton reaction, protein synthesis and activation of protein kinase. Li and Broome (1999) propose that trivalent arsenic induces apoptosis at least in leukemia cells, by binding to tubulin. This results in inhibition of tubulin polymerization and eventual formation of microtubules. Broome suggest that trivalent arsenic binds to cysteine residues (cis-12 and cys-13) of tubulin, which prevents GTP from binding to tubulin. This results in inhibition of microtubule formation, arresting the cells in mitosis, and activation of the genes involved apoptosis.

Tyrosine phosphatases have been proposed as molecular targets for the activity of arsenite. These enzymes play major roles in modulation cellular metabolism. They possess many vicinol thiols therefore are a potential site of interaction with arsenite.

The stress sensor JNK regulates arsenite-induced p53-independent expression of GADD45. Because GADD45 is responsible for the maintenance of the G2/M checkpoint to prevent improper mitosis, therefore, its rapid induction by extracellular signals may be responsible for some of the antiproliferative effects of arsenite (Chen *et al.*, 2001).

There is evidence that antioxidants can attenuate MAPK activity suggesting that MAPK signaling cascades are targets affected by ROS levels in cells. Molecular

mechanisms of oxidant mediated cell growth and its targets during tumor progression remain unclear and need further study.

Chen K., *et al.* (2001), observed that phenotypic properties of endothelium are subject to modulation by oxidative stress, by exposing endothelial cells to H_2O_2 , rapid activation of c-Jun N-terminal kinase (JNK) was observed to involve phosphorylation of JNK and c-Jun. The authors proposed that JNK activation may play some role in nonlethal phenotypic changes in the endothelial cell. The mechanism of JNK activation in endothelial cell is unknown. However, tyrosine kinase inhibitors, genistein, herbimycin A attenuated the effect of H_2O_2 -induced JNK activation. Adenoviral transfection with a dominant negative form of Src in HUVEC implicated that Src is an upstream activator of JNK.

The pathway of H_2O_2 -induced JNK activation was found to be involved with EGFR transactivation through a Src-dependent pathway that is distinct from EGFR ligand activation. Goldkorn *et al.* (1998) also observed that H_2O_2 preferentially induced EGFR tyrosine phosphorylation and this effect was inhibited by genistein implicating an involvement of non-receptor protein tyrosine kinase.

Cell Signaling

Cells need to communicate with their neighbors, monitor the conditions in their environment, and respond appropriately to different stimuli that impinge on their surface. Apparently, cells carry out these interactions by a phenomenon known as *cell signaling*, in which information is relayed across the plasma membrane to the cell interior and often to the cell nucleus.

In most systems, cell signaling includes:

1. Recognition of the stimulus at the outer surface of the plasma membrane by a specific receptor embedded in the membrane.
2. Transfer of a signal across the plasma membrane to its cytoplasmic surface.
3. Transmission of the signal to specific effector molecules on the inner surface of the membrane or within the cytoplasm that trigger the cellular response.
4. Cessation of the response as a result of the destruction or inactivation of the signaling molecule, combined with a decrease in the level of the extracellular stimulus.

However, not all information is transmitted from the extracellular space to the cell interior by way of a cell-surface receptor. Steroid hormones, for example, act on target cells by diffusing through the plasma membrane and binding to a cytoplasmic receptor. Conversely, a few extracellular agents can evoke cellular response directly without having to initiate a signal inside the cell. The neurotransmitter acetylcholine acts by such a mechanism when it binds to a receptor on a skeletal muscle cell, opening an ion channel that lies within the receptor itself (Karp, 1999).

Depending on the type of cell and stimulus, the response may involve a change in gene expression, an alteration of the activity of metabolic enzymes, a reconfiguration of the cytoskeleton, a change in ion permeability, the activation of DNA synthesis, or even the death of the cell.

It is known that cell signaling can affect virtually every aspect of cell structure and function, and is also intimately involved in the regulation of cell growth and division. Therefore, the study of cell signaling is important in understanding how a cell can lose growth control and develop into a malignant tumor.

Signal transduction is a complex process in which information is passed along signaling pathways that consist of a series of distinct proteins. Each protein in the pathway typically acts by altering the conformation of the next protein in the series, an event that activates or inhibits that protein. There are different types of signal transduction pathways: G protein-coupled receptors, receptor tyrosine kinases, and signaling originated from contacts between the cell surface and the substratum (Karp, 1999; Cooper, 2000). These signaling pathways are not linear pathways leading directly from a receptor at the cell surface to an end target. However, in fact, signaling pathways in the cell are much more complex as described below:

- Convergent signaling pathway: signals from a variety of unrelated receptors can converge to activate a common effector.
- Divergent signaling pathway: signals from the same ligand can diverge to activate a variety of different effectors and lead to diverse cellular responses.
- Crosstalk between signaling pathways: signals can be passed back and forth between different pathways.

One of the fundamental mechanisms by which cells in multicellular organisms communicate is the binding of polypeptide ligands to cell surface receptors that possess tyrosine kinase catalytic activity. Receptor tyrosine kinase (RTKs) are transmembrane glycoproteins that are activated by the binding of their cognate ligands, and they transduce the extracellular signal to the cytoplasm by phosphorylating tyrosine residues on the receptor themselves (autophosphorylation) and on downstream signaling proteins. RTKs activate numerous pathways within cells, leading to cell proliferation, differentiation, migration, or metabolic changes (Schlessinger and Ullrich, 1992).

Protein Tyrosine Kinase

Protein tyrosine kinases mediate the transduction and processing of many extra- and intracellular signals. They are critical in regulating cell growth and differentiation and are deeply involved in oncogenesis. There are two general classes of protein tyrosine kinases: the receptor tyrosine kinases and the receptor-associated

tyrosine kinases. The receptor tyrosine kinases possess an extracellular ligand binding domain and an intracellular catalytic domain with intrinsic tyrosine kinase activity.

Binding of a ligand to the receptor leads to a variety of downstream effects including stimulation of other tyrosine kinases, elevation of intracellular calcium levels, activation of serine/threonine kinases, phospholipids C and phosphatidylinositol-3'-kinase, and ultimately changes in gene expression (Medema and Bos, 1993). Many substrates for protein tyrosine kinases contain a structural motif, Src homology 2 domain (SH2) that binds to phosphotyrosine residues and mediates the interaction of substrates with activated protein tyrosine kinases (Koch et al., 1991; Smithgall, 1995). A model pathway leading to the activation of the MAP kinase cascade is depicted in figure 4.

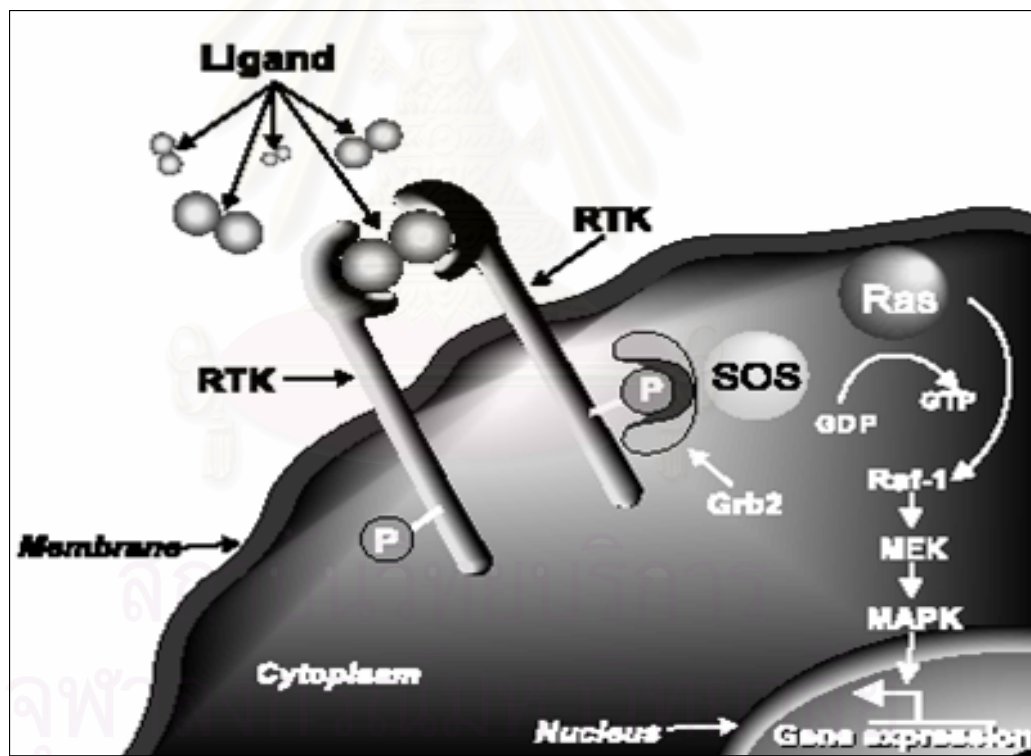


Figure 4. The receptor tyrosine kinase signal transduction pathway. The ligand binds to the receptor tyrosine kinase (RTK) triggering receptor dimerization and autophosphorylation. Grb2 binds to the activated receptor via its SH2 domain and to Sos via its SH3 domain(s). Sos stimulates GDP-GTP exchange on Ras, activating a cascade of Ser/Thr kinases that ultimately leads to changes in gene expression.

EGFR (ErbB-1)

An essential feature of activation of the tyrosine kinase receptors is that binding of the ligand results in dimerization of the receptors. Epidermal growth factor (EGF) is a monomeric ligand and two molecules are needed to bring two receptors together. It is believed that ligand binding changes the conformation in the extracellular domain of the receptor such that the one receptor recognizes the other. The binding of the ligand and subsequent dimerization results in another conformational change which unveils the dormant tyrosine kinase activity. The active protein is then able to phosphorylate the neighboring receptor (autophosphorylation) on a number of tyrosine residues. The tyrosine-phosphorylated dimer receptor complex is the active EGF receptor. At this stage, the receptor is able to phosphorylate and activate other enzymes, and is also able to interact with adaptor proteins.

The dimerized, phosphorylated receptor initiates a series of signal transduction cascades through association with a number of other proteins. The receptor associated with these proteins is called a “receptor signal complex”.

Structure and function

The epidermal growth factor receptor (EGFR) is a single-polypeptide chain with 1186 residues and approximate molecular weight of 170 kDa. The receptor is transmembrane glycoprotein encoded by the c- (erbB) -1 proto-oncogene. It is one of four related growth factor receptors that share similarities in structure and function: EGFR or human EGF-related receptor (HER)-1 (ErbB-1), HER2 (neu or ErbB-2), HER3 (ErbB-3), and HER4 (ErbB-4) (Salomon et al., 1995).

EGFR is composed of three regions with distinct functions:

1. Extracellular region is 662 amino acids with two cysteine-rich domains and ligand-binding domain (binds to different EGF-related growth factors)
2. Transmembrane region is amino acids of hydrophobic nature (anchors the receptor in the cell membrane)
3. The intracellular portion is 542 amino acids and has three function domains.
 - The regulatory domain with serine and threonine residues that are phosphorylated leading to inactivation of the receptor.

- The tyrosine kinase domain that is activated by EGF binding and dimerization of receptors.
- The C-terminal domain with five tyrosine residues that are phosphorylated by the receptor tyrosine kinase and are involved in signal transduction via association with SH2 domain proteins.

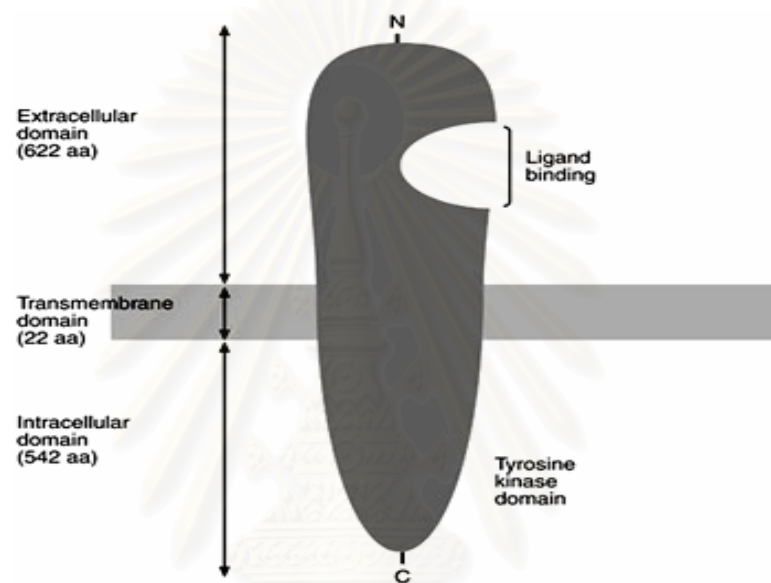


Figure 5. Structure of EGFR.

The other receptor family members are structurally similar to EGFR, but with certain distinct properties. The EGFR extracellular domain is approximately 36-48% homologous with other EGFR family members, with the kinase domain displaying 60-82% homology and the cytoplasmic domain 24-33% homology (Crovello et al., 1998). Notably, the EGFR and HER2 show 82% homology in the tyrosine kinase domain, and cross-reactivity appears to exist between the receptors (Prigent and Lemoine 1992)

EGFR is expressed on healthy cells that originate from all three germ cell layers, particularly those of epithelial origin. Several distinct ligands exist for EGFR, with the most important being epidermal growth factor (EGF) and transforming growth factor- α (TGF)- α (Salomon et al., 1995).

Table 2. EGFR family of receptor tyrosine kinases and their ligands.

| Receptor | Ligand |
|---|---|
| EGFR (erbB-1/HER1) | EGF TGF- α Amphiregulin Epiregulin Heparin-binding EGF Betacellulin Neuregulin 2- α |
| HER2 (erbB-2, c-neu) | Unknown |
| HER3 (erbB-3) | Neuregulin (NRG1*, NRG2) |
| HER4 (erbB-4) | Neuregulin (NRG1-4) Betacellulin |
| *Neuregulin-1 (also called heregulin, Neu differentiation factor) | |

After ligand binding to epidermal growth factor receptor (EGFR), the receptor undergoes dimerization, which may comprise dimerization either between two molecules of the same receptor (homodimerization) or between different members of the human EGF-related receptor (HER) tyrosine kinase family (heterodimerization) (Alroy and Yarden, 1997)

Dimerization is followed by autophosphorylation of tyrosine residues. These phosphorylated residues act as binding sites for the recruitment of adaptor proteins and additional tyrosine kinase substrates. Protein interactions within the activated receptor complex stimulate ras proteins, leading to a cascade of phosphorylation events and activation of mitogen-activated protein (MAP) kinases (Wells, 1999). Alternatively, the signal transducers and activators of transcription (STATS), phosphatidylinositol-3 kinase (PI3K)-Akt, and stress activated protein kinase (SAPK) signaling pathways can be activated (Yarden and Sliwkowski, 2001). These signaling pathways, in turn, trigger gene transcription and pathways controlling cellular proliferation, differentiation and survival are activated (Klapper et al., 2000; Moghal and Sternberg, 1999).

The specificity and potency of the EGFR-mediated signaling pathways depends both on the nature of the activating proteins and the levels of the four EGFR family receptors (Crovello et al., 1998).

HER2 binds to no known ligand but preferentially dimerizes with ligand-activated EGFR when the receptors are co-expressed. The resulting heterodimers have an increased rate of recycling, stability and signaling potency versus EGFR homodimers (Graus-Porta et al., 1997). EGFR also dimerizes with HER3 and HER4, which leads to the enhanced duration and potency of P13K activation.

Endocytosis and degradation of the EGF-receptor complex

The signal is terminated once ligand-bound EGFR is endocytosed and either degraded or recycled to the plasma membrane, depending on the ligand bound (Klapper et al., 2000). For example, bound EGF signals the receptor for degradation, while bound TGF- α results in receptor recycling. Thus, different growth factors affect the magnitude and duration of EGFR signaling.

EGFR signaling pathways have multiple biologic roles. For example, the ras-MAPK signal transduction pathway stimulates cell division and cell migration (Wells, 1999). EGFR is also a critical mediator of multiple receptor pathways, acting as a convergence point for signal integration and diversification (Hackel et al., 1999; Prenzel et al., 2000). For example, transactivation can induce EGFR tyrosine kinase phosphorylation and subsequent signal transduction in response to stress, membrane depolymerization and several non-physiologic stimuli, including oxidants, radiation and alkylating agents.

The major pathway leading to inactivation of signals emanating from ligand-activated growth factor receptors is an endocytic process that sorts active receptors to degradation in lysosomes. For ErbB1, this process is robustly regulated by E3 ubiquitin ligase, called c-Cbl, which binds a specific phosphotyrosine of ErbB1, thereby enhancing receptor ubiquitination and subsequent sorting to endocytosis and degradation (Waterman et al., 1999). However, ligand-induced endocytosis of other ErbBs is slow, because these receptors are weakly coupled to c-Cbl (Levkowitz et al., 1996). Members of the EGFR family of receptors are crucial for normal development, but are often overexpressed and dysregulated in human tumors.

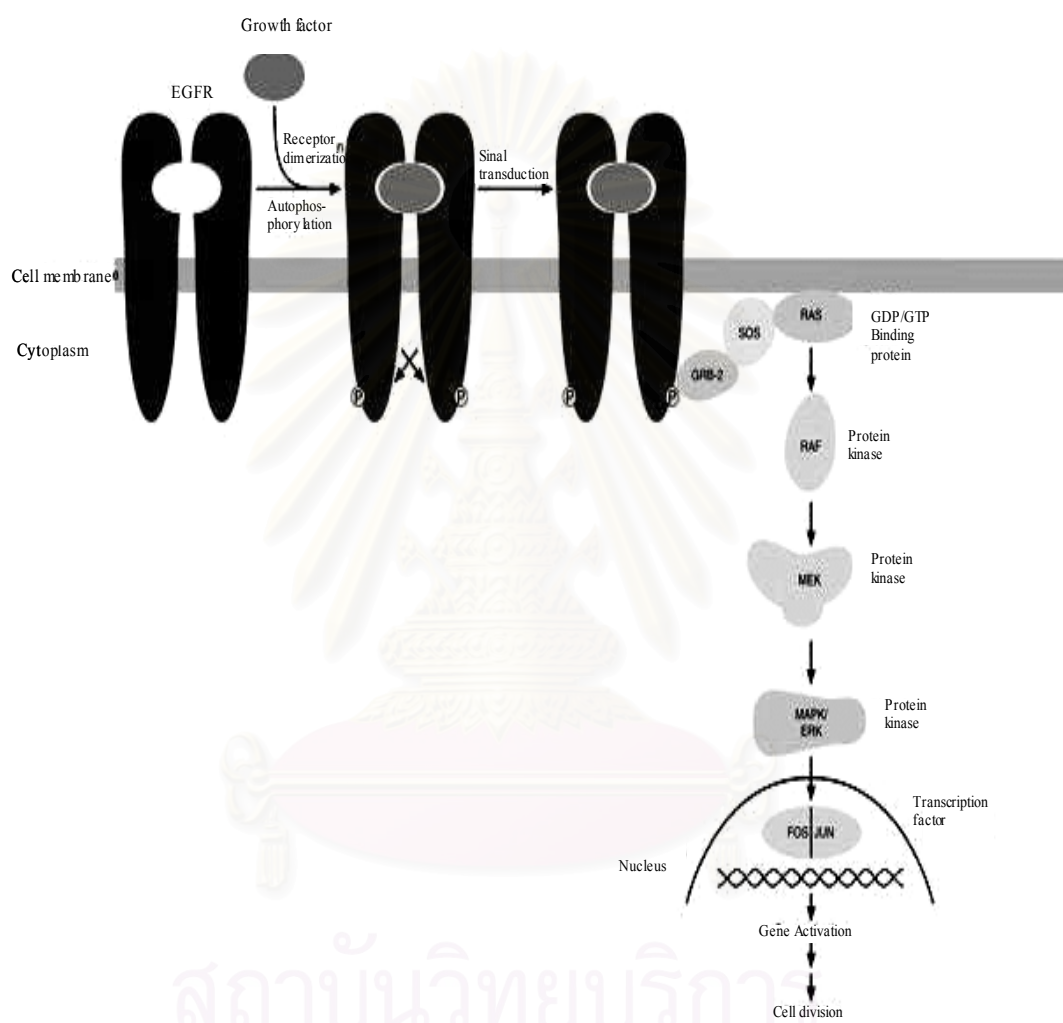


Figure 6. EGFR signal transduction pathway.

EGFR transactivation

RTK tyrosine phosphorylation and signaling can be activated in the absence of physiological ligands. In addition to its function as a receptor for its own ligands, The EGFR is used by different signaling pathways as signal transducer for the activation of downstream targets. Lysophosphatidic acid (LPA), endothelin, carbachol, angiotensin and bradykinin stimulation of G-protein coupled receptors, as well as membrane depolarization-induced Ca^{2+} influx through voltage-gated Ca^{2+} channels (VGCC) induce tyrosine phosphorylation of the EGFR, which is an essential step in the activation of the Ras/MAPK pathway. Besides this mitogenic signaling, carbachol stimulation modulates the activity of a K^+ channel in HEK293 cells or inhibits the Cl^- secretion in T84 cells. LPA activates Rho and induces stressfiber formation via the EGFR. Integrin signaling-mediated EGFR transactivation was shown to be necessary for cell survival. Tyrosine phosphorylation of the EGFR, upon activation of cytokine receptor, does not require the intrinsic EGFR kinase activity but depends on tyrosine phosphorylation of JAK2 (Zwick et al., 1999).

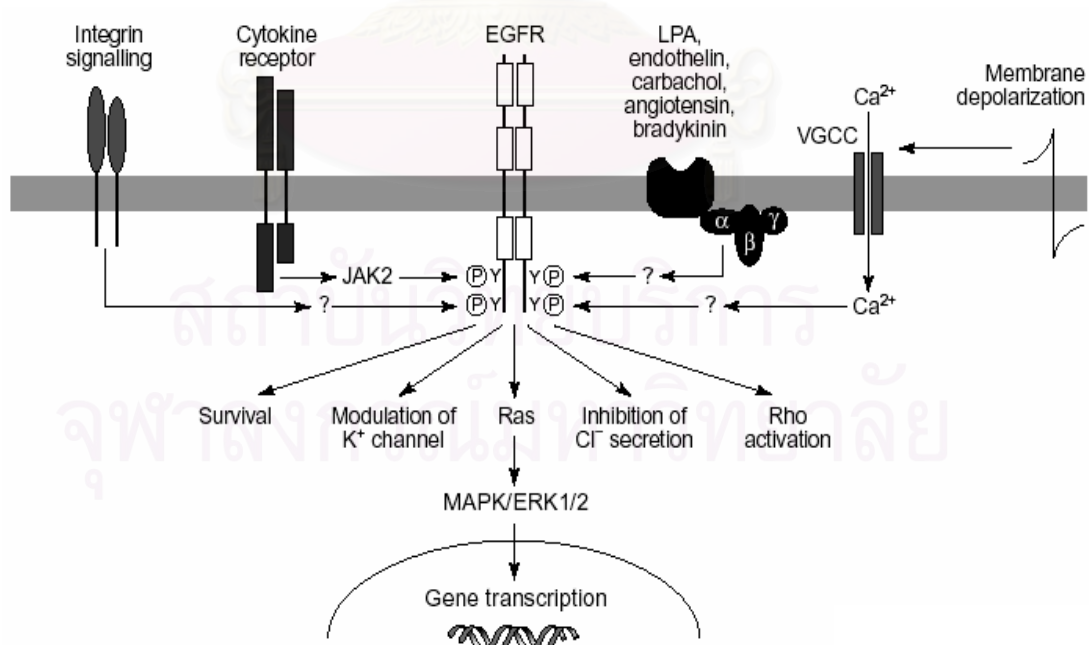


Figure 7. Model of EGFR transactivation.

Nonreceptor Protein-Tyrosine Kinases

Nonreceptor protein-tyrosine kinases are soluble intracellular protein-tyrosine kinases which are non-covalently associated with receptors. They are intermediate conductors of diverse intracellular signal pathways. Many of them are associated with transmembrane receptors, such as hormone receptors, cytokine receptors, and growth factor receptors. There are various classes of nonreceptor protein-tyrosine kinases grouped according to their structural and functional properties with the Src protein as a typical representative of them. In recent years, a considerable body of evidence has been obtained and indicates roles of nonreceptor protein-tyrosine kinases in different cellular processes, such as cell migration, activation of MAPK cascades, induction of DNA synthesis, regulation of the G₂/M transition, and prevention of apoptosis (McCubrey et al., 1993; Frisch and Francis, 1994; Altun-Gultekin and Wagner, 1996; Taylor and Shalloway, 1996; Broome and Hunter, 1997; Klemke et al., 1997; Schlaepfer, Broome, and Hunter, 1997). The nonreceptor protein-tyrosine kinase Src has been now also implicated in the signal switching from G protein-coupled receptor to the MAPK pathway (Fan et al., 2001).

The nonreceptor protein-tyrosine kinases are activated by means of association of receptors with extracellular ligands or cell adhesion components at particular phases of the cell cycle (Wilks, 1993; Shawver, Strawn, and Ullrich, 1995; Taniguchi, 1995). They are mostly required for signaling from cytokine receptors (e.g. interleukin-2 and interleukin-6) and from some polypeptide hormone receptors (e.g. growth hormone).

Mitogen-Activated Protein Kinase (MAPK) Pathways

The MAPK pathways refers to cascades of protein kinases that are highly conserved in evolution and play central roles in signal transduction in all eukaryotic cells, ranging from yeasts to humans. Recently, identified MAPK family members include extracellular signal-regulated kinase (ERK), c-JUN NH₂-terminal protein kinase or stress-activated protein kinase (JNK/SAPK), and p38 MAPK. The central elements in the pathways are a family of protein-serine/threonine kinases that are activated in response to a variety of growth factors and other signaling molecules

(Figure 15). In yeasts, MAPK pathways control a variety of cellular responses, including mating, cell shape, and sporulation. In higher eukaryotes (including *C. elegans*, *Drosophila*, frogs, and mammals), the MAPK pathways are important for the control of cell growth, differentiation, and cell death (Cooper, 2000). The dynamic balance between and the integration of these pathways are important in determining whether a cell survives or undergoes apoptosis (Xia et al., 1995; Chen, Woodruff, and Mayo, 2000).

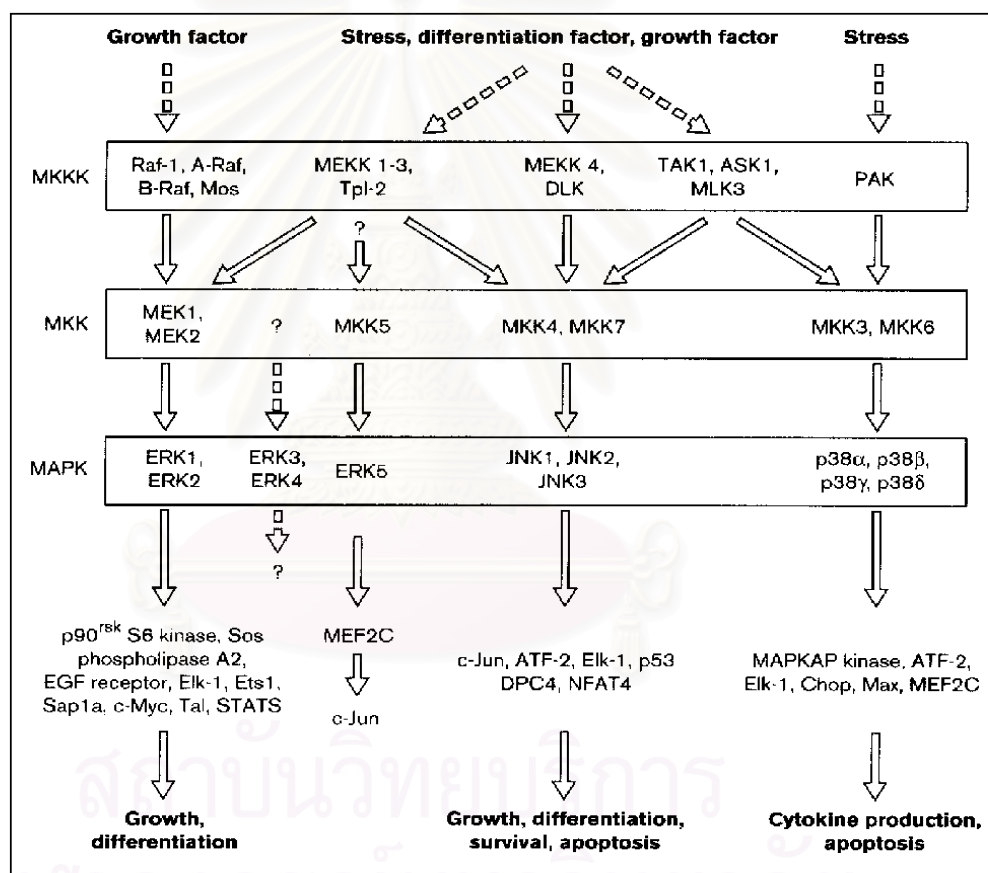


Figure 8. Mitogen activated protein kinase module. The MAPK module consists of MKKKs, MKKs and MAPKs. MKKKs respond to a variety of extracellular signals, including growth factors, differentiation factors and stress responses (Garrington and Johnson, 1999).

Regulation of the Cell Division Cycle and Cell Death

The fundamental processes performed by any single cell are carefully regulated by purely intracellular mechanisms. The total activities of every individual cell in the body fall into two categories: 1) Each cell performs for itself all those fundamental basic cellular processes—movement of materials across its membrane extraction of energy, protein synthesis, and so on—that represent the minimal requirements for maintaining its individual integrity and life; and 2) each cell simultaneously performs one or more specialized activities that, in concert with the activities performed by the other cells of its tissue or organ system, contribute to the survival of the organism by helping maintain the stable internal environment (the extracellular fluid surrounding each cell) required by all cells. A multicellular organism can survive only as long as it is able to maintain the composition of its internal environment in a state compatible with the survival of its individual cell. It is from this fluid that the cells receive oxygen and nutrients and into which they excrete wastes (Vander et al., 1994).

The concept that the composition of the internal environment is maintained relatively constant is known as *homeostasis*. Changes do occur but the magnitudes of these changes are small and are kept within narrow limits. The activities of the cells, tissues, and organs must be regulated and integrated with each other in such a way that any change in the extracellular fluid initiates a reaction to minimize the change. A collection of body components that functions to maintain a physical or chemical property of the internal environment relatively constant is termed a *homeostatic control system* (Vander et al., 1994).

Cell division and cell death are processes controlled by intracellular mechanisms. The consequence of a loss of proliferation control in a cell is cancer, whereas a low cell proliferation may contribute significantly to degenerative diseases. Therefore, in an organism made up of multiple cell types and tissues, it is most important that cell proliferation is tightly regulated (Normal and Lodwick, 1999).

Cell Cycle

Cell division is important for growth, development, repair and replacement of dead cells. The balance of cell proliferation and cell death determines the life cycle of the cell (Normal and Lodwick, 1999).

Phases of the Cell Cycle

The process of cell division is cyclical and unidirectional. The cell cycle can be divided into two major phases: *interphase* and *M (mitosis) phase*. Cells spend the majority of time in interphase, only a small percentage of cells are observed to be in the M phase. Whereas M phase usually lasts only 30 to 60 minutes, interphase may extend for hours, days, weeks, or longer, depending on the cell type and the conditions. The variation in cell cycle length primarily arises from the length of the G₀/G₁ phase¹. Interphase is divided into G₁ (and G₀), S, and G₂ phases; while M phase includes the process of mitosis and cytokinesis (Karp, 1999). (See Figure 9)

G₁ (Gap 1) phase is characterized by gene expression and protein synthesis. This is the only part of the cell cycle regulated primarily by extracellular stimuli (e.g. mitogens and hormones). This phase enables the cell to grow and to produce all the necessary proteins for DNA synthesis. This phase of the cell cycle is the most variable in duration (minutes to months). In non-dividing tissues, cells withdraw from the cell cycle into a **resting state (G₀)**, but can re-enter G₁ upon stimulation.

S (Synthesis) phase, the cell replicates its DNA and has two complete sets of DNA. This allows the cell to divide into two daughter cells, each with a complete copy of DNA.

G₂ (Gap 2) phase, the cell undergoes growth and protein synthesis. The cell needs enough proteins synthesized for two cells.

M (Mitosis) phase is a continuous dynamic process, where *mitosis*, the division of nuclear material, and *cytokinesis*, the process of cytoplasmic division, occur. The result of mitotic cell division is the production of two daughter cells that contain a complete copy of the genomic DNA of the parent cell and the cell cycle has been completed (Normal and Lodwick, 1999).

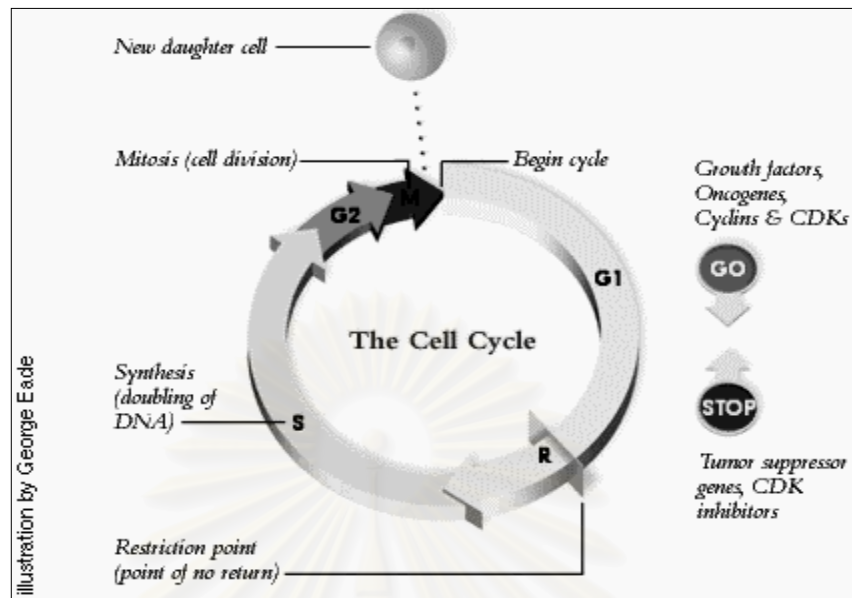


Figure 9. Cell division cycle. This diagram of the cell cycle indicates the phases through which a cell passes from one division to the next. The cell cycle can be divided into two phases: interphase and M phase.

Cells at different stages of the cell cycle can be distinguished by their DNA content (Figure 10).

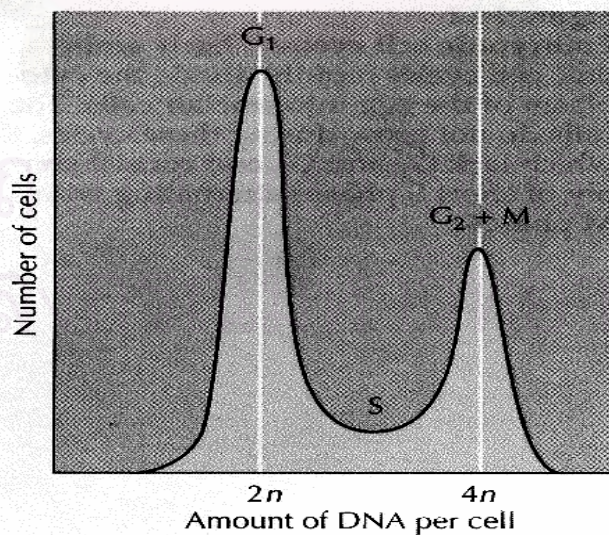


Figure 10. Determination of cellular DNA content.

A population of cells is labeled with a fluorescent dye that binds DNA. The cells are then passed through a flow cytometer, which measures the fluorescence intensity of individual cell number versus fluorescence intensity, which is proportional to DNA content. The distribution shows two peaks, corresponding to cell with DNA contents of $2n$ and $4n$; these cells are in the G1 and G2/M phases of the cycle, respectively. Cell in S phase have DNA contents between $2n$ and $4n$ and are distributed between these two peaks. (Copper, 2000).

G₀ to G₁ Transition (Mitogenesis)

Proliferation of quiescent cells (G₀) can be induced by mitogens in a cell-type-specific manner. Mitogens include growth factors, hormones and cell contact. Signaling pathways activated by mitogens lead to protein expression (includes some cyclins), the expression of responsive genes (e.g. by *myc*, *fos*, *jun* genes), and the progression of the cell through G₁ and past a ‘or check point or restriction point’, where the cell becomes committed to a complete division cycle. Once past the check point, cells no longer require the presence of growth factors and are unresponsive to anti-mitogenic signals (Normal and Lodwick, 1999).

Regulation of the Cell Cycle

Progression through the cell cycle is controlled at three ‘checkpoints’ between the stages of the cycle: restriction point, mitosis entry and mitosis exit. Checkpoints are specialized intracellular signaling pathways that are triggered by defects and malfunctions such as DNA damage. The activation of a checkpoint normally leads to one of the following two phenomenons. The first is cell cycle arrest, which is accompanied by the activation of the DNA repair machinery. The second outcome is a programmed active cell death, also called “apoptosis”, which will be discussed latter.

Checkpoints

In most Eukaryotic cells, there are 3 checkpoints called the G1 checkpoint, the G2 checkpoint and the M-phase checkpoint. Each checkpoint is explicitly triggered by specific types of abnormalities. The G1 and G2 checkpoints

specifically react to DNA damage whereas the M checkpoint is found to react to microtubule and kinetochore damage. The checkpoint pathways and proteins that carry out the responses mainly consist of:

- sensor proteins that detect the abnormality,
- signaling proteins that transduce the signal and
- target proteins that are altered to arrest cell division or cause apoptosis.

There are a number of proteins that regulate and control the cell cycle. These proteins are: 1) cyclins and cyclin-dependent protein kinases (CDKs); 2) CDK inhibitors; and 3) tumor suppressor gene products.

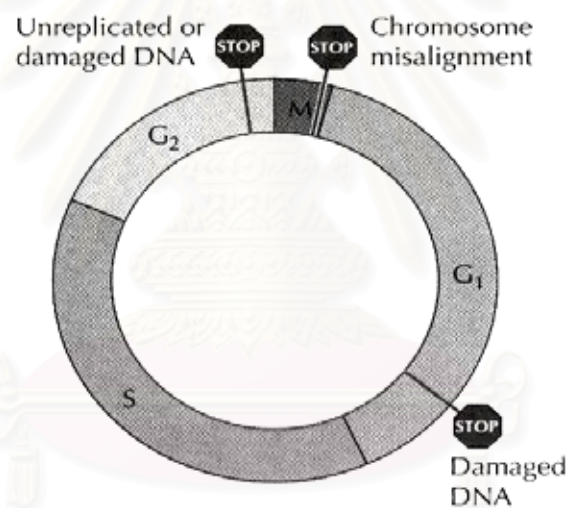


Figure 11. Cell cycle check points. Several checkpoints function to ensure that complete genomes are transmitted to daughter cells: G₁, G₂ and M-phase checkpoint (cooper, 2000).

1) Cyclins and cyclin-dependent protein kinases

Cyclin/CDK (Cyclin-dependent kinases) complexes phosphorylate specific substrates at appropriate phases in the cell cycle, driving the cellular events necessary for progress from one phase to the other. In humans, the active cyclins/CDK complexes in the different phases are shown in Figure 12.

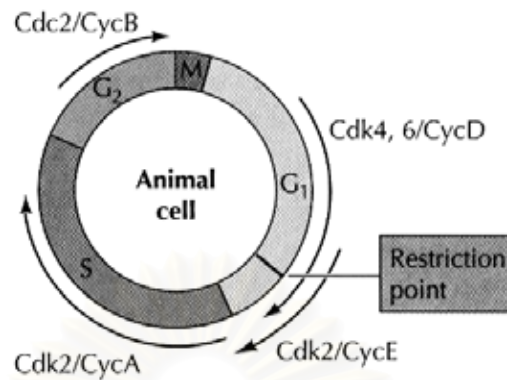


Figure 12. Complexes of cyclins and cyclin-dependent kinases. Combinations between various cyclins and cyclin-dependent kinases are used to control the cell cycle activities at different stages (Cooper, 2000).

Transition between stages is triggered by increased activity of specific CDKs. Levels of CDK proteins remain relatively constant throughout the cell cycle but their activity is regulated at different stages. CDKs are activated primarily by the binding of specific cyclins. The levels of the different cyclins rise and fall at different points in the cell cycle and produce temporal activation of their specific CDKs (figure 12). Each CDK is presumed to phosphorylate and modulate the activity of a subset of cellular target proteins specific for progression through individual transitions within the cell cycle (Normal and Lodwick, 1999).

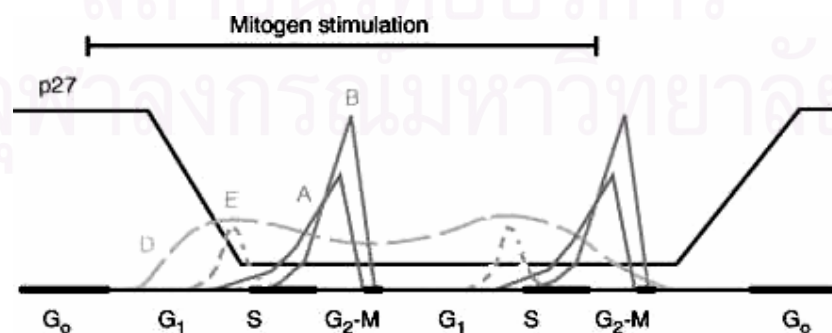


Figure 13. The cycling of the different cyclins. Cycling of the different cyclins depending on the phase of the cell cycle (Sherr, 1996).

Successive waves of synthesis and degradation of different cyclins probably play a key role in driving the cell from one stage to the next. The pairing between cyclins and CDKs is highly specific, and only certain combinations are found. For example, a complex formed between cyclin E and CDK2 is active at the G₁-S transition, whereas a complex between cyclin B and CDK1 is active at the G₂-M transition. Cell cycle activities during G₁ are accomplished primarily by CDKs associated with the D-type cyclins (D1, D2, and D3). Among the substrates for these CDKs are transcription factors that activate genes required for DNA replication. The G₁-S transition, which includes the initiation of replication, is driven by the activity of the cyclin E-CDK2 complex. The transition from G₂ to M is driven by the activity of cyclin A-CDK1 and cyclin B-CDK1 complexes, which are thought to phosphorylate such diverse substrates as cytoskeletal proteins, histones, and proteins of the nuclear envelope. Destruction of cyclin B is a key factor in the inactivation of CDK1 and the transition of the cell from mitosis back into G₁ (Karp, 1999). For example, the synthesis of cyclin B is relatively constant and concentrations rise in a linear manner until a threshold is reached when Cdc2 is activated and the cell proceeds into mitosis. At mitosis the rate of cyclin B breakdown is accelerated and the stimulation of Cdc2 is terminated. The levels of other cyclins, e.g. cyclin E, are more closely controlled at the level of expression and mRNA for these species is only present during limited phases of the cell cycle. For example, the S-phase CDK (CDK2/ cyclin D, E or A) may phosphorylate proteins involved in DNA replication, while mitosis-promoting factor (MPF) (Cdc2 (CDK1)/ cyclin B) may phosphorylate proteins during mitosis such as the nuclear lamins, histones and cytoskeletal proteins involved in chromosome condensation, assembly of the mitotic spindle, dissolution of the nuclear membrane and cell detachment (Normal and Lodwick, 1999).

CDKs are also subject to complex modulation in response to several intracellular signalling pathways. This serves to integrate intra- and extracellular signals reflecting nutritional status and intercellular communication. Whether or not a cell proceeds to the next stage of the cell cycle, therefore, depends on the integration of multiple factors at the level of the CDK (Normal and Lodwick, 1999).

The Cyclin/CDKs are regulated by phosphorylation. The CAK (CDK activating kinase) positively phosphorylates the Cyclin/CDK at its Thr160 residue

whereas, Wee1 and Myt1 kinases negatively phosphorylate the same at the Tyr14 and Thr 15 residues. The inhibitory phosphorylations are removed by Cdc25 phosphatase.

2) CDK inhibitors

In addition to regulation of the CDKs by phosphorylation, their activities can also be controlled by the binding of inhibitory proteins, called CDK inhibitors or CKIs, to cyclin/CDK complexes. In mammalian cells, two families of CKI are responsible for regulating different cyclin/CDK complexes: the INK4 family and the Cip/Kip family (Table 1). The INK4 family consists of p15^{INK4b}, p16^{INK4a}, p18^{INK4c}, and p19^{INK4d}. Basically, the INK4 family binds to and inhibits Cdk4/6 (INK4=Inhibitors of cdk4). By binding, it does not allow cyclin D to bind, and thus prevents the activation of Cdk4/6. Under conditions of stress or other times when a cell should not undergo the cell cycle, the INK4 CKIs are expressed and prevent Rb phosphorylation (see below).

The other family of CKIs consists of p21^{Waf1/Cip1}, p27^{Kip1}, and p57^{Kip2}. These CKIs (unlike the INK4 family) bind to and inhibit cyclin E-Cdk2 and cyclin A-Cdk2. By binding, these CKIs lead to the inhibition of Cdk activity and thus prevent ability to stimulate cell cycle progression. p21^{Waf1/Cip1}, and p27^{Kip1} have been demonstrated to also act as assembly factors for cyclin D-Cdk4/6 and act as a positive regulator of the complex. Roles of p21^{Waf1/Cip1} in cell cycle control and apoptosis will be discussed.

Table 3. Cdk Inhibitors

| Inhibitor | Cdk/cyclin complex | Cell cycle phase affected |
|---|--------------------|---------------------------|
| Cip/Kip family (p21 ^{Waf1/Cip1} , p27 ^{Kip1} , p57 ^{Kip2}) | Cdk4/cyclin D | G1 |
| | Cdk6/cyclin D | G1 |
| | Cdk2/cyclin E | G1/S |
| | Cdk2/cyclin A | S |
| Ink4 family (p15, p16, p18, p19) | Cdk4/cyclin D | G1 |
| | Cdk6/cyclin D | G1 |

The Cyclin-dependent Kinase Inhibitor p21^{Waf1/Cip1}

p21^{Waf1/Cip1} was identified as a mediator of p53-induced growth arrest, a direct regulator of CDK activity, and a gene whose expression is induced in concomitance with cellular senescence. p21^{Waf1/Cip1} belongs to the Cip/Kip family of CKIs (p21^{Waf1/Cip1}, p27^{Kip1}, p57^{Kip2}), which share significant sequence homology in their amino-terminal portions and recognize a broad range of cyclin/CDK targets. p21^{Waf1/Cip1} plays an essential role in growth arrest after DNA damage, and overexpression leads to G₁ and G₂ or S-phase arrest. p21^{Waf1/Cip1} expression has been shown to be regulated largely at the transcriptional level by both p53-dependent and -independent mechanisms. The p21^{Waf1/Cip1} promoter contains two conserved p53-binding sites, and at least one of these is required for p53 responsiveness after DNA damage.

The amino-terminal domain of p21^{Waf1/Cip1}, is necessary and sufficient to inhibit cyclin/CDK activity *in vitro* and *in vivo*. The unique carboxy-terminal domain of p21^{Waf1/Cip1} associates with the proliferating nuclear antigen (PCNA), a subunit of DNA polymerase, and can inhibit DNA replication directly, without affecting DNA repair. It has recently been reported that PCNA binding can be modulated by reversible phosphorylation of p21^{Waf1/Cip1} at its C-terminus. Besides associating with cyclin/CDKs and PCNA, p21^{Waf1/Cip1} has been found to participate in a number of other specific protein–protein interactions (Figure 14). Some of these interactions still bear on cell cycle control. Other interactions are related to a new emerging function for p21^{Waf1/Cip1}, as a modulator of apoptosis. Finally, p21^{Waf1/Cip1} has been found to associate with other, apparently unrelated proteins, which points to the possibility of yet other functions for this molecule. In most of the studies, data are presented and showed that targeted overexpression of p21^{Waf1/Cip1} increases apoptosis, or disruption of p21^{Waf1/Cip1} function lead to a decrease in apoptosis. The mechanisms by which p21^{Waf1/Cip1} promote apoptosis are not currently understood but could be related to its ability to interact with and possibly regulate components of the DNA repair machinery. p21^{Waf1/Cip1} expression may also be regulated posttranscriptionally by both ubiquitin-dependent and -independent proteasome-mediated degradation.

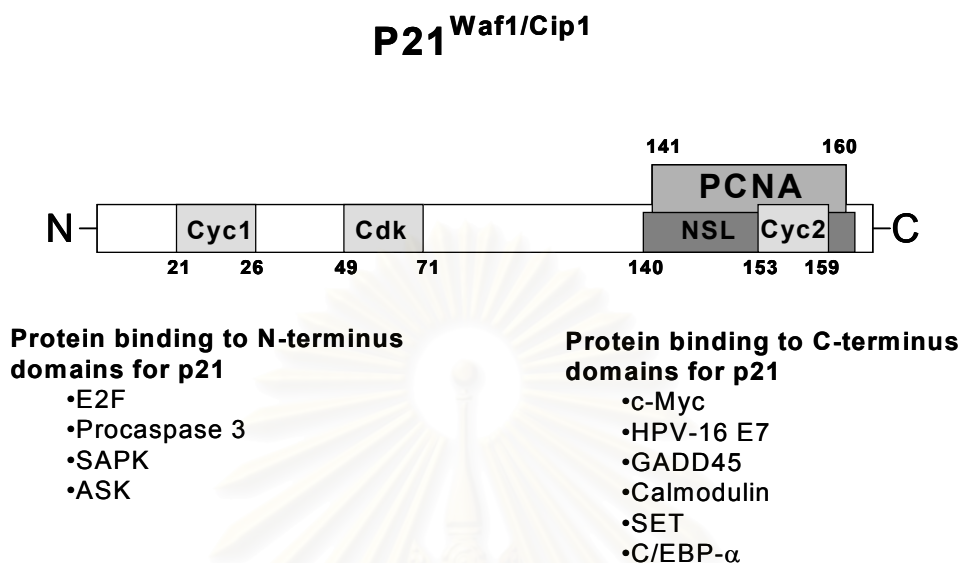


Figure 14. Map of p21^{Waf1/Cip1} and its direct protein-protein interactions (Dotto, 2000).

3) Tumor suppressor gene products

The tumor suppressor genes encode proteins which are normally involved in the regulation of normal cell division and differentiation. The important tumor suppressor gene products are:

p53: p53 is a 393 amino acid nuclear phosphoprotein whose gene lies on the short arm of chromosome 12 in humans and contains 11 exons. It can be divided into 3 domains: an N-terminal acidic trans-activating domain; a central evolutionarily conserved DNA binding domain and a complex C terminal domain that houses, among other things, a homotetramerization domain and a DNA damage recognition site (specifically single stranded DNA). p53 recognizes when there is an irreversibly damaged DNA in the cell and either arrests the cell cycle in G₁ (figure 12), or if all else fails, triggers cell removal by apoptosis (Normal and Lodwick, 1999).

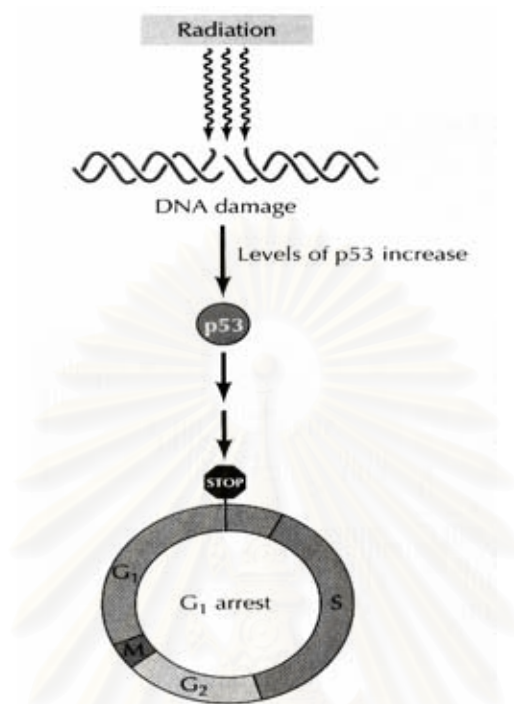


Figure 15. Role of p53 in G₁ arrest induced by DNA damage. DNA damage such as the resulting from irradiation, leads to rapid increases in p53 levels. The protein p53 then signals cell cycle arrest at the G₁ checkpoint (Cooper, 2000).

Activation of p53 following DNA damage is associated with accumulation of the normally short lived protein. This accumulation is not mediated at the transcriptional level. Rather, it is stabilized after DNA damage. This accumulation of p53 transactivates a number of different genes including Bax, GADD45, MDM2 and p21^{waf1/cip1}. These genes contain the consensus binding site PuPuPuC(A/T)(T/A)GPyPyPy in p53 promoter region.

Rb: Most of the substrates for CDKs remain unknown. However, one mechanism at the G₁-S checkpoint may involve the hyperphosphorylation of negative cell cycle regulators, such as the retinoblastoma tumour suppressor gene product (pRb), to overcome their suppression of passage from G₁. In normal quiescent cells

and early G₁, pRb is found in a hypophosphorylated form, which actively binds several cytoplasmic proteins, including transcription factors of the E2F family, which go on to activate transcription of the S-phase genes. Therefore, in G₁, pRb appears to act as a cell cycle suppressor by binding members of the E2F transcription factor family. pRb is absent or inactive in retinoblastoma and several other tumours suggesting that, in its absence, passage through the G₁-S checkpoint goes unchecked (Normal and Lodwick, 1999).

Cell Cycle Arrest

The cell cycle may be arrested at two points (G₁-S and G₂-M) as a result of DNA damage. Mechanisms of cell cycle arrest are not well characterized but appear often to involve inhibition of CDKs as part of their action. The tumor suppressor gene product p53 is also reported important in arresting the cell cycle at G₁ phase. The expression of p53 is normally low but it is increased dramatically when cell DNA is damaged, therefore, it may stimulate DNA repair indirectly. This leads to the suggestion that p53 is a 'guardian of the genome' (Normal and Lodwick, 1999).

Cell Death

As the cell encounters physiologic stresses or pathologic stimuli, it can undergo adaptation, achieving a new steady state and preserving viability. If the adaptive capability of a cell is exceeded, cell injury develops. Up to a point, cell injury is reversible; however, with severe or persistent stress, the cell suffers irreversible injury and ultimately dies.

Cell death can be morphologically and biochemically distinguished and divided into two forms: necrosis and apoptosis. (See Figure 17 and table 3)

1. Necrosis or accidental cell death occurs after severe and sudden injury. It is characterized by the swelling of organelles and a breakdown of the integrity of the plasma membrane, which results in the leakage of cellular contents and an inflammatory response (Normal and Lodwick, 1999).

2. Apoptosis or programmed cell death is a normal physiological form of cell death. It is responsible for balancing cell proliferation (by mitosis) and maintaining constant cell numbers in tissues undergoing cell turn over. In addition, programmed cell death provides a defence mechanism by which damaged and potential dangerous cells can be eliminated for the good of the whole organism (figure 16) (Cooper, 2000).



Figure 16. Balance between cell growth and cell death.

Apoptosis occurs in response to physiological triggers in development (tissue remodelling), defence, homeostasis and ageing. Apoptotic cells initially shrink and lose microvilli and cell junctions. Organelles maintain their structure but the plasma membrane becomes highly convoluted and the cell breaks down into small apoptotic bodies (membrane-enclosed vesicles), which are quickly phagocytosed by macrophages. This occurs without leakage of cellular constituents and, hence, without an inflammatory response. Characteristics of apoptotic cells include DNA fragmentation, chromatin condensation, membrane blebbing, cell shrinkage, and disassembly into apoptotic bodies. *In vivo*, as mentioned above, this process culminates with the engulfment of apoptotic bodies by other cells, preventing complications that would result from a release of intracellular contents. These changes can be completed within 30 to 60 minutes (Thornberry and Lazebnik, 1998; Normal and Lodwick, 1999).

Apoptosis is a major form of cell death that is used to remove excess, damaged or infected cells throughout life. It is important in normal cell turnover, the

immune system, embryonic development, metamorphosis and hormone dependent atrophy, and also in chemical-induced cell death (Arends and Wyllie 1991; Ellis et al., 1991; Cohen et al., 1992). Apoptosis is important in eliminating cells containing damaged DNA that may contribute to the initial development of cancer and in suppressing the neoplastic signals in others. Failure of apoptosis in these situations could contribute to cancers. Moreover, failure to deplete self-reactive T cells by apoptosis may be important in the development of autoimmune disease (Normal and Lodwick, 1999; Bratton and Cohen, 2001).

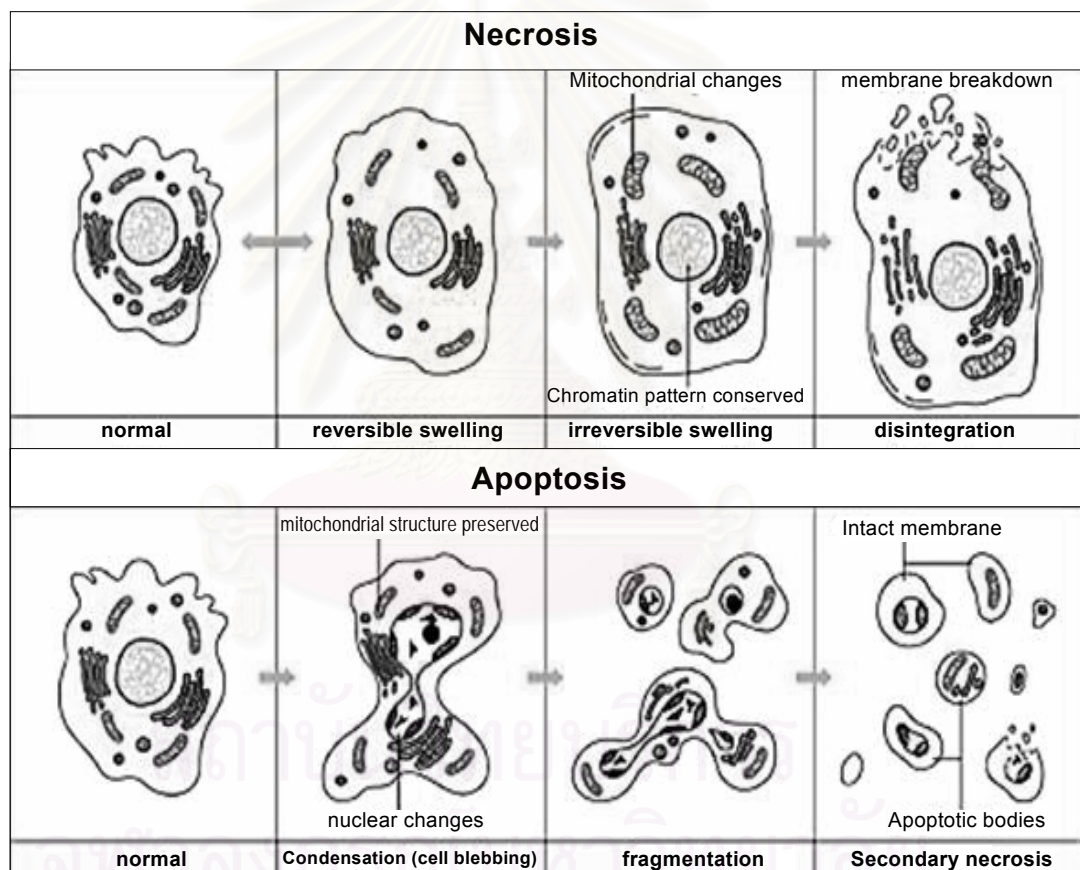


Figure 17. Cell death. The sequential ultrastructural changes seen are different between necrosis and apoptosis. Signs of necrosis include chromatin clumping, organellar swelling, and eventual membrane damage. In apoptosis, the initial changes consist of nuclear chromatin condensation and

fragmentation, followed by cytoplasmic budding and phagocytosis of the extruded apoptotic bodies (Kumar et al., 1997).

Table 3. Apoptosis versus Necrosis Characteristics

| Apoptosis | Necrosis |
|---|---|
| Internal / external signals e.g. <ul style="list-style-type: none"> • Lack of growth factors • Hormonal influences • Mild toxic influences | <ul style="list-style-type: none"> • Ischemia • Physical damage • Chemical damage • Radiation |
| Energy dependent | Not dependent on energy |
| Changes in gene expression, Protein synthesis | - |
| Single cells | Groups of cells |
| The cell shrinks and is engulfed by macrophages or neighboring cells | The cells swell and release their content into the surroundings and the circulation |
| Cell surface protrusion, budding | Cell membrane: smoothing, lysis |
| - | Organelles swelling |
| Nuclear condensation, DNA fragmentation | - |
| No inflammatory reaction | Marked inflammatory reaction |

Possible Mechanisms of Programmed Cell Death

Mechanisms of programmed cell death or apoptosis in cells remain to be elucidated but are clearly very varied. Signals for apoptosis in one cell type can induce cell proliferation and differentiation in other cell types. It is found that raised intracellular calcium concentrations ($[Ca^{2+}]_i$) and increased synthesis of tumour suppressor proteins (e.g. p53), are commonly but not universally implicated in

apoptosis. Whether implicated gene products induce cell proliferation or apoptosis probably depends on their associations with other proteins and reflects the complexity and fine balance of the regulation of the cell cycle.

Apoptotic cell death occurs in two phases: first a commitment to cell death, followed by an execution phase characterized by dramatic stereotypic morphological changes in cell structure (Kamens et al., 1995), suggesting the presence in different cells of a common execution machinery (Jacobson, Burne, and Raff, 1994). Apoptosis, as mentioned above, is characterized by condensation and fragmentation of nuclear chromatin, compaction of cytoplasmic organelles, dilatation of the endoplasmic reticulum (frequently in a subplasmalemmal distribution), a decrease in cell volume and alterations to the plasma membrane resulting in the recognition and phagocytosis of apoptotic cells, so preventing an inflammatory response (Arends and Wyllie, 1991). The nuclear alterations, which are the pre-eminent ultrastructural changes of apoptosis, are often associated with internucleosomal cleavage of DNA (Wyllie, 1980), recognized as a 'DNA ladder' on conventional agarose gel electrophoresis and long considered as a biochemical hallmark of apoptosis (Brown, Sun, and Cohen, 1993; Oberhammer et al., 1993; Cohen et al., 1994). Internucleosomal cleavage of DNA now appears to be a relatively late event in the apoptotic process. Nevertheless, its measurement is simple and it is often used as a major criterion to determine whether a cell is apoptotic (Cohen et al., 1992b; Tomei, Shapiro, and Cope, 1993).

Apoptosis is process requires specialized machinery. The central component of this machinery is a proteolytic system involving an activation of a family of proteases called caspases. These enzymes participate in a cascade that is triggered in response to proapoptotic signals and culminates in cleavage of a set of proteins, resulting in disassembly of the cell (Normal and Lodwick, 1999; Bratton and Cohen, 2001).

Caspases

Caspases are intracellular cysteine proteases, which are highly conserved in mammals, the worm *Caenorhabditis elegans*, and the fly *Drosophila melanogaster*. They are primarily responsible for the stereotypic morphological and biochemical changes that are associated with apoptosis. Exposure of cells to chemicals and

radiation, as well as loss of trophic stimuli, perturb cellular homeostasis and signal the cell to undergo apoptosis by stimulating the formation of unique and/ or common caspase-activating complexes (Bratton and Cohen, 2001).

Caspases participate in apoptosis of the cell by cutting off contacts with surrounding cells, reorganizing the cytoskeleton, destroying DNA, disrupting the nuclear structure, inducing the cell to display signals that mark it for phagocytosis, and disintegrating the cell into apoptotic bodies (Thornberry and Lazebnik, 1998).

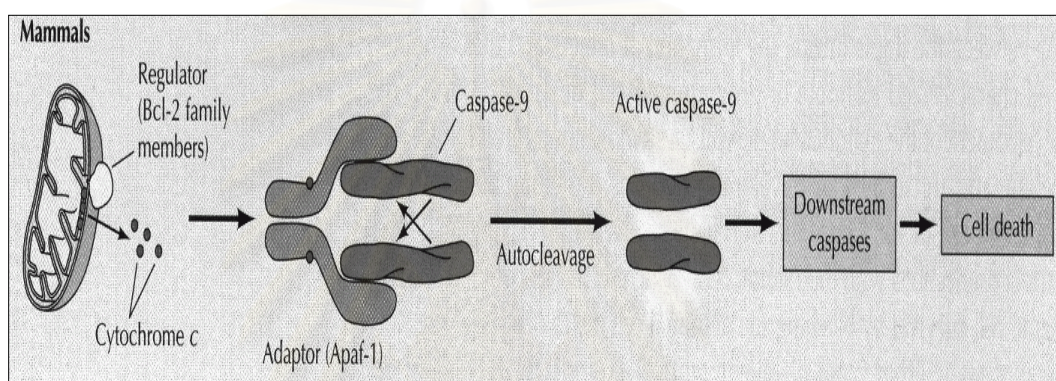


Figure 18. Caspase activation and apoptosis. Mitochondrial is linked with the action of the caspases and the Bcl-2 family; apoptosis-protein inducing factor-1 (Apaf-1); and cytochrome *c* (Cooper, 2000).

Bcl-2 (Schendel et al., 1997)

Bcl-2 proteins are one of apoptosis-regulating proteins. These proteins appear to block a distal step in a common pathway for apoptosis and programmed cell death, with some functioning as suppressors (Bcl-2, Bcl-XL, Mcl-1, Ced-9, BHRF-1, E1b-19 kDa, A1, ASFV-5HL, Bcl-W, and NR13) and others as promoters (Bax, Bcl-XS, Bak, Bad, Bik, and Bid) of cell death. In many cases, these proteins can interact with each other in a complex network of homodimers and heterodimers. Aberrant expression of Bcl-2 and some of its homolog has been described in association with several disease states characterized by either excessive accumulation of cells or inappropriate cell death, including cancer, autoimmunity, ischemic diseases (stroke, myocardial infarction), HIV-associated immunodeficiency, and some neurodegenerative diseases.

p53 and apoptosis (Bratton and Cohen, 2001)

As previously mentioned, DNA damage, induced by irradiation, drugs or environmental toxicants, frequently induces cell death by apoptosis. However, cells have mechanisms involved with initial recognition and assessment of the damage, followed by an appropriate response that involves either DNA repair or cell death. The nuclear protein p53 is one of key sensors of DNA damage. It integrates numerous signals that are crucial to the control of life and death of the cell. The p53 is activated, in part, by various signals that induce its dissociation from its inhibitor. Once activated, p53 binds to specific sequences in DNA and initiates the transcription of many genes involved in genetic stability, cell-cycle inhibition, and apoptosis. For instance, p53 induces or maintains growth arrest through increased expression of cell-cycle regulators, such as p21^{Waf1/Cip1}, an inhibitor of CDKs.

A recent study suggests that p53 relocalizes to mitochondria during p53-dependent apoptosis, preceding changes in mitochondrial membrane potential and cytochrome *c* release. Therefore, the possibility exists that p53 might also induce apoptosis through transcriptionally independent mechanisms.

Oxidative Stress

Oxidative stress is a general term used to describe a state of damage caused by reactive oxygen specie (ROS). This damage can affect a specific molecule or the entire organism. The ROSs, such as free radicals and peroxides, represent a class of molecules that are derived from the metabolism of oxygen and exist in all aerobic organisms. There are many different sources of ROSs that can cause oxidative damage to an organism. Most ROSs come from endogenous sources as by-products of normal and essential reactions, such as energy generation from mitochondria or the detoxification reactions involving the liver cytochrome P-450 system. Exogenous sources include bacterial, fungal or viral infections (figure 12).

However, biologic systems have defensive mechanisms to either block free radical formation or scavenge them once they have formed as shown in figure 13 (Kumar et al., 1997).

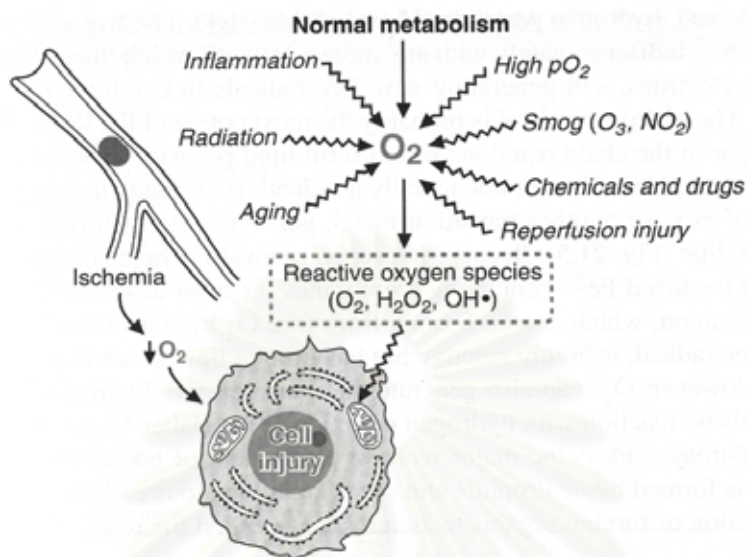


Figure 19. Role of oxygen in cell injury (Marks et al., 1996)

ROS levels can be modulated by changes in endogenous cytochrome P450s or exogenously following the administration of drugs, hormones, xenobiotics and toxicants (figure 13,14). Oxidative damage can induce apoptosis following an increase in ROS (Buttke and Sandstrom, 1994, Suzuki *et al.*, 1997).

From Figure 12 and 13, oxygen (O_2) is converted to superoxide (O_2^-) by oxidative enzymes in the endoplasmic reticulum (ER), mitochondria, plasma membrane, peroxisomes, and cytosol. O_2^- is converted to H_2O_2 by superoxide dismutase (SOD) and then to OH^\bullet by the Cu^{2+}/Fe^{2+} catalyzed Fenton reaction. H_2O_2 is also derived directly from oxidases in peroxisomes. The resultant free radicals can damage lipid (peroxidation), proteins, and DNA. Note that O_2^- catalyzes the reduction of Fe^{3+} to Fe^{2+} , thus enhancing OH^\bullet generation by the Fenton reaction. The major antioxidant enzymes are SOD, catalase, and glutathione peroxidase.

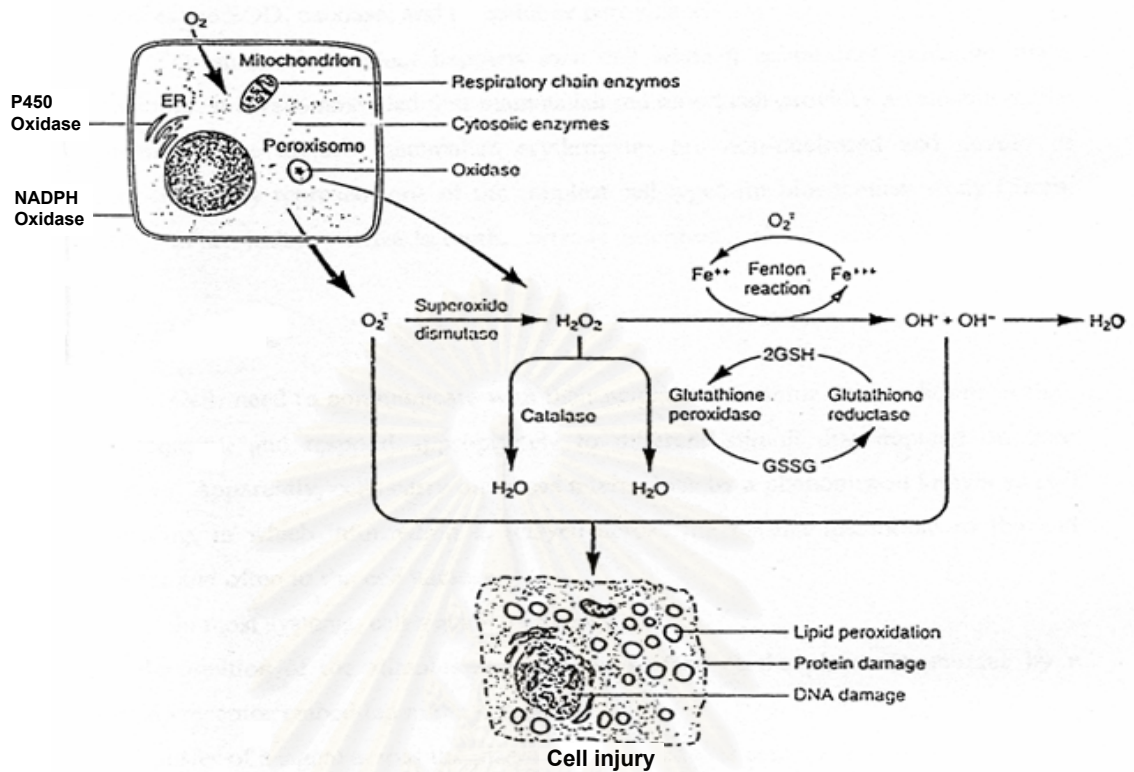


Figure 20 Formation of ROSs and antioxidant mechanisms in biologic systems. GSH, reduced glutathione; GSSG, oxidized glutathione; NADPH, reduced form of nicotinamide-adenine dinucleotide phosphate.

Oxidative stress and apoptosis

Oxidative stress is known to be a key regulator in chemical-induced apoptosis. It also causes DNA damage which may lead to the development of a number of disease states including cancer, diabetes, atherosclerosis and Alzheimer disease (Breimer and Schellens, 1990). Although there is considerable evidence to implicate oxidative damage in the regulation of apoptosis, little is known of its mode of action. Cells and tissues are subjected to oxidative stress when the concentration of reactive oxygen species (ROS) exceeds the antioxidant capability of the cell (figure 14). This occurs following either an increase in free radicals or peroxides such as H_2O_2 , or a decrease in antioxidant levels in the cell.

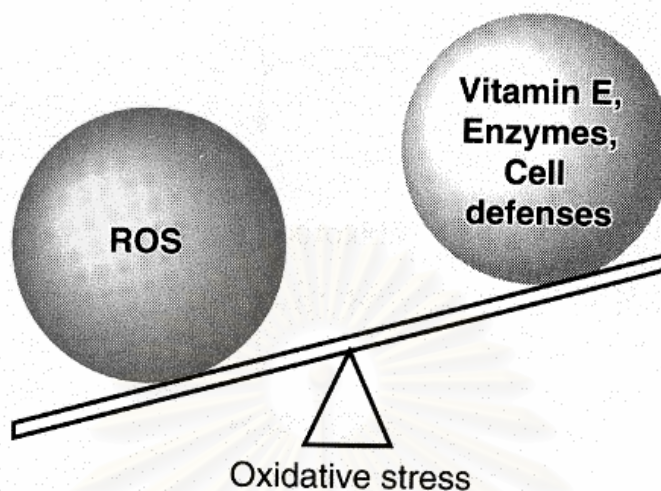


Figure 21. Oxidative stress. Oxidative stress occurs when ROS are produced faster than they can be removed by the cellular defense mechanisms. (Marks et al.,1996).

The molecular pathways that regulate apoptosis provide a possible target for oxidative stress, suggesting a role for transcriptional regulation of genes implicated in cell survival. One such group of genes are members of the family of mitogen activated protein kinases (MAPKs) which play a pivotal role in regulating changes in cell survival and proliferation. This family includes the extracellular signal-regulated protein kinases (ERKs) and the c-jun N-terminal kinase/stress-activated protein kinase (JNK/SAPK). Evidence shows that oxidative damage can activate and suppress the MAPKs since H_2O_2 - induced apoptosis of HeLa cells is preceded by the inhibition of ERK and the activation of JNK/SAPK (Wang *et al.*, 1998). However, in cultured mouse keratinocytes, ERKs can be induced by treatment with H_2O_2 and butylated hydroxytoluene hydroperoxide indicating that cell type is an important factor in determining which signaling pathways are modulated (Guyton *et al.*, 1996a,b). ERK activation also has an important role in protecting cardiac myocytes from apoptotic death following oxidative damage (Aikawa *et al.*, 1997). It is thought that the

dynamic balance between the ERKs and JNK/SAPK pathways is important in determining whether a cell survives or undergoes apoptosis (Xia *et al.*, 1995).

A number of other signaling proteins are involved in ROS-induced apoptosis. The anti-apoptotic protein Bcl-2 is normally downregulated by oxidative damage and its activation can protect cells against apoptosis following treatment with H₂O₂ (Wang *et al.*, 1998). The pro-apoptotic genes p53 and p21^{Waf1/cip1} accumulate during ROS-induced apoptosis in human fibroblast cells (Gansauge *et al.*, 1997). More recently the protein p85, a regulator of the signaling protein phosphatidylinositol-3-OH kinase (PI3 kinase), has been shown to participate in p53-mediated apoptosis following oxidative damage (Yin *et al.*, 1998). The transcription factor NF-κB, which has been implicated in suppression of apoptosis and survival in some cell types, is also activated by ROS (Schreck *et al.*, 1991, 1992; Sen and Packer, 1996). Cells overexpressing the H₂O₂-detoxifying enzyme catalase are unable to activate NF-κB whereas overexpression of Cu/Zn-dependent superoxide dismutase (SOD), which enhances the production of H₂O₂ from superoxide, increases NF-κB activation (Schmidt *et al.*, 1995). In summary, oxidative damage can elevate apoptosis, accompanied by changes in the expression or activation of pro- and anti- apoptotic genes. However, a clear role has been demonstrated with only a limited number of genes to date.

CHAPTER III

MATERIALS AND METHODS

Cells and culture mediums

Human umbilical vein endothelial cell (HUVEC) was obtained from Clonetics. COS 7 cell was provided by the American Type Culture Collection (ATCC, Manassas, VA). Cell culture medium including EGM-2 kit was from Cambrex and Dulbecco's modified Eagle's medium (DMEM) was from Invitrogen (Carlsbad, CA).

Chemicals

Sodium m-arsenite was from Sigma. Protein kinase inhibitors including AG1478, AG825, 4-amino-5-(4-chlorophenyl)-7-(t-butyl)pyrazolo[3,4-D]pyrimidine (PP2), PD98059, SB203580, SB202190, SP600125, LY294002 were obtained from Calbiochem (San Diego, CA). Primary antibodies directed against phospho-JNK, phospho-c-Jun, phospho-ERK1/2, and phospho-p38 were from New England Biolabs (Beverly, MA). p21^{Waf1/Cip1} antibody was from Pharmagen (San Diego, CA). Agarose-conjugated anti-EGFR, anti-p53, anti-MDM2, actin antibodies and rabbit anti-goat secondary antibody were obtained from Santa Cruz Biotechnology (Santa Cruz, CA). Anti-EGFR and anti-ErbB2 were obtained from Neomarker. Anti-phospho p53, anti-phosphotyrosine (PY100) and monoclonal and polyclonal secondary peroxidase-labeled antibodies were from Cell Signaling (Beverly, MA). Short-interfering RNA (SiRNA) for EGFR (ErbB1), ErbB2 and negative control were from Upstate Biotechnology (Waltham, MA). LipofectAMINE Plus reagent was purchased from Invitrogen. Rneasy Mini kit and TransMessenger Transfection Reagent were provided by Qiagen (Valencia, CA). Protein A/G-agarose was from Pierce. 2',7'-dichlorofluorescein diacetate was from Molecular Probe. Dominant-negative mutants for MKK4 (Sanchez, 1994) and MKK7 (Yao, 1997) were kindly provided by Dr. Leonard I. Zon, Children's Hospital, Boston, MA and Dr. Tse-Hua Tan, Baylor College of Medicine, Houston, TX, respectively. All other reagents were obtained from Sigma or as described.

Cell Culture condition

HUVECs were grown in endothelial cell growth medium (EGM-2) and used between passages 3 and 6. COS 7 cells were cultured in DMEM supplemented with 10% FBS, 100 U/ml penicillin G and streptomycin and used in some experiments due to less efficiency for DNA transfection in endothelial cells. Cells were plated onto cell culture containers as described in each experiment and grown at 37 °C in a humidified, 5% CO₂ atmosphere.

Experimental procedures

Cell viability assay

HUVECs were seeded at a density of 2×10^5 cells/ml into 96-well plates or 6-well plates as appropriated. After overnight growth at 37 °C, cells were treated with various concentrations of sodium arsenite for 24 h, or 50 μM sodium arsenite at various time point. Cell viability was determined by MTT assay or by trypan blue exclusion method as indicated. MTT assay was performed by using CellTiter 96 Non-radioactive Cell Proliferation Assay Kit (Promega, Madison, Wisconsin U.S.A.) Briefly, 20 μl of combined solution of tetrazolium compound MTT and an electron-coupling reagent, phenazine methosulphate, was added to each well. After incubation for 2 h at 37 °C in a humidified, 5% CO₂ atmosphere, the absorption of $A_{490 \text{ nm}}$ was recorded using an enzyme-linked immunosorbent assay (ELISA) plate reader. For trypan blue exclusion, after treatments, mediums were collected and the cells were washed with PBS before trypsinization. Trypsinized cells were combined with medium for each sample. The samples were diluted 1:1 with trypan blue dye. Viable cells and deaths cell were counted using hemocytometer.

Immunoprecipitation and Western Blotting

Immunoprecipitation of protein was performed as described previously (Chen et al, 2000). After treatments, cells were washed with ice-cold phosphate buffer saline (PBS) twice and incubated in lysis buffer containing 20 mM Tris-HCl (pH 7.5), 150 mM NaCl, 1% Triton X-100, 1 μg/ml leupeptin, 1 μg/ml aprotinin, 1mM

phenylmethylsulfonyl fluoride, 1 mM sodium vanadate, 2.5 mM sodium pyrophosphate, and 1 mMEGTA, 1mM sodium EDTA, for 30 min on ice followed by brief sonication for 10 s. Cell lysates were then centrifuged at $13,600 \times g$ for 10 min. The supernatants were collected and protein contents were performed by protein assay kit (Biorad). Equal amount of proteins (1 mg/ml) in each cell lysates were incubated with 10 μ g of primary antibody for 16 h at 4°C on rotator, followed by 2 h incubation with protein A/G-agarose. Following a brief centrifugation, pellets were washed twice with lysis buffer and twice with PBS and resuspended in loading buffer (50 mM Tris-HCl (pH 6.8), 2% SDS, 200 mM dithiothreitol, 20% glycerol, and 0.2% bromophenol blue). Samples were then boiled and supernatants were applied to SDS-PAGE. Separated proteins were transferred to a nitrocellulose membrane for 3 h. The membranes were incubated with 5% non fat dry milk, 0.05% Tween 20 in 10 mM Tris pH 8, 150 mM NaCl for 3 h, and incubated with specific primary-antibodies at 4 °C overnight. After washing, the membranes were incubated with polyclonal- or monoclonal-secondary antibodies as appropriate for 1 h at room temperature. Antigen-antibody complexes were detected using an enhanced chemiluminescence (ECL) detection kit (Amersham Biosciences, Buckinghamshire, England). Densitometric analysis of Western blots was carried out using the ImageJ software (<http://rsb.info.nih.gov/ij/>).

Dorminant negative DNA transfection

COS 7 cells were seeded at a density of 2×10^5 cells /ml in 6-well plate. Transfections were carried out using LipofectAMINE Plus reagent (Invitrogen) according to the manufacture's instruction. When cells reached ~70 % confluence, the cells were incubated with SEK wide type or dorminant negative SEK KR (2 μ g/ well). Transfected cells were grown for 24 h before the experiments.

SiRNA Transfections

The protocol for HUVEC transfection with SiRNA (EGFR and ErbB2) and a negative control SiRNA was performed as manufacturer instruction (TransMessenger Transfection Reagent, Qiagen). Briefly, Cells were seeded (1×10^6 /well) in 60 mm

dishes and allowed to reach 50-70% confluence (~24 h). On the day of transfection, SiRNA was mixed with enhancer reagent and incubated the mixture at room temperature for 5 minutes, before adding transmembrane transfection reagent. The mixtures were incubated further for 10 minutes room temperature to allow transfection-complex formation. SiRNA complexes were mixed with OPTI-MEM (Invitrogen) and immediately transferred into cell culture dishes.

RNA extraction and RT PCR

A Total RNA from the cells grown in 6-well plate was isolated using RNeasy Mini Kit (Qiagen, Valencia, CA). The forward and reverse primers corresponding to human p53 and p21^{Waf1/Cip1} were 5'-ACA GCC AAG TCT GTG ACT T-3' and 5'-CAC GCA CCT CAA AGC TGT T-3'; and 5'-GCT GGG GAT GTC CGT CAG AA-3' and 5'-GAG CGA GGC ACA AGG GTA CAA-3', respectively. Constitutively expressed glyceraldehyde-3-phosphate dehydrogenase mRNA was amplified with forward (5'-ACA GTC CAT GCC ATC ACT GCC-3') and reverse (5'-AGG AAA TGA GCT TGA CAA AGT-3') primers in a similar fashion. The RT-PCR products were applied to 1.5% polyacrylamide gel in TBE buffer.

PI Staining

HUVEC cells seeded on six-well plates. After treatment, cells were collected and fixed with 5% formaldehyde in PBS for 30 min room temperature. Cells were stained with 0.5 ml propidium iodide solution (10 µg/ml in PBS) and detected pyknotic nuclei by using fluorescent microscope.

Cell cycle analysis

Cell cycle distribution was determined by measuring the cellular DNA content using flow cytometry. Briefly, 5×10^5 cells were collected and fixed with 1% ice-cold paraformaldehyde. RNaseA (10 µg/ml) was added and the cells were incubated for 30 min at 37 °C. The cells were resuspended in 0.5 ml propidium iodide solution (10 µg/ml in PBS). Propidium iodide stained cells were analyzed with a FACScan cytometer (MoFlo®, Dako Cytomation, Fort Collins, CO).

Statistical Analysis

All experiments were replicated, and representative findings are shown. Statistical significance was determined by one-way analysis of variance.



สถาบันวิทยบริการ
จุฬาลงกรณ์มหาวิทยาลัย

CHAPTER IV

RESULTS

Sodium arsenite inhibits endothelial cells growth

The pleiotropic and sensitivity of arsenic metal are dependent on the species of arsenic, the concentration and the cell types. Vascular endothelial cells have long been suspected as primary target of arsenic exposure. We observed both dose-and time-dependent decreases in HUVEC viability as a function of sodium arsenite exposure (Figures 22-25). These findings were evident by both the MTT assay and trypan blue dye exclusion methods for the detection of endothelial cell viability. Trends for an effect of arsenite were observed with concentrations as low as 5 μM and significant effects were evident at 10 μM arsenite. However, lower concentrations of arsenite (<1 μM) caused a slight increase in cell viability.



สถาบันวิทยบริการ
จุฬาลงกรณ์มหาวิทยาลัย

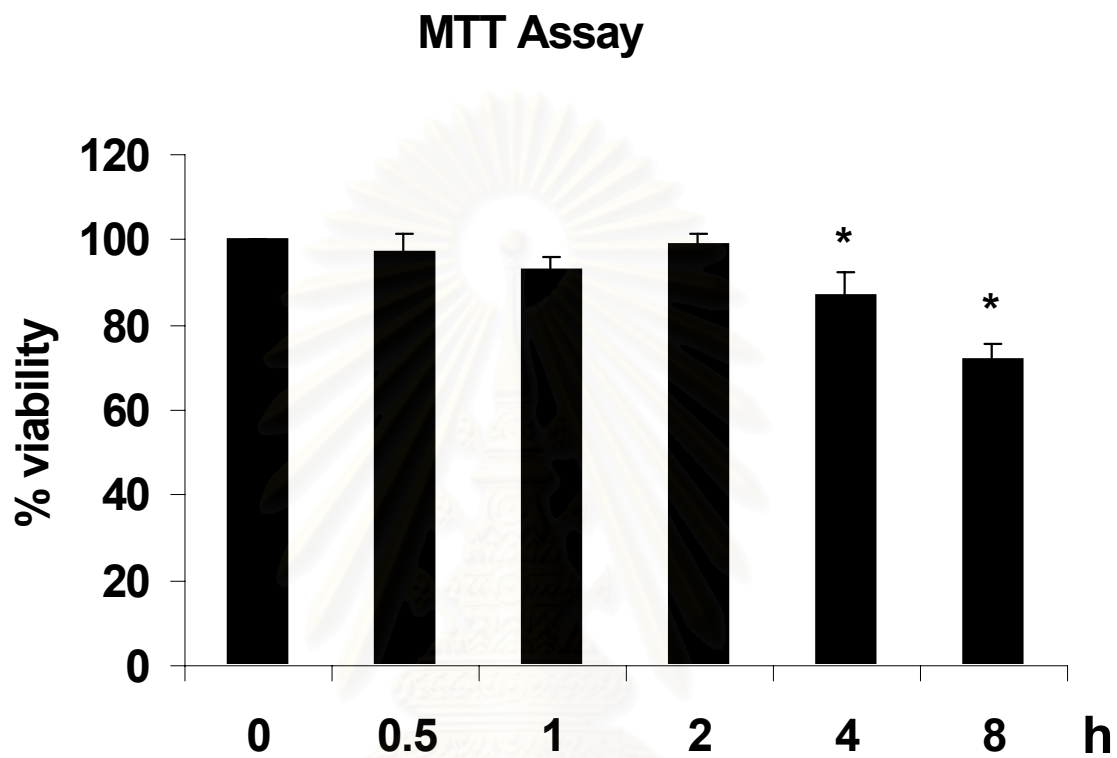


Figure 22. HUVECs were treated with 50 μ M sodium arsenite for the indicated time. After treatment, cell viability was determined by MTT assay. Values are mean \pm SE from 3-5 independent experiments (*, $p < 0.05$ compare with respective untreated control).

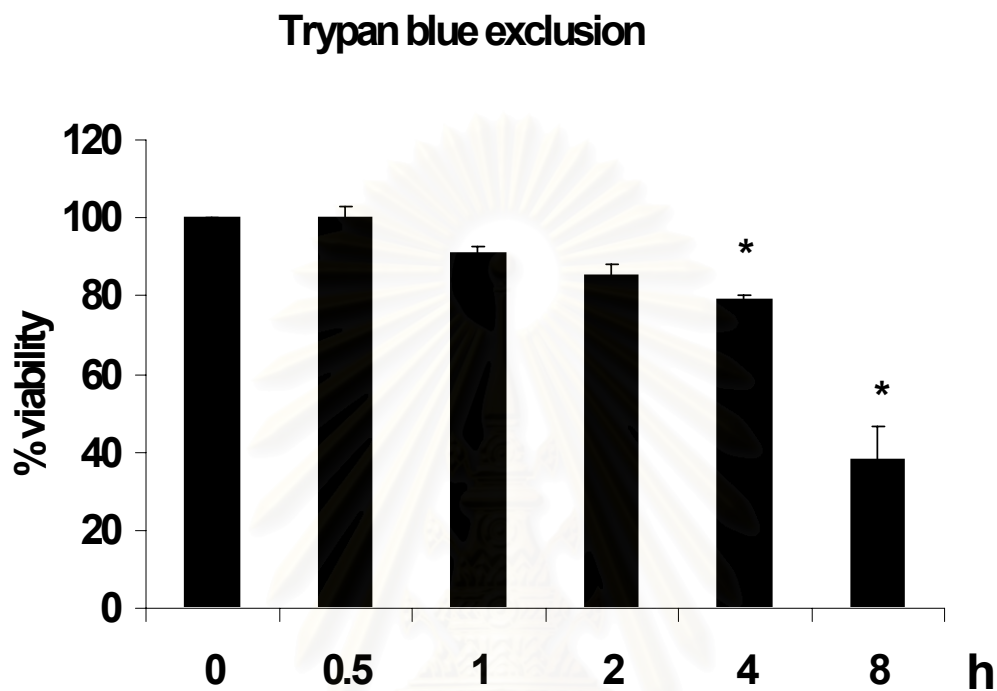


Figure 23. HUVECs were treated with 50 μ M sodium arsenite for the indicated time. After treatment, cell viability was determined by trypan blue exclusion. Values are mean \pm SE from 3-5 independent experiments (*, $p < 0.05$ compare with respective untreated control).

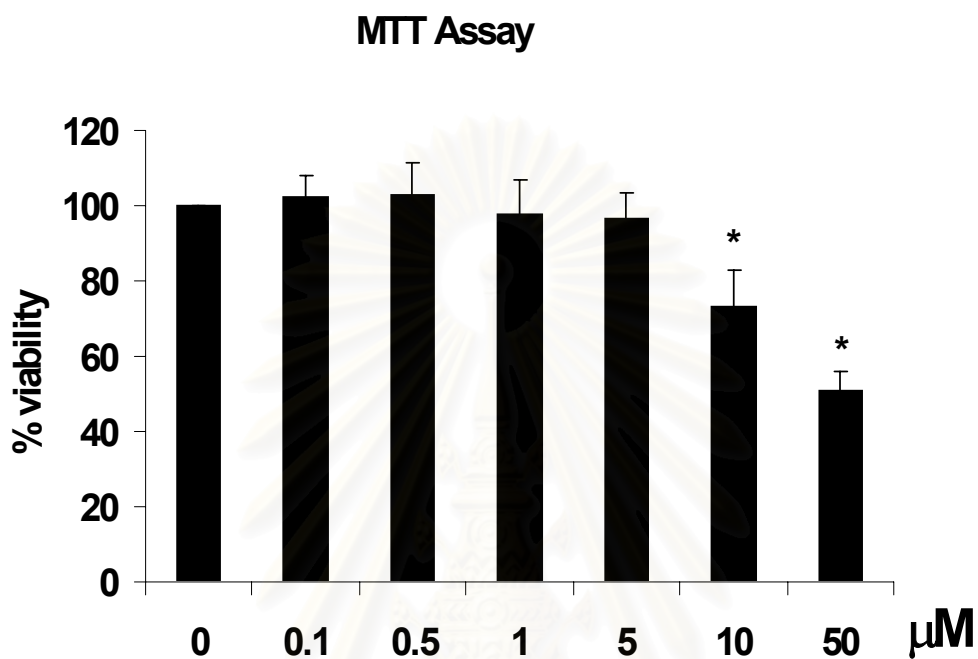


Figure 24. HUVECs were treated with increasing concentrations of sodium arsenite for 24 h. After treatment, cell viability was determined by MTT assay. Values are mean \pm SE from 3-5 independent experiments (*, $p < 0.05$ compare with respective untreated control).

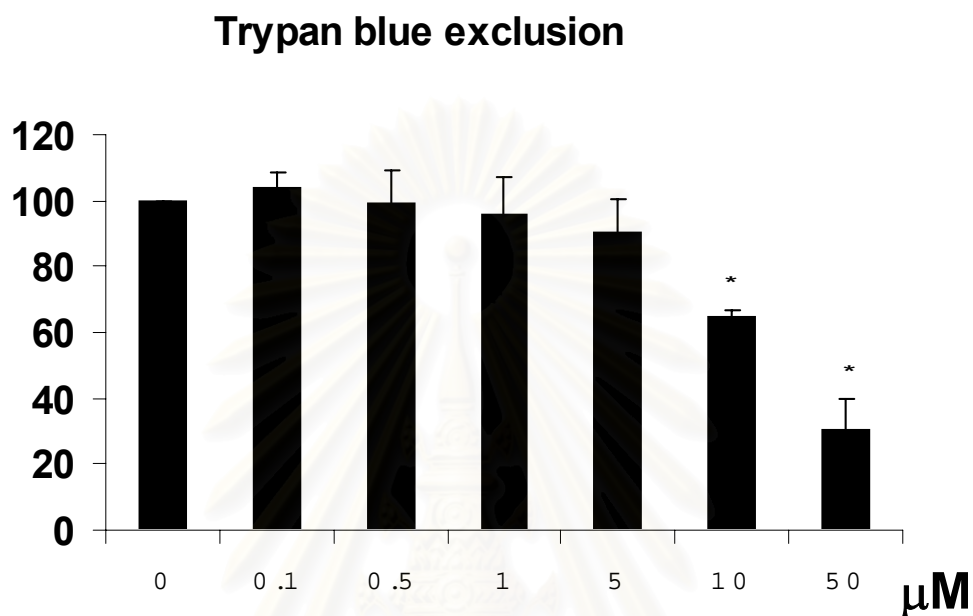


Figure 25. HUVECs were treated with increasing concentrations of sodium arsenite for 24 h. After treatment, cell viability was determined by trypan blue exclusion. Values are mean \pm SE from 3-5 independent experiments (*, $p < 0.05$ compare with respective untreated control).

Sodium arsenite induces p21^{Waf1/Cip1} induction in HUVECs

Arsenite has been linked to DNA damage in the endothelium (Liu and Jan, 2000) and induction of p53 (Yih and Lee). To probe the mechanism(s) involved in arsenite-induced endothelial cell toxicity, we examined its effect on p53 and its downstream target, p21^{Waf1/Cip1}. We found that arsenite produced a potent induction of both p53 and p21^{Waf1/Cip1} (figure 26) after 4h incubation. This effect was also noted at arsenite concentrations as low as 1 – 5 μ M with prolonged incubations (16 h) (figure 27). Induction of p53 and p21^{Waf1/Cip1} in response to arsenite required 4 – 6 hours (figure 28), suggesting a mechanism involving gene transcription. Consistent with this notion, we found that arsenite produced an increase in the steady-state mRNA levels of p53 and p21^{Waf1/Cip1} (figure 29). Arsenite-induced p21^{Waf1/Cip1} upregulation required a novel protein and RNA synthesis, since pretreatment of the cell with Cycloheximide (protein synthesis inhibitor) and actinomycin D (RNA synthesis inhibitor) attenuated the effect of sodium arsenite induced- p21^{Waf1/Cip1} upregulation (figure 30). To determine if p21^{Waf1/Cip1} was also regulated at the post-translational level, we examined the half-life of the protein level of p21^{Waf1/Cip1} in the presence of Cycloheximide. As shown in figure. 31, there was no difference in p21^{Waf1/Cip1} stability between cells with and without arsenite treatment. Thus, these data indicate that arsenite-induced upregulation of p53 and p21^{Waf1/Cip1} is might be, in part, due to increased transcription.

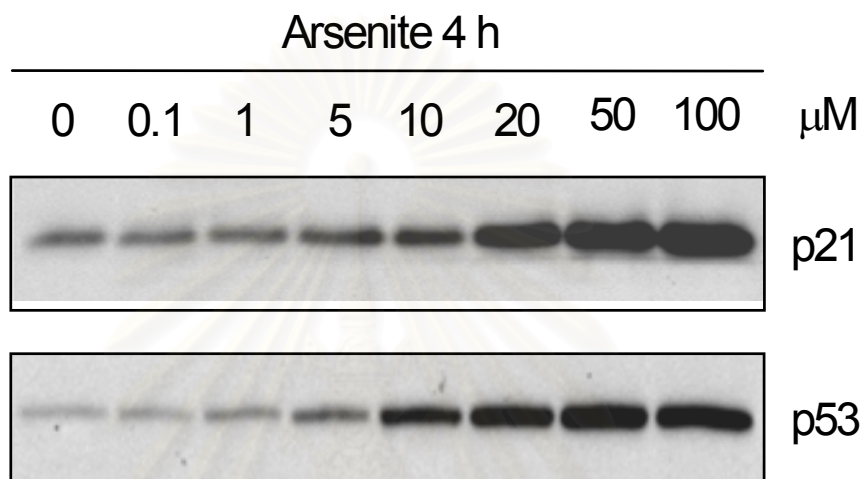


Figure 26. HUVECs were treated with increasing concentrations of sodium arsenite for 4 h. After treatment, total cell lysates were subjected to immunoblot analysis for the levels of p21^{Waf1/Cip1}, and p53.

จุฬาลงกรณ์มหาวิทยาลัย

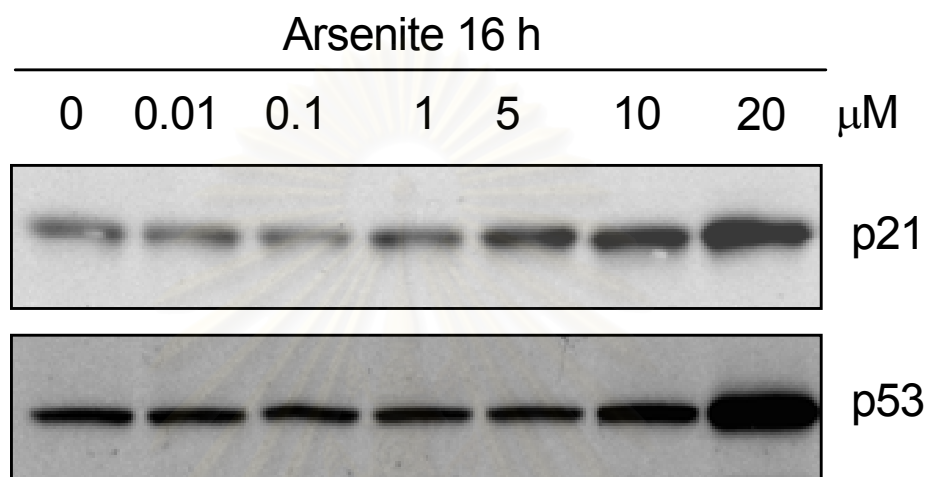


Figure 27. HUVECs were treated with increasing concentrations of sodium arsenite for 16 h. After treatment, total cell lysates were subjected to immunoblot analysis for the levels of p21^{Waf1/Cip1}, and p53.

จุฬาลงกรณ์มหาวิทยาลัย

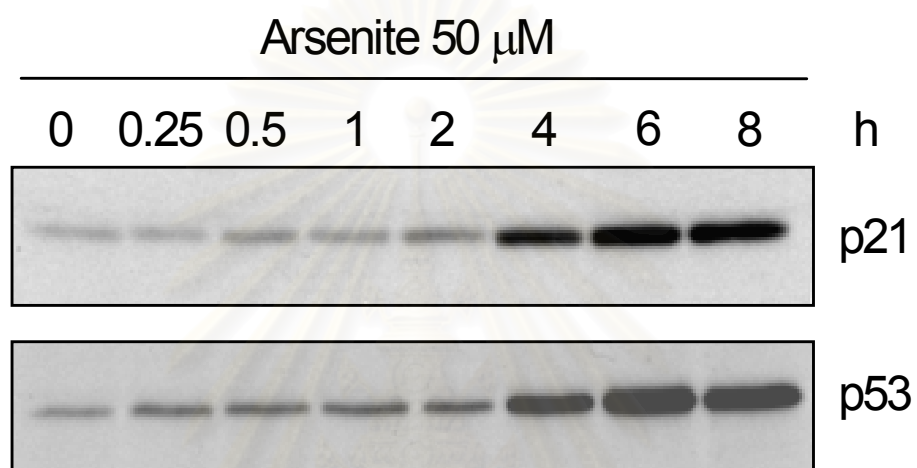


Figure 28. HUVECs were treated with 50 μ M sodium arsenite for the indicated time. After treatment, total cell lysates were subjected to immunoblot analysis for the levels of p21^{Waf1/Cip1}, and p53.

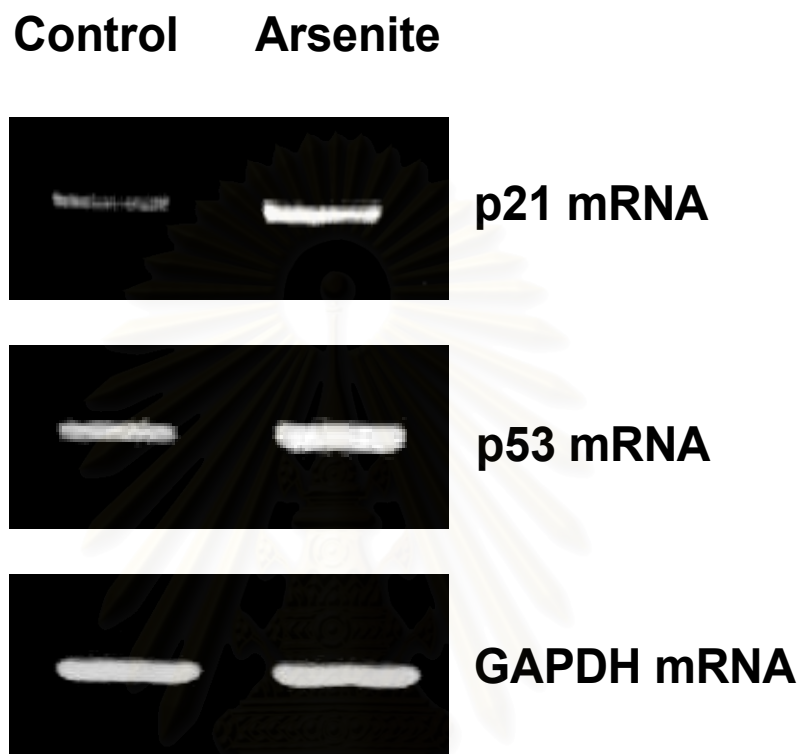


Figure 29. HUVECs were treated with 50 μ M sodium arsenite for 4 h. Total cell RNA was obtained and the mRNA levels of p21^{Waf1/Cip1}, p53 and GAPDH total RNA was measured by RT-PCR.

จุฬาลงกรณ์มหาวิทยาลัย

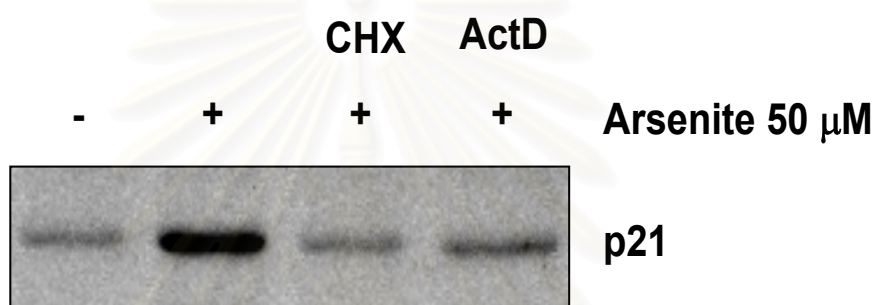


Figure 30. HUVECs were pre-incubated with 5 μ M cycloheximide (CHX) or actinomycine D (ActD) for 30 min prior to exposure to 50 μ M sodium arsenite for 4 h. Immunoblot analysis for p21^{Waf1/Cip1} was performed.

สถาบันวิทยบริการ
จุฬาลงกรณ์มหาวิทยาลัย

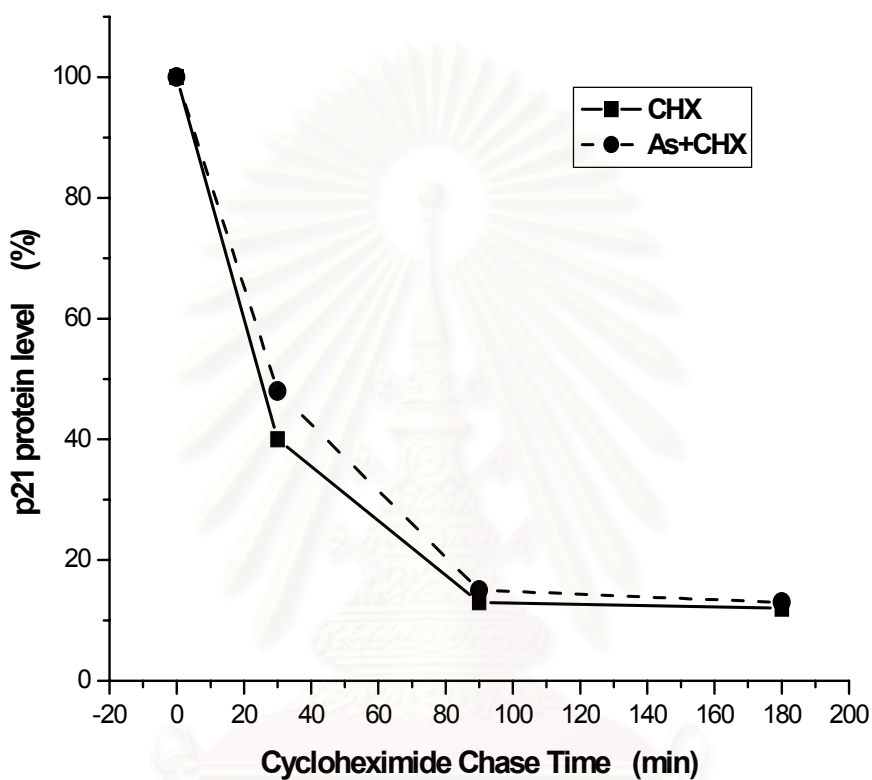


Figure 31. Half-life of p21^{Waf1/Cip1} in HUVECs was measured by cycloheximide chase. Cells were treated with or without 50 μ M sodium arsenite (As) for 4 h and then 5 μ M cycloheximide (CHX) was added to all cell cultures. p21^{Waf1/Cip1} and actin protein level were determined at the indicated time points after administration of cycloheximide. The p21^{Waf1/Cip1} protein levels were quantified as fold induction after normalization to the actin level and presented as percent change compared to time zero of cycloheximide chase.

Arsenite-induced p21^{Waf1/Cip1} and p53 upregulation in HUVECs involved ErbB receptor activation

It is well known that activation of p53 is occurred under oxidative stress. Recently, Chen K et al. (2003) reported that H₂O₂ increased p53 activation required the PDGF β receptor but not EGF receptor (ErbB1). However, the ErbB1 has been implicated in arsenite-induced MAP kinase activation (Chen W et al., 1998). To verify the involvement of these two growth factor receptors in our system, we first used pharmacological inhibitors to block the kinase activity of the receptors. AG1478, a specific inhibitor of ErbB1 receptor, attenuated arsenite-mediated the p21^{Waf1/Cip1} and p53 induction, whereas inhibition of the PDGF receptor with AG1295 or AG1433 was ineffective for (figure 32). Consistent with this finding, AG1478 produced a dose-dependent inhibition of both p53 and the p21^{Waf1/Cip1} induction with arsenite (figure 33). We also found evidence for ErbB2 involvement as selective inhibition of this growth factor receptor impaired arsenite-mediated p53 and p21^{Cip1/Waf1} induction (figure 32 and 34). We were able to confirm activation of both the ErbB1 and ErbB2 receptor in response to arsenite by tyrosine phosphorylation (figure 35-37). In addition, each ErbB isoform receptor tyrosine phosphorylation was dependent upon its intrinsic receptor tyrosine kinase activity and the non-receptor Src-family kinases (figure 38 and 39). To substantiate these results, we utilized siRNA directed against the ErbB1 and ErbB2 receptor. We found that ErbB1 siRNA produced effective gene silencing that significantly attenuated p21^{Waf1/Cip1} induction in response to arsenite (figure 40). Similarly, siRNA against ErbB2 abrogated ErbB2 expression and abolished arsenite-induced p21^{Cip1/Waf1} induction in HUVECs (figure 41). Thus, arsenite-induced p21^{Cip1/Waf1} induction requires the tyrosine kinase activity of both the ErbB receptors.

Involvement of ErbB receptors but not PDGF receptor in sodium arsenite-induced p21^{Waf1/Cip1} and p53 expression in HUVECs.

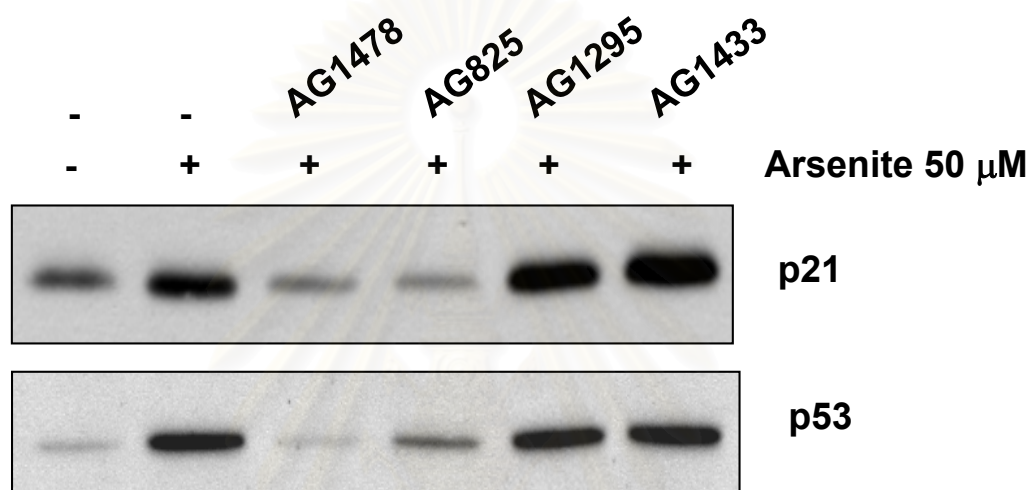


Figure 32. HUVECs were pre-incubated with PDGF receptor tyrosine kinase inhibitor AG1295, AG1433 (40 μM) or ErbB receptor tyrosine kinase inhibitors AG1478 (40 μM) and AG 825 (40 μM) for 30 min prior to exposure to 50 μM sodium arsenite for 4 h. Immunoblot analysis for p21^{Waf1/Cip1} was performed as above. Data are representative of three independent experiments.

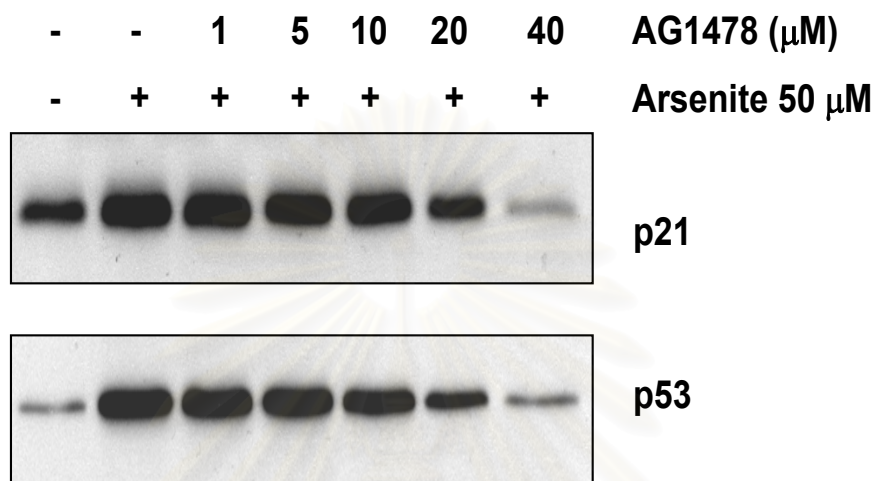


Figure 33 HUVECs were pre-treated with increasing concentrations of EGFR (ErbB1) specific inhibitor AG1478. After treatments, cells were lysed and cell lysates were subjected to immunoblot analysis for p21^{Waf1/Cip1} and p53. Data are representative of three independent experiments.

สถาบันวิทยบริการ
จุฬาลงกรณ์มหาวิทยาลัย

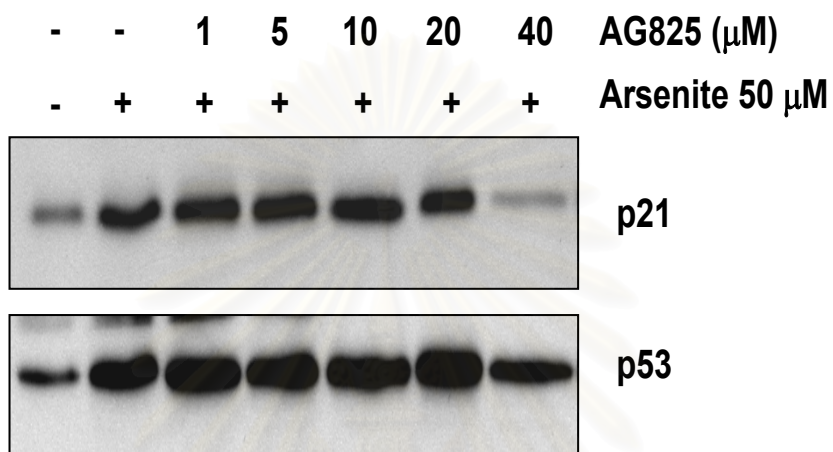


Figure 34. HUVECs were pre-treated with increasing concentrations of ErbB2 specific inhibitor AG825. After treatments, cells were lysed and cell lysates were subjected to immunoblot analysis for p21^{Waf1/Cip1} and p53. Data are representative of three independent experiments.

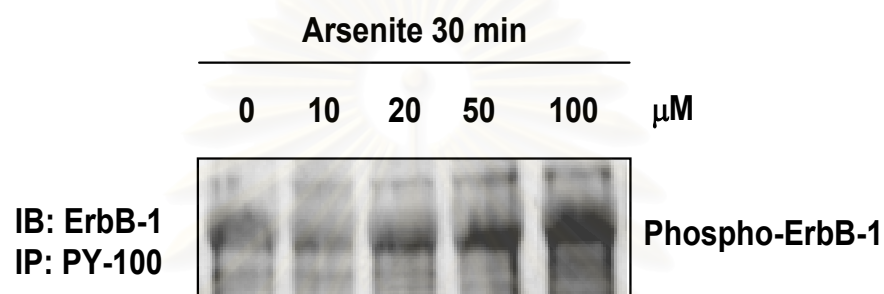


Figure 35. A dose dependent-phosphorylation of ErbB-1 by sodium arsenite? HUVECs were treated with increasing concentrations of sodium arsenite for 4 h. After treatment, cells were lysed, and ErbB-1 tyrosine phosphorylation was assessed by immunoprecipitation (anti-EerbB-1 antibody) and immunoblotting (PY100 antibody).

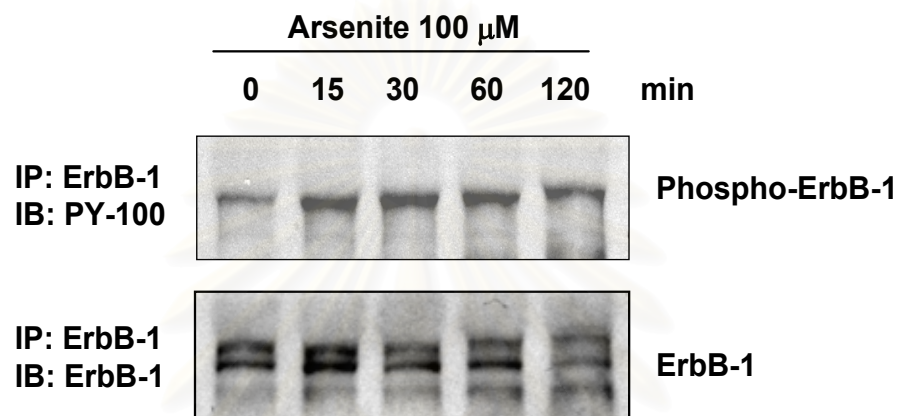


Figure 36. Time-dependent-phosphorylation of ErbB-1 by sodium arsenite HUVECs were treated with 100 μ M sodium arsenite for the indicated time. After treatment, cells were lysed, and ErbB-1 tyrosine phosphorylation was assessed as in figure 35.

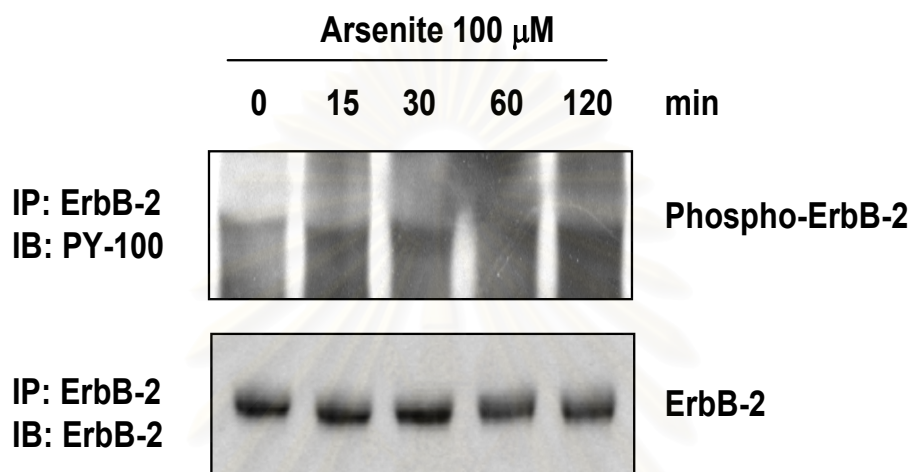


Figure 37. Time-dependent phosphorylation of ErbB-2 by sodium arsenite. HUVECs were treated with 100 μ M sodium arsenite for the indicated time. After treatment, cells were lysed, and ErbB-2 tyrosine phosphorylation was assessed by immunoprecipitation (anti-ErbB-2 antibody) and immunoblotting (PY100 antibody).

สถาบันวิทยบริการ
จุฬาลงกรณ์มหาวิทยาลัย

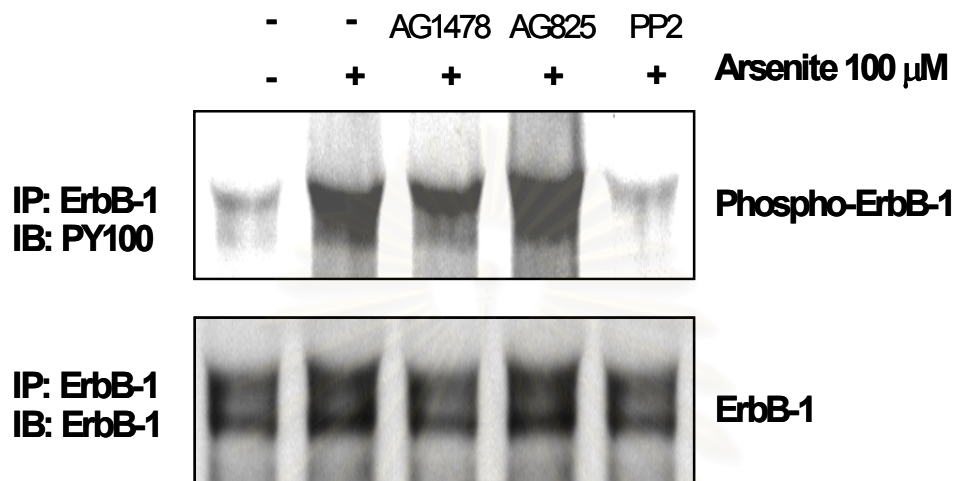


Figure 38. HUVECs were pre-treated with AG1478 (40 μ M), AG825 (40 μ M) or PP2 (20 μ M) for 30 min prior to exposure to 100 μ M sodium arsenite for 30 min. Cells were then lysed, and EGFR tyrosine phosphorylation was assessed by immunoprecipitation (anti-EGFR antibody) and immunoblotting (PY100 antibody). The blots were then reprobbed with anti-EGFR antibody. The blots shown are representative of 3 independent experiments.

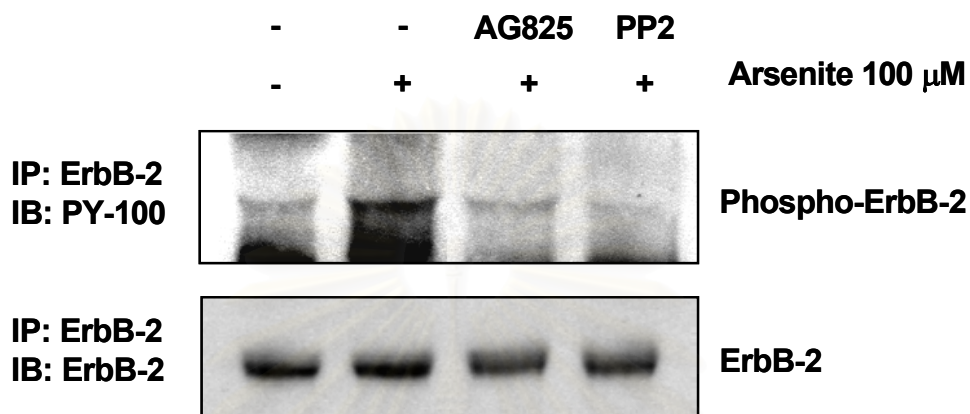


Figure 39. HUVECs were pre-treated with AG1478 (40 μ M), AG825 (40 μ M) or PP2 (20 μ M) for 30 min prior to exposure to 100 μ M sodium arsenite for 30 min. Cells were then lysed, and ErbB2 tyrosine phosphorylation was assessed by immunoprecipitation (anti-ErbB2 antibody) and immunoblotting (PY100 antibody). The blots were then reprobbed with anti-ErbB2 antibody. The blots shown are representative of 3 independent experiments.

สถาบันวิทยบริการ
จุฬาลงกรณ์มหาวิทยาลัย

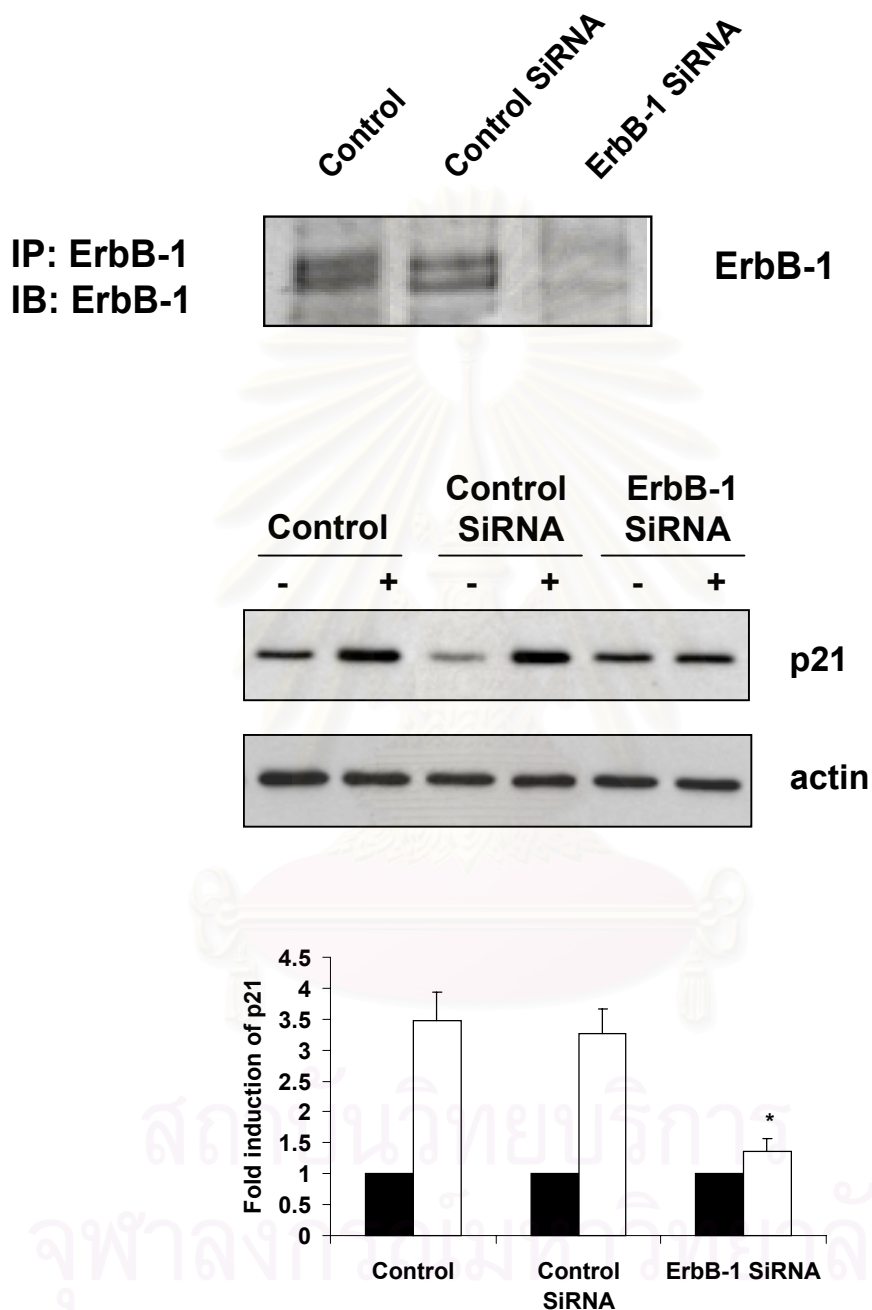


Figure 40. HUVECs were transfected with EGFR siRNA in combination with negative control siRNA. After 48 h, EGFR expression level was determined by immunoprecipitation and immunoblot analysis. HUVECs after siRNA transfection were treated with 50 μ M sodium arsenite for 4 h and cell lysates were assessed for expression of p21^{Waf1/Cip1} and actin with bar graphs representing composite (mean \pm SE; *, $p < 0.05$ compare with respective controls).

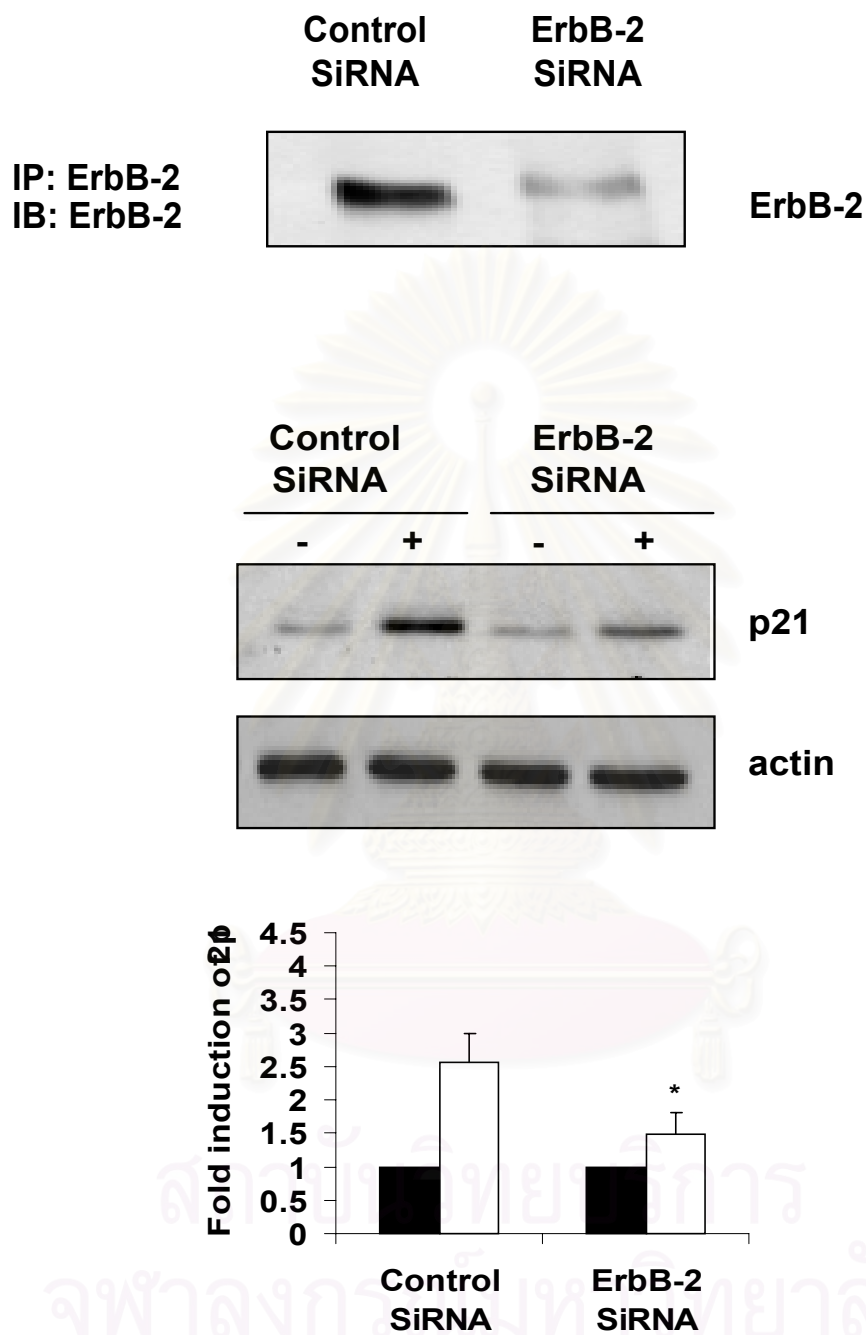


Figure 41. HUVECs were transfected with ErbB2 siRNA in combination with negative control siRNA. After 48 h, ErbB2 expression level was determined by immunoprecipitation and immunoblot analysis. HUVECs after siRNA transfection were treated with 50 μ M sodium arsenite for 4 h, then cell lysates were assessed for expression of p21^{Waf1/Cip1} and actin with bar graphs representing composite (mean \pm SE; *, $p < 0.05$ compare with respective controls).

Arsenite-induced p21^{Waf1/Cip1} and p53 upregulation involve distinct MAP kinases

Because growth factor receptors are often upstream components of MAP kinase activation, we probed MAPKs (p38 MAPK, JNK, and ERK1/2) and in HUVECs exposed to arsenite. We found that arsenite induced activation of p38 MAPK, JNK but not ERK1/2 in our system (figure 42). Moreover, inhibition of p38 MAPK with SB203580 inhibited both p21^{Waf1/Cip1} and p53 induction (figure 43), whereas the selective JNK inhibitor SP600125 did not inhibit arsenite-mediated p53 induction (figure 44). These data are most consistent with a p53-independent signaling pathway directly between JNK and the p21^{Waf1/Cip1} that is distinct from p38 MAPK-mediated activation of p53. To assess this hypothesis directly, we transfected cells with dominant-negative isoforms of MAP kinase kinases MKK4 or MKK7 and examined the implications for arsenite-induced p21^{Waf1/Cip1} upregulation. It's known that MKK4 activates both JNK and p38 MAPK, while MKK7 serves as a specific activator of JNK. As shown in figure 45, inhibition of MKK4 or MKK7 significantly attenuated arsenite-induced p21^{Waf1/Cip1} induction with distinct effect on p53. Inhibition of MKK4 inhibited both p21^{Waf1/Cip1} and p53 induction, whereas inhibition of MKK7 significantly attenuated arsenite-mediated p21^{Waf1/Cip1} induction without any material affect on p53. Thus, arsenite-induced p21^{Waf1/Cip1} upregulation involves a unique role for ErbB1/JNK that is independent of p53 (figure 46).

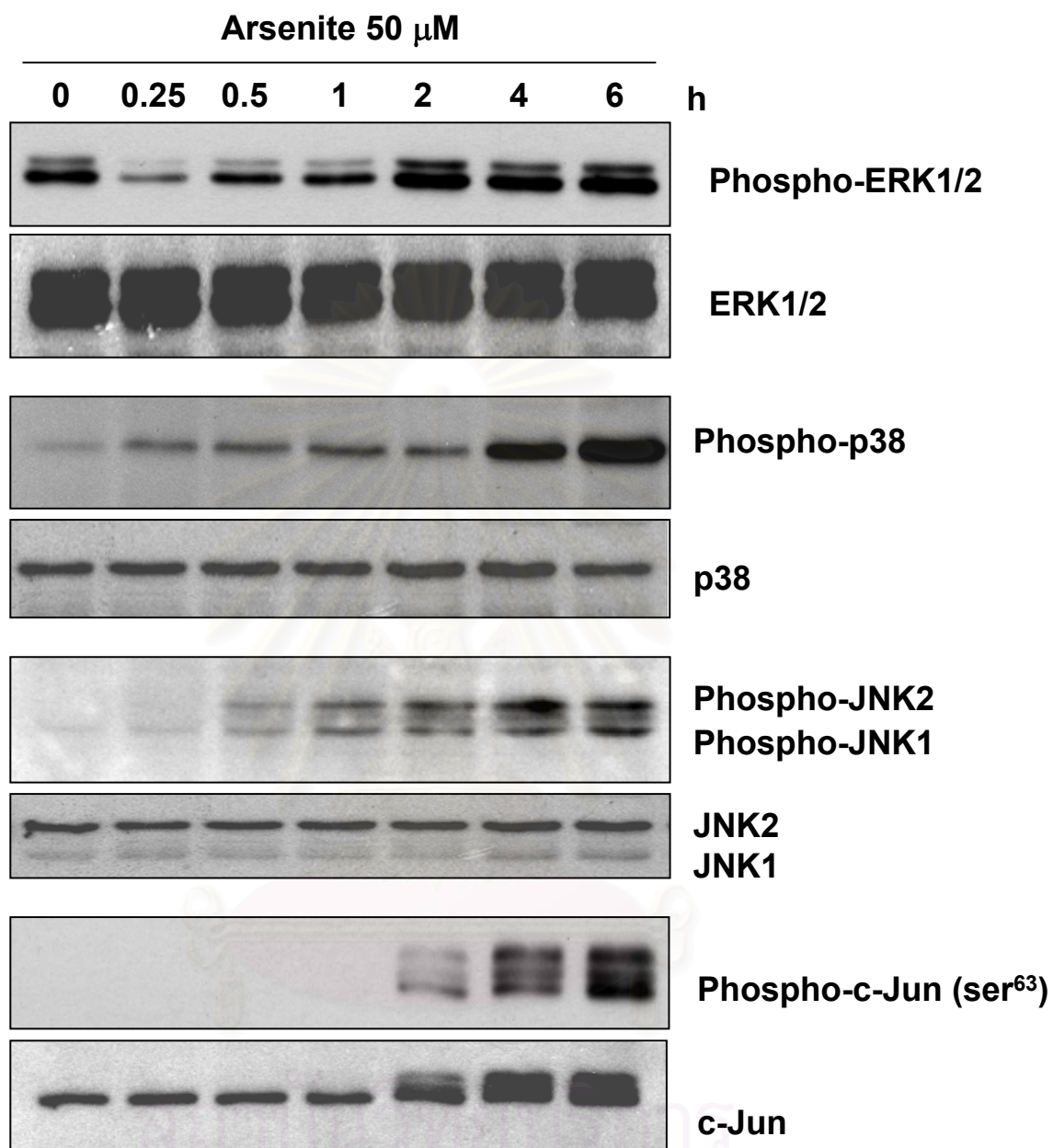


Figure 42. HUVECs were treated with 50 μ M sodium arsenite for the indicated time. Cell lysates were subjected to immunoblotting with phospho-specific antibodies for several kinases.

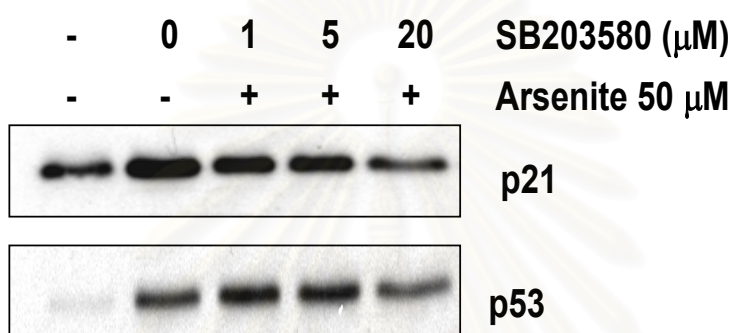


Figure 43. HUVECs were pre-treated with increasing concentrations of SB203580. p21^{Waf1/Cip1} and p53 induction was determined.

สถาบันวิทยบริการ
จุฬาลงกรณ์มหาวิทยาลัย

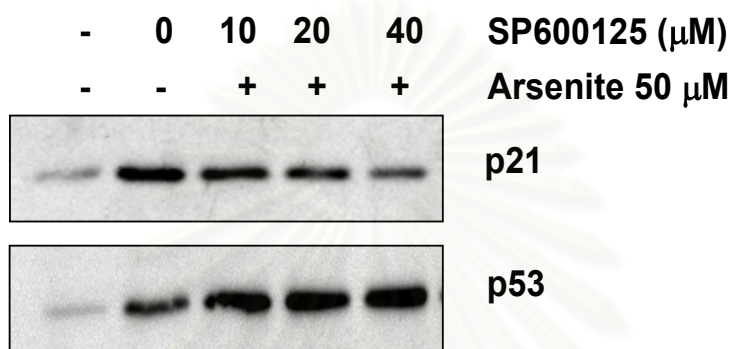


Figure 44. HUVECs were pre-treated with increasing concentrations of SP600125. p21^{Waf1/Cip1} and p53 induction was determined.

สถาบันวิทยบริการ
จุฬาลงกรณ์มหาวิทยาลัย

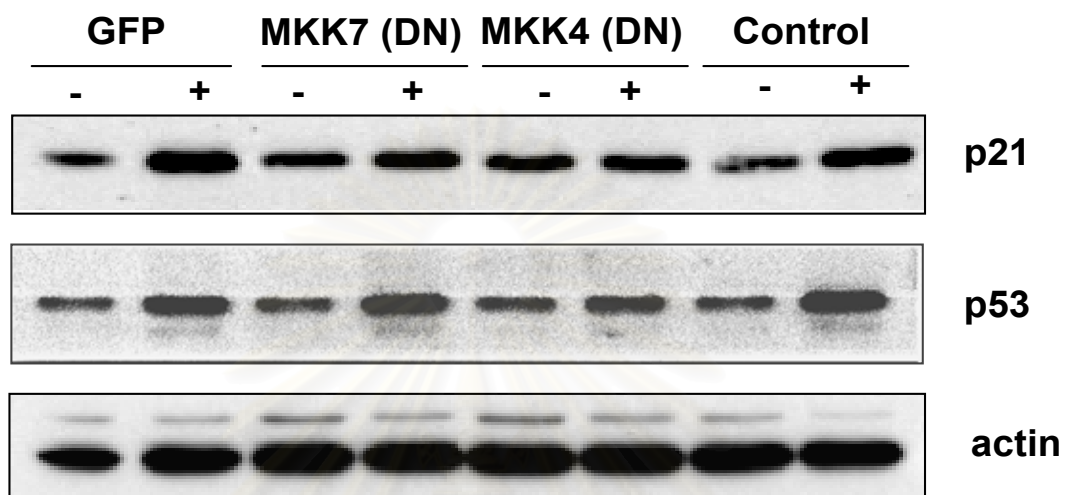


Figure 45 COS-7 cells were transfected with dominant negative MKK7 (MKK7-KE) or dominant negative MKK4 (MKK4-KR) prior to exposure to 50 μ M sodium arsenite for 14 h. A GFP vector transfection was served as a control. All blots were reprobbed for actin to ensure equal protein loading.

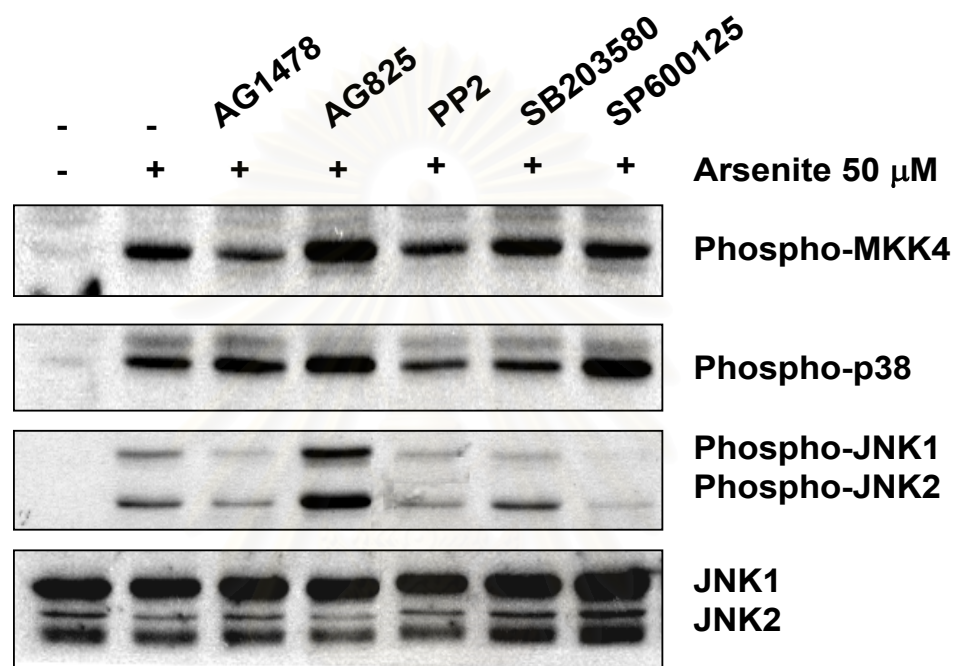


Figure 46, HUVECs were pretreated with inhibitors for EGFR (AG1478, 40 μ M), ErbB2 (AG825, 40 μ M), p38 (SB203580, 20 μ M), and JNK (SP600125, 40 μ M) for 30 min prior to sodium arsenite treatment (50 μ M, 4 h). Immunoblot analysis was performed as above. Data are representative of three independent experiments.

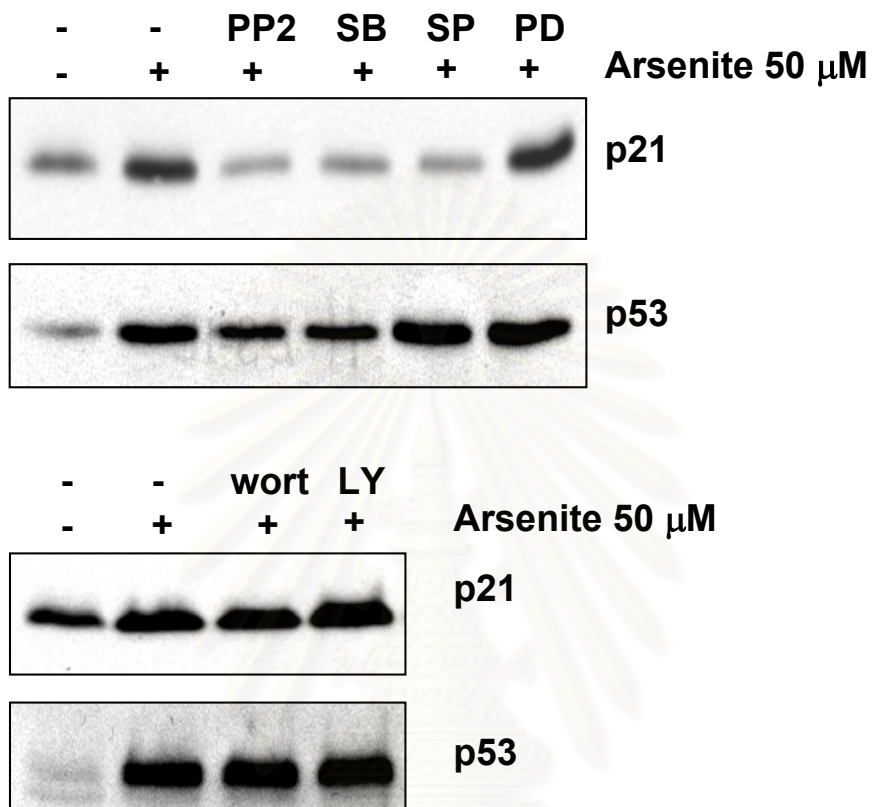


Figure 47. HUVECs were pretreated with inhibitors for Src kinase (PP2, 20 μ M), p38 (SB203580, 20 μ M), JNK (SP600125, 40 μ M), ERK1/2 (PD98059 20 μ M), Akt (LY, 5 μ M), or PKC (wortmanin, 5 μ M) for 30 min prior to sodium arsenite treatment (50 μ M, 4 h). Immunoblot analysis for p21^{Waf1/Cip1} and p53 was performed. Data are representative of three independent experiments.

Role of sodium arsenite-induced p21^{Waf1/Cip1} in apoptosis.

To determine the functional consequences of this pathway, we manipulated arsenite-induced p21^{Waf1/Cip1} upregulation and determined the implications for apoptosis. Arsenite exposure produced a significant decrease in cell numbers and pyknotic nuclei, an effect that was substantially reversed with inhibition of p21^{Waf1/Cip1} upregulation by interruption of arsenite signaling using AG1478, SP600125, SB203580, or EGFR siRNA (figure 48-51). Thus, these data are consistent with the notion that arsenite upregulates p21^{Waf1/Cip1} through multiple pathways resulting in cell apoptosis.



สถาบันวิทยบริการ
จุฬาลงกรณ์มหาวิทยาลัย

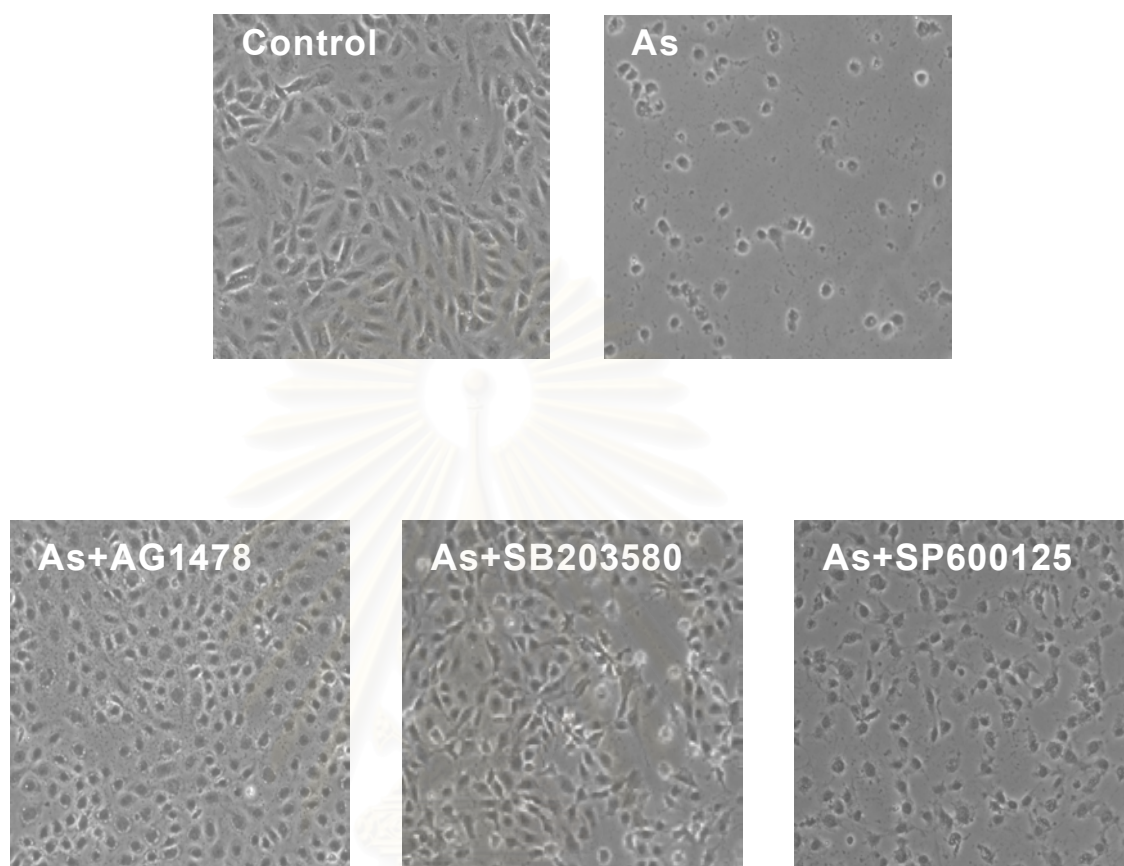


Figure 48. HUVECs were incubated with 100 μ M sodium arsenite for 8 h in the presence or absence of AG1478, SB203580 or SP600125. After treatment, cell morphology was observed using phase contrast microscopy.

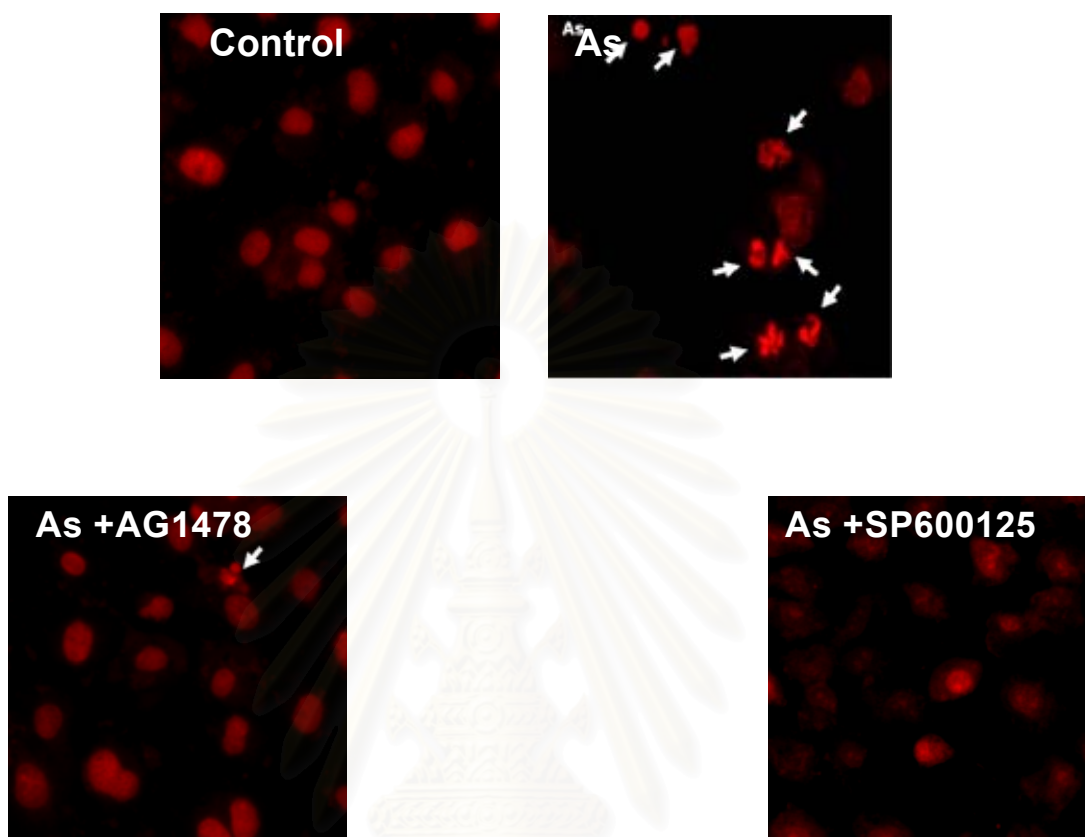


Figure 49 Cells after treatments as in figure 47 were then fixed and stained with 10 $\mu\text{g/ml}$ propidium iodide to detect pyknotic nuclei by using fluorescent microscope.

สถาบันวิทยบริการ
จุฬาลงกรณ์มหาวิทยาลัย

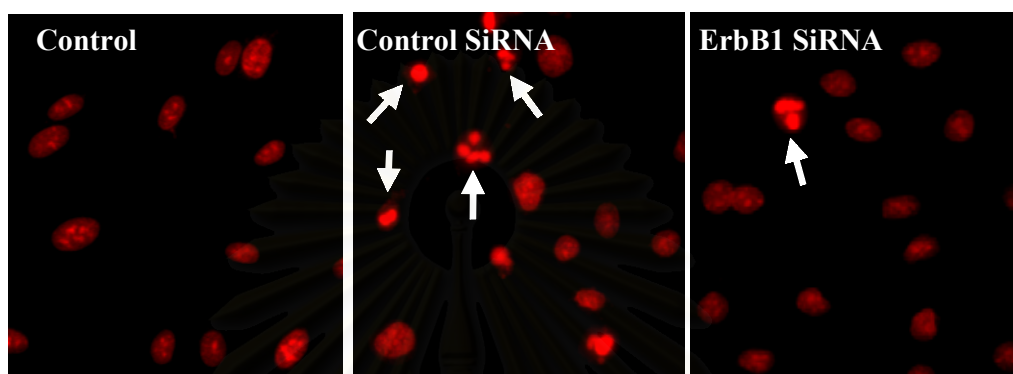


Figure 50. Cells after treatments with control SiRNA and ErbB1 SiRNA were then fixed and stained with 10 $\mu\text{g/ml}$ propidium iodide to detect pyknotic nuclei by using fluorescent microscope.

สถาบันวิทยบริการ
จุฬาลงกรณ์มหาวิทยาลัย

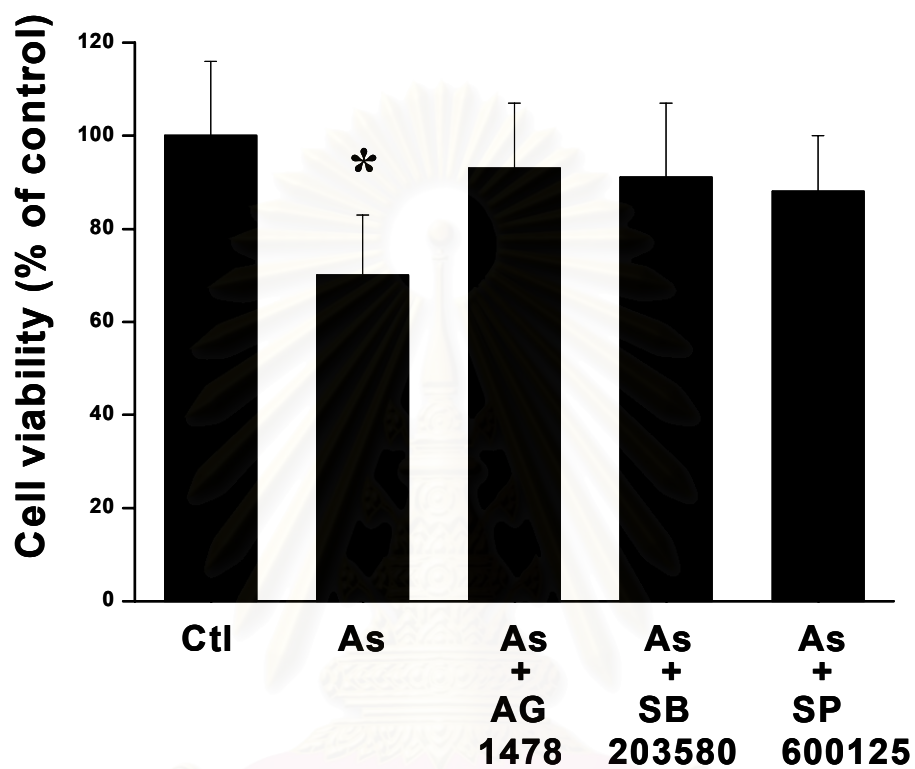


Figure 51. HUVECs were treated as in figure 47, cell viability was measured by MTT assay (mean \pm SE; *, $p < 0.05$ compare with other groups).

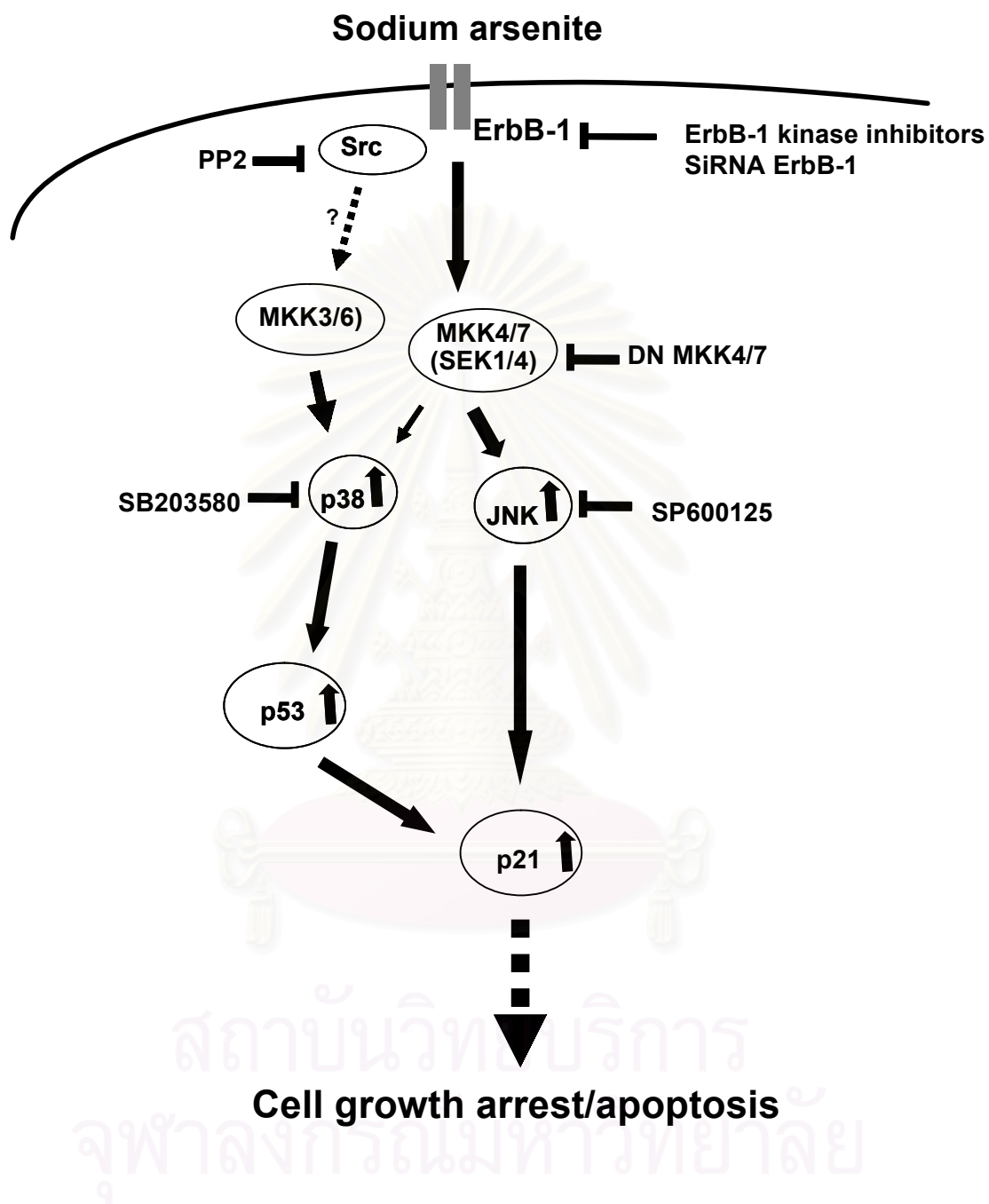


Figure 52. Schematic model depicting the signaling pathways involved in arsenite-induced p21^{Waf1/Cip1}.

CHAPTER V

DISCUSSION

In the present report, we provide evidence that arsenite triggers membrane receptor-dependent signaling pathways that ultimately lead to endothelial cell toxicity. As an initial step of our study, we observed an evident toxicity in HUVEC at 10 μ M arsenite after 24-h treatment. This toxic effect is in agreement with that previously reported by Kao et al. (2003) in HUVEC, and appears to be cell type-dependent with more resistance in porcine endothelial cells (Yeh et al., 2003). The discrepancies with regard to species could be explained by differences in the genetic background. Although this paper focuses on elucidating the signaling pathways by arsenite at toxic levels, it's important to note that the proliferative effect of arsenite at lower levels (<1 μ M) (Kao et al., 2003) may involve distinct mechanisms which remain elusive. We found that arsenite produced transactivation of the EGF (ErbB1) and ErbB2 receptors leading to induction of both p53 and p21waf1/cip1 in endothelial cells, although each process appears distinct (Fig. 52). In particular, we found that EGF receptor activation was required for JNK stimulation that facilitated p21waf1/cip1 induction and this pathway was independent of p53. In contrast, we also found that arsenite induces ErbB2 and p38 MAPK activation independently leading to increased p53 transcription that also contributes, in part, to p21waf1/cip1 expression. Finally, we have established the importance of these pathways in arsenite-mediated endothelial cell apoptosis as we were able to attenuate both p21waf1/cip1 induction and apoptosis by inhibiting ErbB receptors, JNK, or p38 MAP kinase. Thus, ErbB receptors are involved in coordinated MAP kinase activation that determines endothelial cell fate in response to arsenite-mediated injury. These data provide further information on the mechanisms of arsenite-mediated endothelial cell toxicity. Arsenic, a pervasive carcinogen in the environment, is known to promote DNA damage.

Indeed, very low physiologically relevant doses of arsenite induce DNA strand breaks and DNA-protein crosslinks in a variety of cell types (Bau et al., 2002; Schwerdtle et al., 2003). Although typically associated with carcinogenesis,

increasing evidence now links oncogenes and tumor suppressors such as Ras and p53 with vascular disease (Guevara et al., 1999; Minamino et al., 2003). We have recently demonstrated that oxidative DNA damage induces p53 expression through protein stabilization via a PDGF β receptor-mediated process. Despite the similar propensity for DNA damage, however, it appears that arsenite and oxidative stress act on p53 via distinct mechanisms. In particular, we found here that arsenite-induced p53 upregulation was largely a consequence of increased transcription (Fig. 29) that was independent of the PDGF β receptor (Fig. 32) and appears to involve ErbB receptors instead. Thus, arsenite and oxidative stress facilitate increases in cellular p53 levels via different mechanisms. Although distinct with regard to p53 activation, arsenite and oxidative stress do share some common features pertaining to ErbB receptors. In this study, we found that arsenite induced EGF and ErbB2 receptor activation in a manner dependent upon both receptor kinase activity and Srcfamily kinases (Fig. 38-39). This finding is reminiscent of previously reported data on H₂O₂-mediated EGF receptor transactivation (Chen et al., 2001). They have demonstrated that endothelial cells treated with H₂O₂ exhibit activation of the EGF receptor in a Src-dependent manner that is distinct from EGF receptor autophosphorylation. This “transactivation” of the EGF receptor has been described with respect to a number of diverse stimuli including G-protein-coupled receptors, cytokines, and cellular stress (Zwick et al., 1999). This similarity between the response to H₂O₂ and arsenite is consistent with other data that arsenite exposure leads to the intracellular generation of ROS (Wedi et al., 1999) and participation of the EGF receptor in redox-sensitive signal transduction (Chen et al., 1998; Meves et al., 2001). Thus, arsenite and H₂O₂ share common features with regard to the EGF receptor transactivation reported here.

The similarities between the responses to arsenite and H₂O₂ may be consistent with putative mechanisms of signal transduction. For example, arsenite is a well-recognized sulfhydryl reactant that modifies cysteinyl residues of many cellular proteins including the EGF receptor and protein tyrosine phosphatase (PTPase) (Brown et al., 1987). The EGF receptor contains an extracellular cysteine-rich domain that has proven important with regard to receptor dimerization (Heldin, 1995). A similar scenario has been proposed that arsenite, through reaction with vicinal dithiols, alters the conformation of the EGF receptor and produces an increase in its

intrinsic tyrosine kinase activity (Tanaka-Kagawa et al., 2003). Upstream kinases are also targets of arsenite as Simeonova and colleagues (Simeonova et al., 2002) have demonstrated that activation of Src was induced by arsenite in epithelial cells and this process produced EGF receptor transactivation and stimulation of ERK. In that study, PP2 significantly inhibited arsenite-induced EGF receptor phosphorylation, consistent with both the results reported here and our previous study demonstrating H₂O₂ transactivation of the EGF receptor in a Src-dependent manner (Chen et al., 2001). Finally, PTPase activity is subject to modulation by arsenite and inhibition of PTPases has received considerable attention as a mechanism for signal transduction with ligand-induced growth factor activation (Meng et al., 2002; Rhee et al., 2003; Salmeen et al., 2003; Souza et al., 2001). The link between arsenite and activation of the MAP kinase pathway has been studied in some detail. Arsenite has been shown to induce ERK, JNK and p38 kinase components of the MAP kinase cascade in a number of human cell lines (Porter et al., 1999; Souza et al., 2001; Tanaka-Kagawa et al., 2003). For example, arsenite-treated human bronchial epithelial cells exhibit EGF receptor tyrosine phosphorylation, MEK1/2 activation, ERK1/2 phosphorylation, and enhanced transcriptional activity of Elk-1 (Wu et al., 1999). With regard to the current study, the p38 kinase and JNK components of the MAP kinase pathway have been linked to cell cycle regulation, particularly in response to external cellular stress (Daly et al., 1999; Lee et al., 1999; Wang et al., 1999). Treatment of NIH 3T3 cells with sodium arsenite induced growth inhibition through a mechanism that involved p38 kinase-mediated induction of p21^{waf1/cip1} (Kim et al., 2002). Our data is in general agreement with this literature as we found both JNK and p38 kinase activation in response to arsenite and inhibition of p38 kinase attenuated arsenite-induced p21^{waf1/cip1} induction (Fig. 42-44). However, our data add new information in that we found distinctions between p38 kinase and JNK activation. For example, activation of JNK required arsenite-induced ErbB receptor activation, whereas p38 MAP kinase did not. In addition, we found no role for p53 in the linear pathway of p21^{waf1/cip1} induction mediated by EGFR and JNK in response to arsenite. This latter finding is consistent with published reports that growth factors such as PDGF α and basic fibroblast growth factor (bFGF) have also been shown to induce p53-independent transcription of p21^{waf1/cip1} (Micheili et al., 1994; Yu et al., 2003).

With regard to PDGF α , the mechanism of p21waf1/cip1 induction appears to involve JNK-1-responsive cis-acting regulatory elements residing in the p21 promoter (Yu et al., 2003). There is precedent for this mechanism as c-Jun, a substrate of JNK1, mediates p53-independent p21waf1/cip1 promoter activation via physical interaction with the Sp1 protein (Kadssis et al., 1999). Thus, our results are consistent with the model depicted in Figure 8 that indicates arsenite induces p21waf1/cip1 through a pathway that involves EGF receptor-mediated JNK activation. Our data is also consistent with the pathways involving ErbB2 and p38 kinase-mediated p53 induction that contributes to the p21waf1/cip1 upregulation in response to arsenite. The precise nature of the coordination between these pathways, however, is not yet known. Given the important role of both p53 and p21waf1/cip1 in regulating cell growth and apoptosis, however, one might submit that such coordination would be expected.

In summary, the data presented here indicate that arsenite induces endothelial cell death via a mechanism that involves p21waf1/cip1 induction. These data are in keeping with a large body of literature indicating that arsenite produces abnormalities in endothelial function. In this study we have linked the mechanism of arsenite-induced injury, in part, to ErbB receptor activation and coordinated activation of the MAP kinase cascade. The data presented here suggest that p21waf1/cip1 may represent an attractive target to ameliorate arsenite-induced endothelial cell dysfunction.

REFERENCES

- Abernathy, O., Liu, P., Longfellow, D. (1999). Arsenic: health effects, mechanisms of actions and research issue. Environ. Health Perspect. 107:593-7.
- ATSDR (2000). Arsenic. Toxicological Profile. Agency for Toxic Substances and Disease Registry, Public Health Service, U.S. Department of Health and Human Services, Atlanta, GA.
- Barchowsky, A., Roussel, R.R., Klei, L.R., James, P.E., Ganju, N., Smith, K.R., Dudek, E.J. (1999). Low levels of arsenic trioxide stimulate proliferative signals in primary vascular cells without activating stress effector pathways. Toxicol. Appl. Pharmacol. 159:65-75.
- Barchowsky, A., Dudek, E.J., Treadwell, M.D., Wetterhahn, K.E. (1996). Arsenic induces oxidant stress and NF-kappa B activation in cultured aortic endothelial cells. Free Radic. Biol. Med. 21:783-90.
- Barchowsky, A., Klei, L.R., Dudek, E.J., Swartz, H.M. and James, P.E. (1999). Stimulation of reactive oxygen, but not reactive nitrogen species, in vascular endothelial cells exposed to low levels of arsenite. Free Radic. Biol. Med. 27: 1405–1412.
- Bau, D.T., Wang, T.S., Chung, C.H., Wang, A.S., Wang, A.S., and Jan, K.Y. (2002). Oxidative DNA adducts and DNA-protein cross-links are the major DNA lesions induced by arsenite. Environ. Health Perspect. 110 (Suppl 5):753-756.
- Bazuine, M., Ouwens, D.M., et al. (2003). Arsenite stimulated glucose transport in 3T3-L1 adipocytes involves both Glut4 translocation and p38 MAPK activity. Eur. J. Biochem. 270: 3891-3903.
- Brown, S. B., Turner, R. J., Roche, R. S., and Stevenson, K. J. (1987). Spectroscopic characterization of thioredoxin covalently modified with monofunctional organoarsenical reagents. Biochemistry. 26:863-871.
- Brugge, J.S., McCormick, F. (1999). Cell regulation intracellular networking. Curr. Opin. Cell Biol. 11:173-176.
- Bunderson, M., Coffin, J.D. and Beall, H.D. (2002). Arsenic induces peroxynitrite generation and cyclooxygenase-2 protein expression in aortic endothelial cells: possible role in atherosclerosis. Toxicol. Appl. Pharmacol. 184:11–18.

- Cai, H. and Harrison, D.G. (2000). Endothelial dysfunction in cardiovascular diseases: the role of oxidant stress. Circ. Res. 87:840–844.
- Chang, W.C., Chen, S.H., Wu, H.L., Shi, G.Y., Murota, S., and Morita, I. (1991). Cytoprotective effect of reduced glutathione in arsenical-induced endothelial cell injury. Toxicology. 69:101-110.
- Chen, C.J., Chiou, H.Y., Chiang, M.H., Lin, L.J. and Tai, T.Y. (1996). Dose-response relationship between ischemic heart disease mortality and long-term arsenic exposure. Arterioscler. Thromb. Vasc. Biol. 16:504–510.
- Chen, C.J., Wu, M.M., Lee, S.S., Wang, J.D., Cheng, S.H. and Wu, H.Y. (1988). Atherogenicity and carcinogenicity of high-arsenic artesian well water. Multiple risk factors and related malignant neoplasms of blackfoot disease. Arteriosclerosis. 8:452–460.
- Chen, F., Lu, Y. et al. (2001). Opposite effect of NF- κ B and c-Jun N-terminal kinase on p53-independent GADD45 induction by arsenite. J. Biol. Chem. 276: 11414-11419.
- Chen, G.S., Asai, T., Suzuki, Y., Nishioka, K., Nishiyama, S. (1990). A possible pathogenesis for Blackfoot disease--effects of trivalent arsenic (As_2O_3) on cultured human umbilical vein endothelial cells. J. Dermatol. 17:599-608.
- Chen, K., Albano, A., Ho, A., and Keane, J.F., Jr. (2003). Activation of p53 by oxidative stress involves platelet-derived growth factor- β receptor-mediated ataxia telangiectasia Mutated (ATM) kinase activation. J. Biol.Chem. 278:39527-39533.
- Chen, K., Gunter, K. and Maines, M.D. (2000). Neurons overexpressing heme oxygenase-1 resist oxidative stress-mediated cell death. J. Neurochem. 75: 304-313.
- Chen, K., Thomas, S.R. and Keane, J.F., Jr. (2003). Beyond LDL oxidation: ROS in vascular signal transduction. Free Radic. Biol. Med. 35:117–132.
- Chen, K., Vita, J.A, Berk, B.C., Keane, J.F., Jr. (2001). c-Jun N-terminal kinase activation by hydrogen peroxide in endothelial cells involves SRC-dependent epidermal growth factor receptor transactivation. J. Biol. Chem. 276:16045-16050.

- Chen, W., Martindale, J.L., Holbrook, N.J., and Liu, Y. (1998). Tumor promoter arsenite activates extracellular signal-regulated kinase through a signaling pathway mediated by epidermal growth factor receptor and Shc. Mol. Cell. Biol. 18:5178-5188.
- Chopin, V, Toillon, R-A., Jouy, N., Bourhis, X. (2004). p21waf1/cip1 is dispensable for G1 arrest, but indispensable for apoptosis induced by sodium butyrate in MCF-7 breast cancer cells. Oncogene. 21-29.
- Collins, T. and Cybulsky, M.I. (2001). NF-kB: pivotal mediator or innocent bystander in atherogenesis?. J. Clin. Invest. 107: 255–264.
- Cooper, G.M. (2000). The cell: A molecular approach. 2nd ed. Washington, D.C., ASM Press.
- Cushing, S.D., Berliner, J.A., Valente, A.J., Territo, M.C., Navab, M., Parhami, F., Gerrity, R., Schwartz, C.J. and Fogelman, A.M., (1990). Minimally modified low density lipoprotein induces monocyte chemotactic protein 1 in human endothelial cells and smooth muscle cells. Proc. Natl. Acad. Sci. U.S.A. 87: 5134–5138.
- Daly, J.M., Olayioye, M.A., Wong, A.M., Neve, R., Lane, H.A., Maurer, F.G., Hynes, N.E. (1999). NDF/herregulin-induced cell cycle changes and apoptosis in breast tumour cells: role of PI3 kinase and p38 MAP kinase pathways. Oncogene. 18:3440-51.
- Daugherty, A. and Roselaar, S.E., (1995). Lipoprotein oxidation as a mediator of atherogenesis: insights from pharmacological studies. Cardiovasc. Res. 29: 297–311.
- De la Torre, J.C. (2004). Is Alzheimer's disease a neurodegenerative or a vascular disorder? Data, dogma, and dialectics. Lancet Neurol. 3:184-90
- Dong, J.T and Luo, X.M. (1993). Arsenic-induced DNA-strand breaks associated with DNA-protein crosslinks in human fetal lung fibroblasts. Mutat. Res. 302: 97-102.
- Dyndam, M. C. A., S. T. M. Hulscher, et al. (2003). “Evidence for a role of p38 kinase in hypoxia-inducible factor 1-independent induction of vascular endothelial growth factor expression by sodium arsenite. J. Biol. Chem. 278: 6885-6895.

- Engel, R., Hopenhayn-Rich, C., Receveur, O., Smith, H. (1994). Vascular effects of chronic arsenic exposure: a review. Epidemiol. Rev. 16:184-209.
- Engel, R.R., Smith, A.H. (1994). Arsenic in drinking water and mortality from vascular disease: an ecologic analysis in 30 counties in the United States. Arch. Environ. Health. 49:418-27.
- Foreman, J.C., and Johansen, T. (1996). Textbook of receptor pharmacology. New York: CRC Press.
- Fotedar, R., Brickner, H., Saadatmandi, N., Rousselle, T., Diederich, L., Munshi, A., Jung, B., Reed, J.V., and Fotesar, A. (1999). Oncogene. 18:3652-3658.
- Germolec, D.R., Spalding, J., Yu, H.S., Chen, G.S., Simeonova, P.P., Humble, M.C., Bruccoleri, A., Boorman, G.A., Foley, J.F., Yoshida, T. and Luster, M.I., (1998). Arsenic enhancement of skin neoplasia by chronic stimulation of growth factors. Am. J. Pathol. 153: 1775–1785.
- Gibbons, G.H. and Dzau, V.J., (1996). Molecular therapies for vascular diseases. Science. 272: 689–693.
- Guevara, N.V., Kim, H.S., Antonova, E.I., and Chan, L. (1999). The absence of p53 accelerates atherosclerosis by increasing cell proliferation in vivo. Nat. Med. 5, 335-339.
- Haffner, R., Oren, M. (1995). Biochemical properties and biological effects of p53. Curr. Opin. Genet. Dev. 84-90.
- Han, J.W., Ahn, S.H., Kim, Y.K., Bae, G.U., Yoon, J.W., Hong, S., Lee, H.Y., Lee, Y.W., Lee, H.W. (2001). Activation of p21(WAF1/Cip1) transcription through Sp1 sites by histone deacetylase inhibitor apicidin: involvement of protein kinase C. J. Biol. Chem. 276:42084-90.
- Harrison, D., Griendling, K.K., Landmesser, U., Hornig, B. and Drexler, H., (2003). Role of oxidative stress in atherosclerosis. Am. J. Cardiol. 91: 7A–11A.
- Haudenschild, C.C., Zahniser, D., Folk, J., and Klagsbrun, M. (1976). Human vascular endothelial cells in culture. Exp. Cell Res. 98:175-183.
- Heldin, C.H. (1995). Dimerization of cell surface receptors in signal transduction. Cell. 80: 213-223.
- Hirano, S., Cui, X., Li, S., Kanno, S., Kobayashi, Y., Hayakawa, T. and Shraim, A., (2003). Difference in uptake and toxicity of trivalent and pentavalent

- inorganic arsenic in rat heart microvessel endothelial cells. Arch. Toxicol. 77: 305–312.
- Huang, H-S., Chang, W., Chen, C. (2002). Involvement of reactive oxygen species in arsenic-induced downregulation of phospholipid hydroperoxide glutathione peroxidase in human epidermoid carcinoma A431 cells. Free Rad. Biol. Med. 864-873.
- Jaffe, E.A., Nachman R.L., Becker, G.C., and Ninick, C.R. (1973). Culture of human endothelial cells derived from umbilical veins. J Clin. Invest. 52:2745-2756.
- Jung, D. K., Bae G.-U., et al. (2003). Hydrogen peroxide mediates arsenite activation of p70s6k and extracellular signal-regulated kinase. Exp. Cell Res. 290:144-154.
- Kao, Y.H., Yu, C.L., and Yu, H.S. (2003). Low concentration of arsenic induce vascular endothelial growth factor and nitric oxide release and stimulate angiogenesis in vitro. Chem. Res. Toxicol. 16: 460-468.
- Kapahi, P., Takahashi, T. Natoli, G., et al. (2000). Inhibition of NF-kappa B activation by arsenite through reaction with a critical cysteine in the activation loop of Ikappa B kinase. J. Biol. Chem. 275:36062-36066.
- Kardassis, D., Papakosta, P., Pardali, K., and Moustakas, A. (1999). c-Jun transactivates the promoter of the human p21(WAF1/Cip1) gene by acting as a superactivator of the ubiquitous transcription factor Sp1. J. Biol. Chem. 274:29572-29581.
- Karnes, W.E., Weller, S.G., Adjei, P.N., Kottke, T.J., Glenn, K.S., Gores, G.J., Kaufmann SH. (1998). Inhibition of epidermal growth factor receptor kinase induces protease-dependent apoptosis in human colon cancer cells. Gastroenterology. 1998:114:930-939.
- Kim, J.Y., Choi, J.A., Kim, T.H., Yoo, Y.D., Kim, J.I., Lee, Y.J., Yoo, S.Y., Cho, C.K., Lee, Y.S., Lee, S.J. (2002). Involvement of p38 mitogen-activated protein kinase in the cell growth inhibition by sodium arsenite. J. Cell Physiol. 190:29-37.
- Kita, T., Kume, N., Minami, M., Hayashida, K., Murayama, T., Sano, H., Moriwaki, H., Kataoka, H., Nishi, E., Horiuchi, H., Arai, H. and Yokode, M., (2001).

- Role of oxidized LDL in atherosclerosis. Ann. N. Y. Acad. Sci. 947: 199–205.
- Kondo, S., Barna, B.P., Kondo, Y., Tanaka, Y., Casey, G., Liu, J., Morimura, T., Kaakaji, R. Arsenic-induced malignant transformation with DNA hypomethylation and aberrant gene expression. Proc. Natl. Acad. Sci. USA. 94:10907-10912.
- Lee, A.M. and Fraumeni Jr., J.F., (1969). Arsenic and respiratory cancer in man: an occupational study. J. Natl. Cancer Inst. 42: 1045–1052.
- Lee, R.J., Albanese, C., Stenger, R.J., Watanabe, G., Inghirami, G., Haines, G.K., 3rd., Webster, M., Muller, W.J., Brugge, J.S., Davis, R.J., Pestell, R.G. (1999). pp60(v-src) induction of cyclin D1 requires collaborative interactions between the extracellular signal-regulated kinase, p38, and Jun kinase pathways. A role for cAMP response element-binding protein and activating transcription factor-2 in pp60(v-src) signaling in breast cancer cells. J. Biol. Chem. 274:7341-7350.
- Lewis, D.R., Southwick, J.W., Ouellet-Hellstrom, R., Rench, J. and Calderon, R.L., (1999). Drinking water arsenic in Utah: a cohort mortality study. Environ. Health Perspect. 107: 359–365.
- Libby, P., (2000). Changing concepts of atherogenesis. J. Intern. Med. 247: 349–358.
- Liu, F. and Jan, K. Y. (2000). DNA damage in arsenite- and cadmium-treated bovine aortic endothelial cells. Free Radic. Biol Med. 28: 55-63.
- Lundberg, A.S, Weinberg, R.A (1999). Control of the cell cycle and apoptosis. Eur. J. Cancer. 35:1886-1894.
- Mark, D.B., Marks, A.D., and Smith, C.M. (1996). Basic medical biochemistry: A clinical approach. Baltimore: Willium&Wilkins.
- Mathas, S., A. Lietz, et al. (2003). Inhibition of NF-kB essentially contributes to arsenic-induced apoptosis. Blood. 102: 1028-1034.
- Meng, T. C., Fukada, T., and Tonks, N. K. (2002). Reversible oxidation and inactivation of protein tyrosine phosphatases in vivo. Mol. Cell. 9: 387-399.
- Meves, A., Stock, S. N., Beyerle, A., Pittelkow, M. R., and Peus, D. (2001). H(2)O(2) mediates oxidative stress-induced epidermal growth factor receptor phosphorylation. Toxicol.Lett. 122: 205-214.

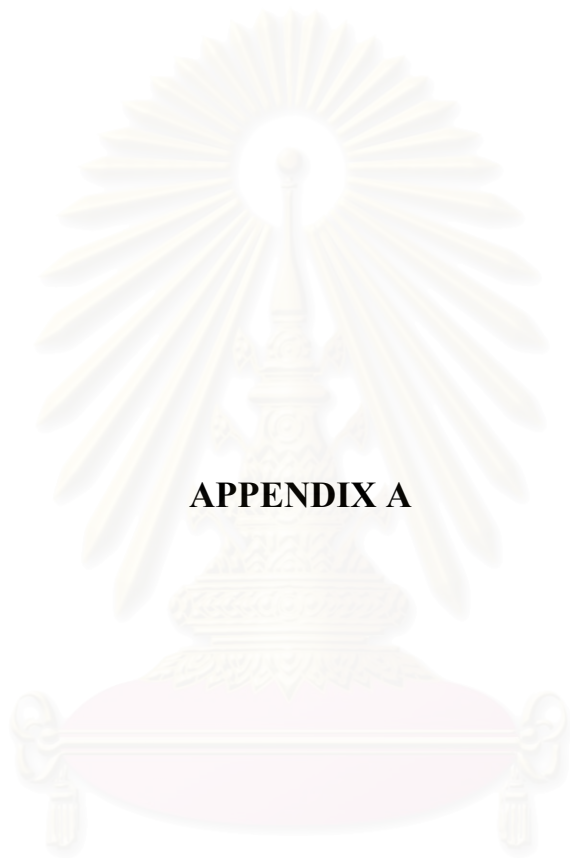
- Michieli, P., Chedid, M., Lin, D., Pierce, H., Mercer, E., Givol, D. (1994). Induction of p21 waf1/cip1 by a p53-independent pathway. Cancer Res. 54: 3391-3395.
- Minamino, T., Yoshida, T., Tateno, K., Miyauchi, H., Zou, Y., Toko, H., and Komuro, I. (2003). Ras induces vascular smooth muscle cell senescence and inflammation in human atherosclerosis. Circulation. 108: 2264-2269.
- Porter, A.C., G.R. Fanger, et al. (1999). Signal transduction pathways regulated arsenate and arsenite. Oncogene. 18: 7794-7802.
- Price, J.T, Wilson, H.M, Haites, N.E. (1996). Epidermal growth factor (EGF) increases the in vitro invasion, motility and adhesion interactions of the primary renal carcinoma cell line A704. Eur. J. Cancer. 32A:1977-1982.
- Rhee, S.G., Chang, T.S., Bae, Y.S., Lee, S.R., and Kang, S.W. (2003). Cellular regulation by hydrogen peroxide. J. Am. Soc. Nephrol. 14: S211-S215.
- Roebuck, K.A., (1999). Oxidant stress regulation of IL-8 and ICAM-1 gene expression: differential activation and binding of the transcription factors AP-1 and NF-kappa b. Int. J. Mol. Med. 4: 223–230.
- Ross, R. (1999). Atherosclerosis is an inflammatory disease. Am. Heart. J. 138:S419-420.
- Salmeen, A., Andersen, J.N., Myers, M.P., Meng, T.C., Hinks, J.A., Tonks, N.K., and Barford, D. (2003). Redox regulation of protein tyrosine phosphatase 1B involves a sulphenyl-amide intermediate. Nature. 423:769-773.
- Salomon, D.S., Brandt, R., Ciardiello, F., Normanno, N. (1995). Epidermal growth factor-related peptides and their receptors in human malignancies. Criti. Rev. Oncol. Hematol. 19: 183-232.
- Sanchez, I., Hughes, R. T., Mayer, B. J., Yee, K., Woodgett, J. R., Avruch, J., Kyriakis, J. M., and Zon, L. I. (1994). Role of SAPK/ERK kinase-1 in the stress-activated pathway regulating transcription factor c-Jun. Nature. 372: 794-798.
- Schwerdtle, T., Walter, I., Mackiw, I., and Hartwig, A. (2003). Induction of oxidative DNA damage by arsenite and its trivalent and pentavalent methylated metabolites in cultured human cells and isolated DNA. Carcinogenesis. 24: 967-974.

- Simeonova, P.P. and Luster, M.I., (1996). Asbestos induction of nuclear transcription factors and interleukin 8. Am. J. Respir. Cell Mol. Biol. 15: 787–795.
- Simeonova, P.P. and Luster, M.I., (2002). Arsenic carcinogenicity: relevance of c-Src activation. Mol. Cell. Biochem. 234/235: 277–282.
- Simeonova, P.P., Hulderman, T., Harki, D. and Luster, M., (2003). Arsenic exposure accelerates atherogenesis in apolipoprotein E^{-/-} mice. Environ. Health Perspect. 111: 1744–1748.
- Simeonova, P.P., Leonard, S., Flood, L., Shi, X. and Luster, M.I., (1999). Redox-dependent regulation of interleukin-8 by tumor necrosis factor-alpha in lung epithelial cells. Lab. Invest. 79: 1027–1037.
- Simeonova, P.P., Wang, S., Toriuma, W., Kommineni, V., Matheson, J., Unimye, N., Kayama, F., Harki, D., Ding, M., Vallyathan, V. and Luster, M.I., (2000). Arsenic mediates cell proliferation and gene expression in the bladder epithelium: association with activating protein-1 transactivation. Cancer Res. 60: 3445–3453.
- Simeonova, P.P., Luster, M.I. (2002). Arsenic carcinogenicity: relevance of c-Src activation. Mol. Cell Biochem. 234-235(1-2):277-282.
- Simeonova, P.P., Wang, S., Hulderman, T., Luster, M.I. (2002). c-Src-dependent activation of the epidermal growth factor receptor and mitogen-activated protein kinase pathway by arsenic: Role in carcinogenesis. J. Biol. Chem. 277: 2945-2950.
- Smith, A.H., Steinmaus, C.M. (2002). Arsenic in urine and drinking water. Environ. Health Perspect. 108:A494-A495.
- Souza, K., Maddock, D. A., Zhang, Q., Chen, J., Chiu, C., Mehta, S., and Wan, Y. (2001). Arsenite activation of P13K/AKT cell survival pathway is mediated by p38 in cultured human keratinocytes. Mol. Med. 7:767-772.
- Steinberg, D., Parthasarathy, S., Carew, T.E., Khoo, J.C. and Witztum, J.L., (1989). Beyond cholesterol. Modifications of low-density lipoprotein that increase its atherogenicity. N. Engl. J. Med. 320: 915–924.
- Sunderman, F.W., Jr. (1984). Recent advances in metal carcinogenesis. Ann. Clin. Lab. Sci. 14: 93-122.

- Takei, A., Huang, Y. and Lopes-Virella, M.F., (2001). Expression of adhesion molecules by human endothelial cells exposed to oxidized low density lipoprotein. Influences of degree of oxidation and location of oxidized LDL. Atherosclerosis. 154: 79–86.
- Tanaka-Kagawa, T., Hanioka, N., Yoshida, H., Jinno, H., Ando, M. (2003). Arsenite and arsenate activate extracellular signal-regulated kinases 1/2 by an epidermal growth factor receptor-mediated pathway in normal human keratinocytes. Br. J. Dermatol. 149:1116-1127.
- Theodosiou, A., Ashworth, A. (2002). Differential effects of stress stimuli on a JNK-inactivating phosphatase. Oncogene. 21: 2387-2397.
- Thomas, S.R., Chen, K. and Keane, J.F., Jr. (2002). Hydrogen peroxide activates endothelial nitric oxide synthase through coordinated phosphorylation and dephosphorylation via a phosphoinositide 3-kinase-dependent signaling pathway. J. Biol. Chem. 277:6017-6024.
- Thomas, S.R., Chen, K. and Keane, J.F., Jr. (2003). Oxidative stress and endothelial nitric oxide bioactivity. Antioxid. Redox Signal. 5:181–194.
- Tian, H., Faje, A.T., Lee, S.L., Jorgensen, T.J. (2002). Radiation-induced phosphorylation of Chk1 at S345 is associated with p53-dependent cell cycle arrest pathways. Neoplasia. 4:171-180.
- Tsai, S.H., Liang, Y.C., Chen, L., Ho, F.M., Hsieh, M.S. and Lin, J.K., (2002). Arsenite stimulates cyclooxygenase-2 expression through activating I kappa b kinase and nuclear factor kappaB in primary and ECv304 endothelial cells. J. Cell. Biochem. 84: 750–758.
- Tseng, C.H., Chong, C.K., Chen, C.J. and Tai, T.Y., (1996). Dose–response relationship between peripheral vascular disease and ingested inorganic arsenic among residents in Blackfoot disease endemic villages in Taiwan. Atherosclerosis. 120: 125–133.
- Tseng, C.H., Chong, C.K., Tseng, C.P., Hsueh, Y.M., Chiou, H.Y., Tseng, C.C. and Chen, C.J., (2003). Long-term arsenic exposure and ischemic heart disease in arseniasis-hyperendemic villages in Taiwan. Toxicol. Lett. 137: 15–21.
- Tseng, W.P. (1989). Blackfoot disease in Taiwan: a 30-year follow-up study. Angiology. 40: 547–558.

- Tsou, T.C., Tsai, F.Y., Wu, M.C., Chang, L.W. (2003). The protective role of NF-kappaB and AP-1 in arsenite-induced apoptosis in aortic endothelial cells. Toxicol. Appl. Pharmacol. 191:177-187.
- Valen, G., Yan, Z.Q. and Hansson, G.K., (2001). Nuclear factor kappa-b and the heart. J. Am. Coll. Cardiol. 38: 307–314.
- Voisin, L., Foisy, S., Giasson, E., Lambert, C., Moreau, P., Meloche, S. (2002). EGF receptor transactivation is obligatory for protein synthesis stimulation by G protein-coupled receptors. Am. J. Physiol. Cell Physiol. 283: C446-C455.
- Wang, C.H., Jeng, J.S., Yip, P.K., Chen, C.L., Hsu, L.I., Hsueh, Y.M., Chiou, H.Y., Wu, M.M. and Chen, C.J., (2002). Biological gradient between long-term arsenic exposure and carotid atherosclerosis. Circulation. 105: 804–809.
- Wang, S., Nath, N., Minden, A. and Chellappan, S. (1999). Regulation of Rb and E2F by signal transduction cascades: divergent effects of JNK1 and p38 kinases. EMBO J. 18: 1559-1570.
- Wang, X., Gorospe, M., Holbrook, N.J. (1999). Gadd45 is not required for activation of c-Jun N-terminal kinase or p38 during acute stress. J. Biol. Chem. 274:29599-29602.
- Welch, K., Higgins, I., Oh, M. and Burchfiel, C., (1982). Arsenic exposure, smoking, and respiratory cancer in copper smelter workers. Arch. Environ. Health. 37: 325–335.
- Woodburn, J.R. (1999). The epidermal growth factor receptor and its inhibition in cancer therapy. Pharmacol. Ther. 82:241-250.
- Wu, X., Fan, Z., Masui, H., Rosen, N., Mendelsohn, J. (1995). Apoptosis induced by an anti-epidermal growth factor receptor monoclonal antibody in a human colorectal carcinoma cell line and its delay by insulin. J. Clin. Invest. 95:1897-1905.
- Wu, M.M., Kuo, T.L., Hwang, Y.H. and Chen, C.J., (1989). Dose–response relation between arsenic concentration in well water and mortality from cancers and vascular diseases. Am. J. Epidemiol. 130: 1123–1132.
- Wu, W., Graves, L.M., Jaspers, I., Devlin, R.B., Reed, W., Samet, JM. (1999) Activation of the EGF receptor signaling pathway in human airway epithelial cells exposed to metals. Am. J. Physiol. 277:L924-931.

- Xiao, E.H., Hu, G.D., Li, J.Q. (2002). Relationship between apoptosis and invasive and metastatic potential of hepatocellular carcinoma. Hepatobiliary Pancreat. Dis. Int. 1:574-6.
- Yao, Z., Diener, K., Wang, X.S., Zukowski, M., Matsumoto, G., Zhou, G., Mo, R., Sasaki, T., Nishina, H., Hui, C.C., Tan, T.H., Woodgett, J.P., and Penninger, J.M. (1997). Activation of stressactivated protein kinases/c-Jun N-terminal protein kinases (SAPKs/JNKs) by a novel mitogen-activated protein kinase kinase. J. Biol. Chem. 272: 32378-32383.
- Yeh, J.Y, Cheng, .LC, Liang, Y.C and Ou, B.R. (2003). Modulation of the arsenic effects on cytotoxicity, viability, and cell cycle in porcine endothelial cells by selenium. Endothelium. 10:127-139.
- Yeh, J.Y., Cheng, L.C., Ou, B.R., Whanger, D.P. and Chang, L.W. (2002). Differential influences of various arsenic compounds on glutathione redox status and antioxidative enzymes in porcine endothelial cells. Cell. Mol. Life Sci. 59: 1972–1982.
- Yih, L.-H., Lee, T.-C. (2000). Arsenite induces p53 accumulation through an ATM-dependent pathway in human fibroblasts. Cancer Res. 60: 6346-6352.
- Yu, J., Liu, X. W., and Kim, H. R. (2003). Platelet-derived growth factor (PDGF) receptor-alphaactivated c-Jun NH2-terminal kinase-1 is critical for PDGF-induced p21WAF1/CIP1 promoter activity independent of p53. J. Biol. Chem. 278:49582-49588.
- Zhang, W., Ohnishi, K., Shigeno, K, Fugisawa, S. et al. (1998). The induction of apoptosis and cell cycle arrest by arsenic trioxide in lymphoid neoplasms. Leukemia. 12:1383-1391.
- Zierler, S., Theodore, M., Cohen, A., Rothman, K.J. (1988). Chemical quality of maternal drinking water and congenital heart disease. Int. J. Epidemiol. 17:589-594.
- Zwick, E., Hackel, P. O., Prenzel, N., and Ullrich, A. (1999). The EGF receptor as central transducer of heterologous signalling systems. Trends Pharmacol. Sci. 20, 408-412.



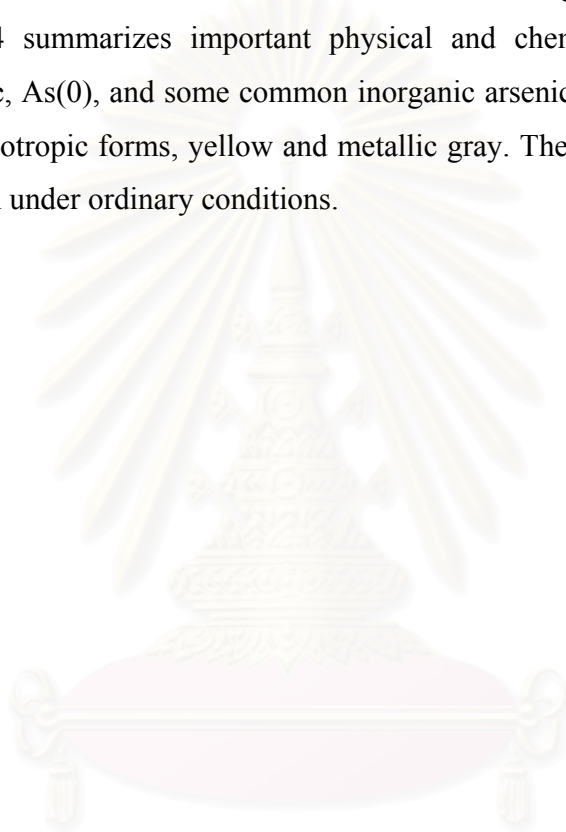
APPENDIX A

สถาบันวิทยบริการ
จุฬาลงกรณ์มหาวิทยาลัย

ARSENIC


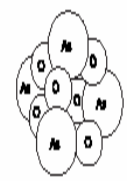
CHEMICAL AND PHYSICAL INFORMATION

Arsenic appears in Group V of the periodic table. It exists in four oxidation states: -3, 0, +3, and +5. Table 3 summarizes information on the chemical identity of elemental arsenic and some common inorganic compounds of arsenic. Table 4 summarizes important physical and chemical properties of elemental arsenic, As(0), and some common inorganic arsenic compounds. As(0) occurs as two allotropic forms, yellow and metallic gray. The metallic gray form is the stable form under ordinary conditions.



สถาบันวิทยบริการ
จุฬาลงกรณ์มหาวิทยาลัย

Table 5. Chemical Identity of Arsenic and Selected Inorganic Arsenic Compounds

| Characteristic | Arsenic | Arsenic acid | Arsenic pentoxide | Arsenic trioxide |
|--------------------------|--|---|--|---|
| Synonym(s) | Arsenic black; colloidal arsenic; gray arsenic | Orthoarsenic acid | Arsenic (V) oxide; arsenic acid anhydride; diarsenic pentoxide | Arsenic oxide; arsenious acid; arsenious oxide; white arsenic |
| Registered trade name(s) | No data | Dessican L-10 ^{®b} ; Scorch ^{®b} | No data | Arsenolite ^{®c} ; Claudelite ^{®c} |
| Chemical formula | As | H ₃ AsO ₄ | As ₂ O ₅ (As ₄ O ₁₀) | As ₂ O ₃ (As ₄ O ₆) |
| Chemical structure | As | $\begin{array}{c} \text{OH} \\ \\ \text{HO}-\text{As}=\text{O} \\ \\ \text{OH} \end{array}$ |  |  |
| Identification numbers: | | | | |
| CAS registry | 7440-38-2 | 7778-39-4 | 1303-28-2 | 1327-53-3 |

| Characteristic | Calcium arsenate | Gallium arsenide | Disodium arsenate | Sodium arsenite |
|--------------------------|---|----------------------|--|---|
| Synonym(s) | Calcium orthoarsenate; arsenic acid, calcium salt | Gallium monoarsenide | Sodium arsenate, dibasic; Disodium hydrogen arsenate; arsenic acid, disodium salt | Arsenious acid, sodium salt; sodium metaarsenite |
| Registered trade name(s) | Pencal ^{®b} ; Spra-cal ^{®c} | No data | No data | Atlas A ^{®b} ; Chem Sen ^{®b} ; Kill-All ^{®b} |
| Chemical formula | Ca ₃ (AsO ₄) ₂ | GaAs | Na ₂ HAsO ₄ | NaAsO ₂ ^d |
| Chemical structure | $\begin{array}{c} \text{O} \\ \\ (\text{Ca}^{2+})_3(\text{O}-\text{As}-\text{O}^{-})_2 \\ \\ \text{O} \end{array}$ | Ga:As | $\begin{array}{c} \text{O} \\ \\ \text{Na}^+-\text{O}-\text{As}-\text{OH} \\ \\ \text{O}-\text{Na}^+ \end{array}$ | O=As-O-Na ⁺ |
| Identification numbers: | | | | |
| CAS registry | 7778-44-1 | 1303-00-0 | 7778-43-0 | 7784-46-5 |

Table 6. Physical and Chemical Properties of Arsenic and Selected Inorganic Arsenic Compounds

| Property | Arsenic | Arsenic acid | Arsenic pentoxide | Arsenic trioxide |
|--|---|----------------------------------|---|---|
| Molecular weight | 74.92 | 150.95 ^b | 229.84 | 197.84 |
| Color | Gray | White | White | White ^e |
| Physical state | Solid | Solid | Solid | Solid ^c |
| Melting point | 817 °C at 28 atm | 35.5 °C | Decomposes at 315 °C | 312.3 °C |
| Boiling point | 613 °C sublimes | Loses H ₂ O at 160 °C | No data | 465 °C |
| Density ^a | 5.727 g/cm ³ | 2.0–2.5 g/cm ³ | 4.32 g/cm ³ | 3.738 g/cm ³ |
| Odor | Odorless ^g | No data | No data | Odorless ^d |
| Odor threshold: | | | | |
| Water | No data | No data | No data | No data |
| Air | No data | No data | No data | No data |
| Solubility: | | | | |
| Water | Insoluble | 3,020 g/L at 12.5 °C | 1,500 g/L at 16 °C 767 g/L at 100 °C | 37 g/L at 20 °C 115 g/L at 100 °C |
| Organic solvent(s) | No data | Soluble in alcohol | Soluble in alcohol | Slightly soluble in alcohol ^f |
| Acids | Soluble in nitric acid | No data | Soluble in acid ^d | Soluble in hydrogen chloride ^g |
| Partition coefficients: | | | | |
| Log K _{ow} | No data | No data | No data | No data |
| Log K _{oc} | No data | No data | No data | No data |
| Vapor pressure | 1 mm Hg at 373 °C ^d 40 mm Hg at 483 °C ^d 100 mm Hg at 518 °C ^d | No data | No data | 66.1 mmHg at 312 °C ^d |
| Henry's law constant at 24.8 °C | No data | No data | No data | No data |
| Autoignition temperature | No data | No data | No data | Nonflammable ^d |
| Flashpoint | No data | No data | No data | No data |
| Flammability limits in air | No data | No data | No data | No data |
| Conversion factors: | No data | No data | No data | No data |
| ppm (v/v) to mg/m ³ in air at 25 °C | | | | |
| mg/m ³ to ppm (v/v) in air at 25 °C | | | | |
| Explosive limits | No data | No data | No data | No data |
| Valence states | 0 ^e | +5 ^e | +5 ^e | +3 ^e |

| Property | Calcium arsenate | Gallium arsenide | Disodium arsenate | Sodium arsenite |
|--|--------------------------------------|-------------------------------------|--|-----------------------------|
| Molecular weight | 398.08 | 144.64 | 185.91 ^c | 129.91 |
| Color | Colorless ^f | Dark gray | No data | Gray-white |
| Physical state | Solid | Solid | Solid ^f | Solid |
| Melting point | No data | 1238 •C • | No data | No data |
| Boiling point | No data | No data | No data | No data |
| Density ^g | 3.62 g/cm ³ | 5.31 ^c g/cm ³ | 1.87 ^{ch} g/cm ³ | 1.87 g/cm ³ |
| Odor | Odorless ^d | No data | Odorless ^d | No data |
| Odor threshold: | | | | |
| Water | No data | No data | No data | No data |
| Air | No data | No data | No data | No data |
| Solubility: | | | | |
| Water | 0.13 g/L at 25 •C • | No data | Soluble in water, glycerol ^h | Very soluble |
| Organic solvents | Insoluble | No data | Slightly soluble in alcohol ^h | Slightly soluble in alcohol |
| Acids | Soluble in dilute acids ^d | No data | No data | No data |
| Partition coefficients: | | | | |
| Log K _{ow} | No data | No data | No data | No data |
| Log K _{oc} | No data | No data | No data | No data |
| Vapor pressure at 25 •C • | No data | No data | No data | No data |
| Vapor pressure at 30 •C • | No data | No data | No data | No data |
| Henry's law constant at 24.8 •C • | No data | No data | No data | No data |
| Autoignition temperature | No data | No data | No data | No data |
| Flashpoint | No data | No data | No data | No data |
| Flammability limits in air | No data | No data | No data | No data |
| Conversion factors: | No data | No data | No data | No data |
| ppm (v/v) to mg/m ³ in air at 25 •C • | | | | |
| mg/m ³ to ppm (v/v) in air at 25 •C • | | | | |
| Explosive limits | No data | No data | No data | No data |
| Valence states | +5 ^g | -3 | +5 | +3 |

^aAll information obtained from Weast 1985, except where noted.

^bValue for H₂AsO₄ • ½ H₂O

^cMerck 1989

^dHSDB 1990

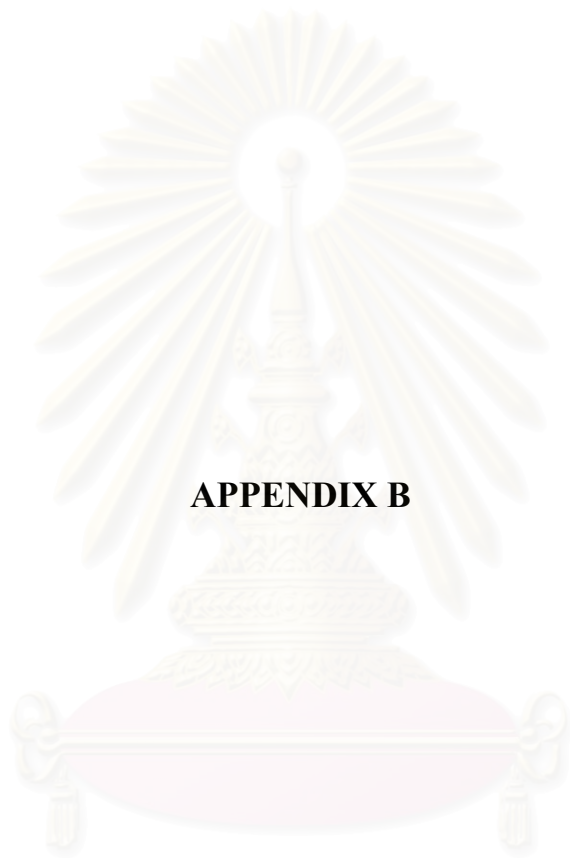
^eEPA 1982d

^fSax and Lewis 1989

^gWhen a property is a function of temperature, the temperature is at room temperature unless otherwise specified.

^hHeptahydrate

สถาบันวิทยบริการ
จุฬาลงกรณ์มหาวิทยาลัย



APPENDIX B

สถาบันวิทยบริการ
จุฬาลงกรณ์มหาวิทยาลัย

SDS-PAGE

A. Stock Solution and Reagents

1. 30% Acrylamide/Bis Solution (37.5:1)

(Bio-Rad, Cat. No. 161-0158~ 500 mL)

Store at 4°C.

2. TEMED

(Sigma, Cat. No. T8133, 50 mL) ./

Store at room temperature.

3. 1.5 M Tris-HCl, pH 8.8 (200 mL)

Tris base 36.3 g

DDW 150 mL

Adjust to pH 8.8 With 6N HCl

Make to 200 mL With DDW.

Store at room temperature.

4. 0.5 M Tris-HO, pH 6.8 (100 mL)

Tris base 6 g

DDW 60 mL

Adjust to pH 6.8 with 6N HCl

Make to 100 mL with DDW.

Store at room temperature.

5. 10% SDS (100 mL)

Dissolve 10 g SDS in 90 mL DDW with gentle stirring and bring to 100mL with

DDW. Store at room temperature.

6. 3X SDS Sample Buffer (SDS reducing buffer)

DDW 2.5 mL

| | |
|------------------------|---------|
| 0.5 M Tris-HCl, pH 6.8 | 3.75 mL |
| Glycerol | 3.0 mL |
| SDS | 0.6 g |
| DTT (Dithiothreitol) | 231 mg |
| Bromophenol blue | 30 mg |

| | |
|-------|-------|
| Total | 10 mL |
|-------|-------|

Loading buffer = 1X SDS Sample Buffer (dilute 3X SDS Sample Buffer to 1X)

7. 10X Electrophoresis Buffer (EP buffer)

| | |
|-----------|--------|
| Tris base | 30.2 g |
| Glycine | 150 g |
| DDW to | 1 L |

8. Running Buffer

| | |
|---------------|--------|
| 10X EP Buffer | 100 mL |
| 10% SDS | 10 mL |
| DDW | 890 mL |

9. Transfer Buffer

| | |
|---------------|--------|
| 10X EP Buffer | 100 mL |
| Methanol | 200 mL |
| DDW | 700 mL |

10. 10% APS

| | |
|---------------------|-------|
| Ammonium persulfate | 1 g |
| DDW | 10 mL |

250 μ l aliquot in eppendoff tube and store at -20°C .

B. Gel Preparation

1. Assembling the Glass Plate Sandwiches

2. Preparing Separating Gel

(total volume 10 ml for two mini-gels with spacer thickness of 1 mm)

| | |
|------------------------|---------|
| | 15 % |
| DDW | 2.35 ml |
| 1.5 M Tris-HCl, pH 8.8 | 2.5 ml |
| 30 % Arc/Bis (37.5:1) | 5.0 ml |
| 10% SDS | 100 ul |
| Mix | |
| 10% APS | 50 ul |
| Mix | |
| TFMED | 5 ul |

Mix, and immediately pour the solution smoothly to the gel sandwiches (4.0 mL for each). Immediately overlay the solution with DDW water. Allow the gel to polymerize for 45 min to 1 h.

After polymerized, rinse off the overlay DDW. Dry the area above the separating gel with filter paper before pouring the stacking gel.

3. Preparing Stacking Gel

(Total volume 10 ml)

| | |
|------------------------|---------|
| DDW | 6.1 ml |
| 0.5 M Tris-HCl, pH 6.8 | 2.5 ml |
| 30% Arc/Bis (37.5:1) | 1.33 ml |
| 10% SDS | 100 ul |
| Mix | |
| 10% APS | 50 ul |
| TEMED | 10 .ul |

Mix and immediately pour the stacking gel solution smoothly to completely fill the gel sandwich and insert the comb. Let the gel polymerize for 30 min -1 h. Remove the comb by pulling it straight up slowly and gently. Rinse the wells completely with DDW. The gels are now ready for use. ,

C. Loading The Samples and Running The Gel

1. Place the gel cassette in to the buffer chamber
2. Fill the buffer chamber with 1X running buffer
3. Load the samples into the wells under the running buffer. (Note: The sample buffer must contain 10% glycerol in order to underlay the sample in the well without mixing). Load molecular weight marker (Rainbow Marker is good) into one well
4. Apply power to begin electrophoresis. The, recommended power condition for optimal resolution with minimal thermal band distortion is 120-150 V, constant voltage setting. Run the gel until bromophenol blue reaches the level about 5 mm from the bottom of the gel.

Western Blot

A. Stock Solutions and Reagents

1. 1X Transfer Buffer (1 L)

| | |
|---------------|--------|
| 10X EP buffer | 100 ml |
| Methanol | 200 ml |
| DDW | 700 ml |

Mix. Store at 4°C.

2. 10X TBST (Tris-buffered saline with Tween-20)

To prepare 1 L of 10X TBST

| | |
|------|--------|
| Tris | 24.2 g |
| NaCl | 80 g |
| DDW | 800 mL |

Adjust pH to 7.6 with

Make to 1 L with DDW

| | |
|----------|-------|
| Tween-20 | 10 mL |
|----------|-------|

Mix with a stirrer. Store at room temperature

3. Primary Antibody

Specific to target protein. The antibody (IgG) is better to be dissolved in 10 mM HEPES {pH 7.5}. 100 μ g/mL BSA. 50% glycerol Store at -20°C .

4. Secondary Antibody

Anti-rabbit or anti-mouse antibody conjugated to horseradish peroxidase (HRP). Store at -20°C .

5. ECL (Western blotting detection reagents)

Amersham, Catalog No. RPN 2106.

Store at 4°C .

6. Transfer Membrane

Hybond

7. Filter Paper (for transfer)

Biorad

8. Nonfat Dry Milk

Biorad

9. Hyperfilm

Amersham, Catalog No. RPN1678H.

10. Stripping Buffer

| | |
|--------------------------|-------------|
| 1 M Tris, pH 6.8 | 1.25 ml |
| 10% SDS | 2.0 ml |
| β -mercaptoethanol | 150 μ l |
| DDW | 15 ml |

B. Western Immunoblotting -

I Protein Transfer

- 1) Prewet the filter papers and transfer membranes with transfer buffer.
- 2) Place a piece of wetted filter paper on a Scotch-Brite pad.
- 3) Place the gel (cut off stacking gel). Onto this filter paper. Remove any air bubbles between gel and filter paper.
- 4) Place a piece of wetted transfer membrane onto the gel and remove any air bubbles.
- 5) Place another piece of wetted filter paper on the transfer membrane and remove all air bubbles.
- 6) Place another Scotch-Brite pad on top of this filter paper.
- 7) Place this sandwich into a plastic support (It is important to orientate the sandwich so that the transfer membrane side faces the anodal (i.e., positively charged) side of the transfer tank
- 8) Place the support containing the sandwich into the transfer tank in the correct orientation.
- 9) Fill the tank with transfer buffer.
- 10) Connect the leads of the power supply to the corresponding anodal and cathodal sides of the transfer apparatus.
- 11) Electrophoretically transfer the proteins from the gel to the transfer membrane at 60

II Membrane Blocking and Antibody Incubations

- 1) After transfer, wash membrane with 25 ml TBST for 5 min at room temperature.
- 2) Incubate membrane in 25 mL of Blocking Buffer for 1-3 h at room temperature or overnight at 4°C. (Blocking Buffer: dissolve 5 g of nonfat dry milk in 100 ml TBST.)
- 3) Incubate membrane and primary antibody in 5-10 ml Blocking Buffer (at the appropriate dilution, usually 1:500-1: 3000 or 1 µg IgG in 0.5-3.0 ml) with gentle agitation overnight at 4 °C.)

- 4) Wash 3 times for 5 min each with 25 ml TBST
- 5) Incubate membrane with HRP-conjugated anti-rabbit (1:2000) or HRP-conjugated anti-mouse (1:5000) secondary antibody in 5-10 ml Blocking Buffer" with gentle agitation for 1 h at room temperature. (The selection of secondary antibody depend on the source of primary antibody. If primary antibody is from rabbit then use HRP-conjugated anti-rabbit. If primary antibody is from mouse, then use HRP-conjugated anti-mouse.)
- 6) Wash membrane twice for 5 min each with 25 ml TBST, and then wash membrane with 25 ml TBST for at least 30 min with gentle agitation at room temperature.
- 7) Incubate membrane with 10 ml ECL (5 mL A + 5 mL B) with gentle agitation for 30 s - 1 min at room temperature.
- 8) Drain membrane of excess solution. wrap in Saran Wrap and expose to Hyperfilm for a few seconds to a few minutes depends on the signal strength.

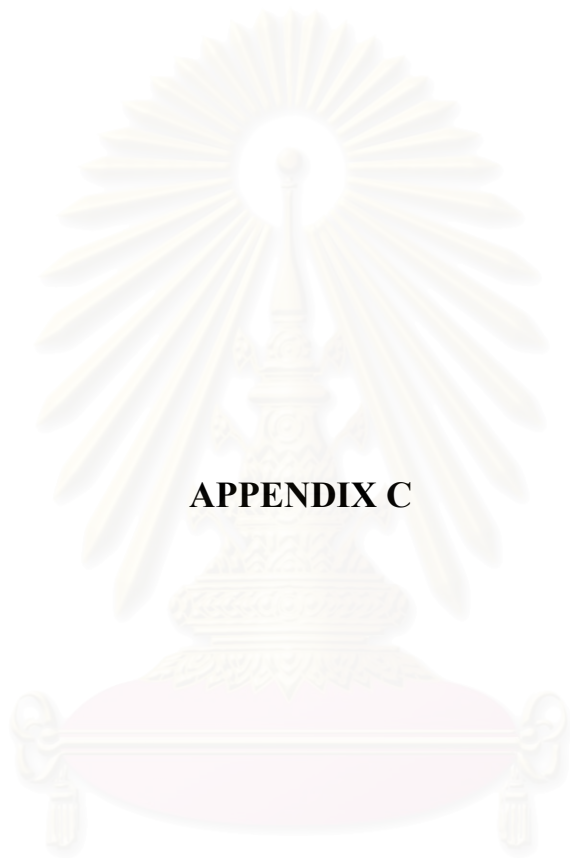
Immunoprecipitation of Proteins

1. Wash adherent cells twice in the dish or flask with ice-cold PBS and drain off PBS. Wash non-adherent cells in PBS and centrifuge at 800 to 1000 rpm in a table-top centrifuge for 5 minutes to pellet the cells.
2. Add ice-cold lysate buffer to cells (1 ml per 10^7 cells/100 mm dish/150 cm² flask; 0.5 ml per 5×10^6 cells/60 mm dish/75 cm² flask).
3. Scrape adherent cells off the dish or flask with either a rubber policeman or a plastic cell scraper that has been cooled in ice-cold distilled water. Transfer the cell suspension into a centrifuge tube. Gently mix the suspension on either a rocker or an orbital shaker at 4°C for 15 minutes to lyse cells.

4. Centrifuge the lysate at 14,000 x g in a precooled centrifuge for 15 minutes. Immediately transfer the supernatant fraction to a fresh centrifuge tube and discard the pellet.
5. To prepare protein A or G agarose/sepharose, wash the beads twice with PBS and restore to a 50% slurry with PBS. It is recommended to cut the tip off of the pipette tip when manipulating agarose beads to avoid disruption of the beads.
6. Pre-clear the cell lysate by adding 100 microliters of either protein A or G agarose/sepharose bead slurry (50%) per 1 ml of cell lysate and incubating at 4°C for 10 minutes on a rocker or orbital shaker. Pre-clearing the lysate will reduce non-specific binding of proteins to the agarose or sepharose when it is used later on in the assay.
7. Remove the protein A or G beads by centrifugation at 14,000 x g at 4°C for 10 minutes. Transfer the supernatant to a fresh centrifuge tube.
8. Determine the protein concentration of the cell lysate.
9. Add the recommended volume of the immunoprecipitating antibody to 500 microliters (i.e., 500 micrograms) of cell lysate. The optimal amount of antibody that will quantitatively immunoprecipitate the protein of interest should be empirically determined for each cell model.
10. Gently mix the cell lysate/antibody mixture for either 2 hours or overnight at 4°C on a rocker or an orbital shaker. A 2 hour incubation time is recommended for the immunoprecipitation of active enzymes for kinase or phosphatase assays.
11. Capture the immunocomplex by adding 100 microliters protein A or G agarose/sepharose bead slurry (50 microliters packed beads) and gently rocking on either a rocker or orbital shaker for either 1 hour or overnight at 4°C. In many instances, immunocomplex capture can be enhanced by adding 2 micrograms of a bridging antibody (e.g., rabbit-anti-mouse IgG). This is especially important with

antibodies that bind poorly to protein A such as mouse IgG₁ or antibodies generated in chicken.

12. Collect the agarose/sepharose beads by pulse centrifugation (5 seconds in the microcentrifuge at 14,000 rpm). Discard the supernatant fraction and wash the beads 3 times with 800 microliters ice-cold lysate buffer.
13. Resuspend the agarose/sepharose beads in 60 microliters 2 x sample buffer and mix gently. This will allow for sufficient volume to run three lanes.
14. The agarose/sepharose beads are boiled for 5 minutes to dissociate the immunocomplexes from the beads. The beads are collected by centrifugation and SDS-PAGE is performed with the supernatant fraction. Alternatively, the supernatant fraction can be transferred to a fresh microcentrifuge tube and stored frozen at -20°C for later use. Frozen supernatant fractions should be reboiled for 5 minutes directly prior to loading on a gel.



APPENDIX C

สถาบันวิทยบริการ
จุฬาลงกรณ์มหาวิทยาลัย

Transient Transfection

Protocol:

1. Seed a six-well tissue culture plate with $1-2 \times 10^5$ COS-7 cells in 2 ml of DMEM supplemented with 10% fetal bovine serum. Incubate for 18-24 hours at 37°C in a CO₂ humidified incubator or until the cells are 40-60% confluent.
2. Dilute 1-2 micrograms of DNA into 100 microliters OPTI-MEM (serum free MEM) in a sterile tube. To this tube, add 6 microliters of PLUS Reagent found in the LIPOFECTAMINE™ PLUS Reagent kit (Life Technologies). Allow mixture to stand for 15 minutes at room temperature. In a second tube dilute 4 microliters of LIPOFECTAMINE™ Reagent into 100 microliters OPTI-MEM.
3. Combine the two solutions, mixing gently and incubate at room temperature for 10-15 minutes.
4. Wash cells once with 2 ml OPTI-MEM.
5. For each transfection, add 0.8 ml serum-free medium to each tube containing the LIPOFECTAMINE™ PLUS Reagent - DNA complexes. Mix gently and overlay the complexes onto cells.
6. Incubate the cells for 3 hours at 37°C in a CO₂ humidified incubator.
7. Remove the DNA-containing medium and replace with 2 ml of DMEM supplemented with 10% fetal bovine serum. Incubate cells at 37°C in a CO₂ humidified incubator for an additional 48-72 hours.
8. Assay cell extracts for gene expression or activity at 24-48 hours post-transfection.

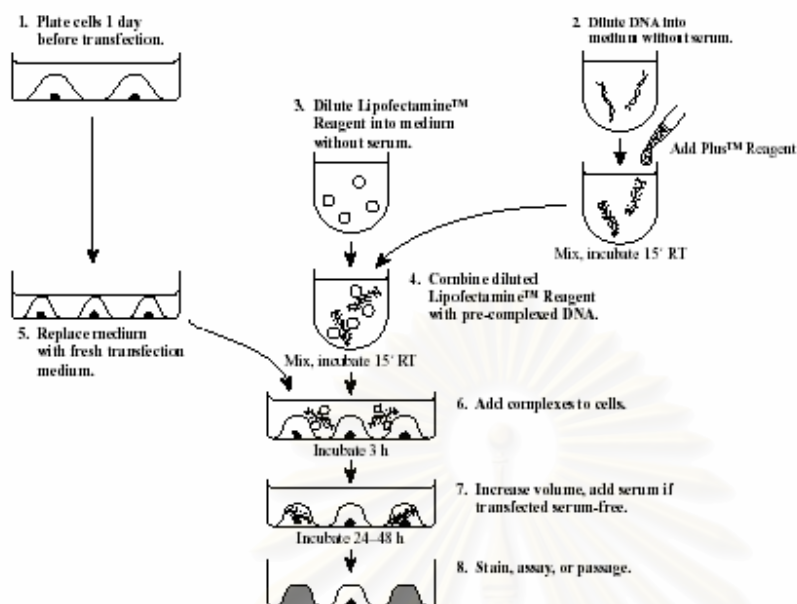


Figure 53. Diagram of transfection procedure with Lipofectamine Reagent.

สถาบันวิทยบริการ
จุฬาลงกรณ์มหาวิทยาลัย



APPENDIX D

สถาบันวิทยบริการ
จุฬาลงกรณ์มหาวิทยาลัย

Cell viability assay

Cell Counting Using a Hemacytometer

Proper use of a hemacytometer is critical for obtaining an accurate count of cells.

Procedure

1. Prepare a cell suspension in growth medium.
2. Prepare a hemacytometer for use.
 - a. Carefully clean all surfaces of the hemacytometer and coverslip.
 - b. Take care to ensure that all surfaces are completely dry using non-linting tissue.
 - c. Center the coverslip on the hemacytometer.
3. Pipet approximately 9 μl (this volume will vary with the brand of hemacytometer) of the cell suspension into one of the two counting chambers.
 - a. Use a clean pipette tip.
 - b. Be sure that the suspension is thoroughly, but gently, mixed before drawing the sample.
 - c. Fill the chambers slowly and steadily.
 - d. Avoid injecting bubbles into the chambers.
 - e. Do not overfill or under fill the chambers.
4. Count the Cells.
 - a. Allow the cell suspension to settle for at least 10 seconds.
 - b. Count all the cells in each of the four 1 mm^3 corner squares.
 - c. DO count the cells touching the top or left borders.
 - d. DO NOT count the cells touching the bottom or right borders.
5. Determine the Cell Count.
 - a. Calculate the total cells counted in the four corner squares.
 - b. If the total cell count is less than 100, or if more than 10% of the cells counted appear to be clustered, carefully re-mix the original cell suspension and repeat steps 2 through 4 above.
 - c. If the total cell count is greater than 400, dilute the suspension so the count will be 100-400 cells. Then repeat steps 2 through 4 above.
6. Calculate the cell count using the equation:

$$\frac{\text{cells}}{\text{ml}} = (n) \times 10^4$$

(n = the average cell count per square of the four corner squares counted.)

Example: If the calculated average (n) of cells in the four 1 mm corner squares of the hemacytometer is 30:

$$\frac{\text{cells}}{\text{ml}} = (n) \times 10^4 \quad (\text{or}) \quad \frac{\text{cells}}{\text{ml}} = 30 \times 10,000 = 300,000 \frac{\text{cells}}{\text{ml}}$$

7. Determine the total number of cells in the total suspension volume.

- a. Determine the total volume of the cell suspension.
- b. Multiply the volume of the cell suspension by the cells/ml value calculated above.

Example: If the initial suspension volume is 2 ml:

$$\frac{\text{cells}}{\text{ml}} \times \text{total volume} = 300,000 \frac{\text{cells}}{\text{ml}} \times 2 \text{ ml} = 600,000 \text{ cells}$$

สถาบันวิทยบริการ
จุฬาลงกรณ์มหาวิทยาลัย

Assessment Of Cell Viability with Trypan Blue

Trypan blue is a dye that enables easy identification of dead cells. Dead cells take up the dye and appear blue with uneven cell membranes. By contrast, living cells repel the dye and appear refractile and colorless. Evaluate on bright field and not phase.

Procedure

1. Prepare the hemacytometer for use.
 - a. Carefully clean all surfaces of the hemacytometer and cover slip.
2. Stain the cells
 - a. Transfer 50 μ l of 0.4% Trypan Blue into a clean tube.
 - b. Add 50 μ l of the prepared cell suspension into the tube containing the stain.
 - c. Mix the solution thoroughly, but gently. Take care to avoid making excessive bubbles.
 - d. Allow the mixture to sit for 2 to 3 minutes after mixing.

Note: Do not let the cells sit in the dye for more than five minutes because both the living and dead cells will begin to take-up the dye after five minutes.

3. Pipet approximately 9 μ l of the Trypan Blue/cell suspension mixture (this volume will vary with brand of hemacytometer) into one of the two counting chambers.
 - a. Use a clean pipette tip.
 - b. Be sure that the suspension is mixed thoroughly but gently before drawing the samples.
 - c. Fill the chambers slowly and steadily.
 - d. Avoid injecting bubbles into the chambers.
 - e. Do not overfill or under fill the chambers.
4. Determine Cell Viability
 - a. Allow the suspension to settle in the chambers for at least 10 seconds.
 - b. Count all of the stained cells in each of the four corner squares of the hemacytometer.
 - c. Separately count all of the unstained cells in the same squares.

5. Calculate the cell viability using the equation:

$$\% \text{ Cell Viability} = \frac{\text{number of unstained (living) cells}}{\text{Total cells counted (stained + unstained)}} \times 100\%$$

Example: If a total of 300 cells (stained + unstained) are counted and 200 are identified as living cells (unstained), then the viability is calculated as:

$$\% \text{ Cell Viability} = \frac{200 \text{ live cells}}{300 \text{ total cells}} \times 100\% = 67\%$$



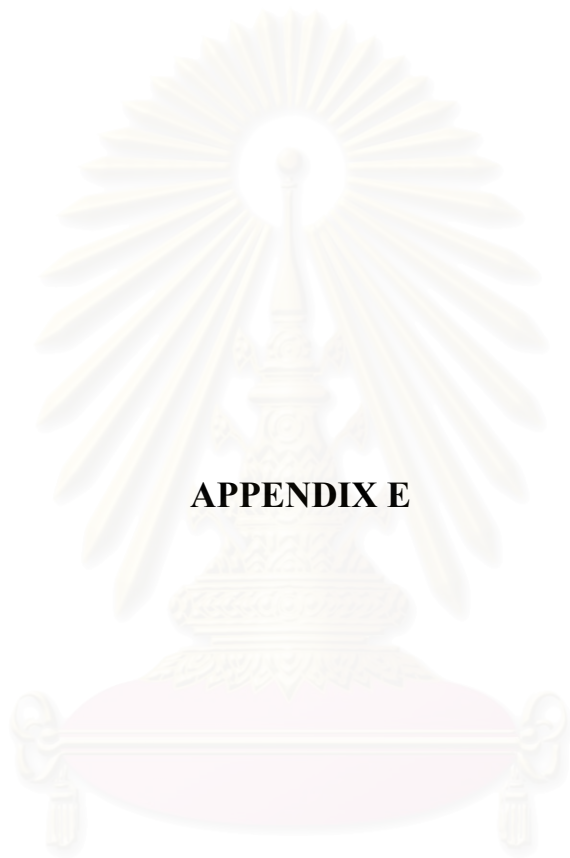
สถาบันวิทยบริการ
จุฬาลงกรณ์มหาวิทยาลัย

MTT Cell Proliferation Assay

The MTT Cell Proliferation Assay is a sensitive method for the measurement of cell proliferation based upon the reduction of the tetrazolium salt 3,[4,5-dimethylthiazol-2-yl]-2,5-diphenyltetrazolium bromide (MTT). MTT is reduced to an insoluble formazan dye by mitochondrial enzymes associated with metabolic activity. The reduction of MTT is primarily due to glycolytic activity within the cell and is dependent upon the presence of NADH and NADPH.

procedure

1. MTT solution: 5 mg/ml MTT (Sigma). This solution is filtered through a 0.2 μm filter and stored at 2-8°C.
2. Add MTT working solution into wells being assayed, for example 10 μl for each well of 24-well plate. Incubate at 37°C for 1-4 hrs (this time depends on cell density and cell type).
3. At the end of the incubation period, the medium can be moved if working with attached cells.
4. The converted dye is solubilized with 400 μl DMSO. Pipette up and down several times to make sure the converted dye dissolves completely.
5. Absorbance of the converted dye is measured at a wavelength of 570nm



APPENDIX E

สถาบันวิทยบริการ
จุฬาลงกรณ์มหาวิทยาลัย

siRNA Technology

Silencing the Messenger

Small interfering RNA (siRNA) is a tool that is revolutionizing bioscience research. The increased use of siRNA in peerreviewed publications clearly demonstrates that it is an incredibly powerful means to specifically knock-down a gene's message, and subsequently the protein level of the targeted gene. In this manner, cellular-based assays can be conducted in the absence and presence of the targeted gene's protein. The value of such an experiment has long been known as researchers the world over have employed genetic knock-out technologies, dominantnegatives and chemical inhibitors of protein activities to perform such experiments. The use of siRNA is replacing all three of these methodologies.

LIMITATIONS OF TRADITIONAL METHODOLOGIES

Traditional methodologies for generating cellular "null" backgrounds have significant limitations. Genetic knock-out models, generated by interrupting a gene through the use of a targeting vector, are very labor intensive and costly to not only produce but also maintain. In addition, a developmental lethality resulting from the knock-out of the targeted gene may prevent the knock-out from ever being studied in an adult organism. Dominant negatives, much like genetic knock-outs, are often difficult to make. Furthermore, to conclusively demonstrate a dominant negative's ability to reduce or rid a cell of a targeted protein's function can be immensely challenging. Chemical inhibitors of protein activity have limitations in that they are very often not specific for the targeted protein. Therefore, any result that is obtained from their experimental usage must always be questioned as to whether the outcome seen was the result of an off-target effect.

ADVANTAGES OF siRNA OVER ALTERNATIVES

The advantages that siRNA provides over the alternative technologies are numerous: decreased time, decreased cost and increased specificity. Using siRNA to generate a knock-down of a targeted gene can be performed in days versus months or years as compared to the time necessary using the traditional methods. Additionally, with siRNA,

the researcher can simultaneously perform experiments in any cell type of interest, as opposed to genetic knock-outs which are typically done in mouse embryonic stem cells (ES cells). If the siRNA cell culture experiments require further *in vivo* testing, the option to adapt siRNA usage to rodent models exists. As important as speed is for many researchers, cost is equally important. Experiments using siRNA can be performed at a fraction of the cost of generating genetic knock-out models and dominant negatives. In addition, siRNA mediated gene knock-down has been shown to be highly sequence specific. This specificity is also characteristic of genetic knock-out models, but that comes at the cost of time and money when compared to using siRNA. In contrast, chemical inhibitors of protein activity and dominant negatives can be inexpensive and quick to use, but often are not specific for their intended target. In particular, chemical inhibitors provide a level of specificity for their target that is undesirable to many peerreviewed journals today. The use of siRNA in place of chemical inhibitors adds significantly to the specificity of the experiment making the resulting data far more credible without adding to its cost or time.



สถาบันวิทยบริการ
จุฬาลงกรณ์มหาวิทยาลัย

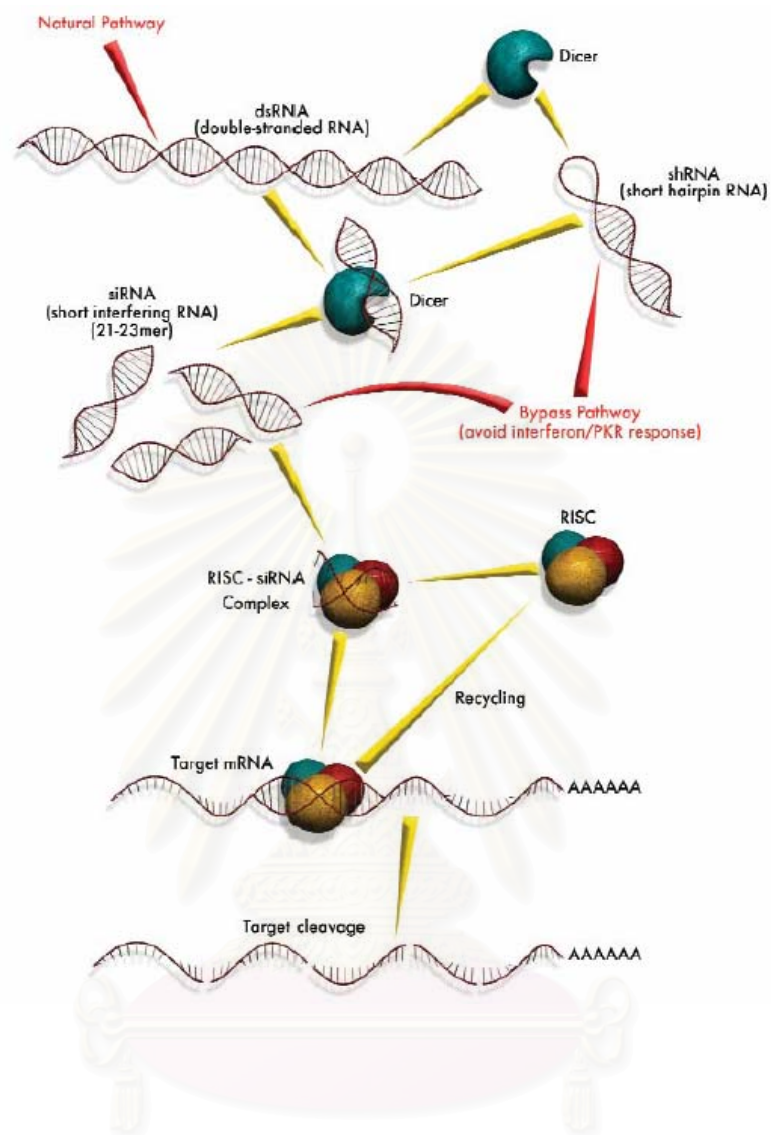


Figure 54. siRNA – Mediated mRNA Degradation Pathway

RNA interference was originally characterized in lower eukaryotes as a cellular illustration, this is noted as the "natural pathway". Upon entry to the cell, the enzyme "dicer" recognizes the dsRNA and processes it into 21-23 nucleotide duplexes that are called small interfering RNA (siRNA). In mammalian cells, introduction of long dsRNA has been shown to activate the interferon/PKR response which results in the cell shutting down its protein translation machinery. This interferon response can be bypassed in mammalian cells if siRNA or short hairpin RNA (shRNA) are introduced. Synthetic

siRNA requires no further processing, but shRNA, it is proposed, is processed by dicer. This processing serves to remove the loop from the shRNA and create a siRNA duplex. siRNA then associates with numerous proteins to form the RNA-induced silencing complex (RISC). In an ATP dependent manner, RISC unwinds the siRNA duplex whereby the antisense strand guides the activated RISC-siRNA complex to its targeted mRNA for hybridization and ultimately its degradation.



สถาบันวิทยบริการ
จุฬาลงกรณ์มหาวิทยาลัย



APPENDIX F

สถาบันวิทยบริการ
จุฬาลงกรณ์มหาวิทยาลัย

HUMAN UMBILICAL VEIN ENDOTHELIAL CELLS

(HUVECs)

HUVECs is isolated from human umbilical cord vein by trypsin digestion. It is identified by the "cobblestone" on morphology exhibited by confluent monolayer (figure 40) and positive staining for factor VIII-related antigen and Weibel-Palade body.

HUVEC (from Clonetics™), cryopreserved, in EGM-2 >500,000 cells/amp

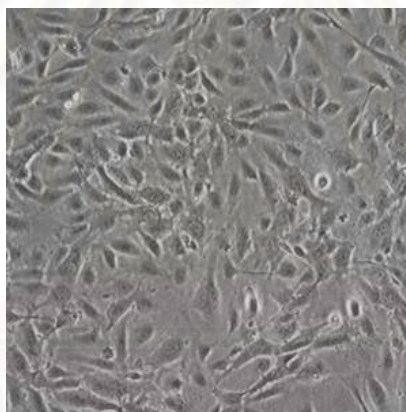


Figure 40 HUVEC: Photograph from phase contrast microscopy.

EGM-2 (Endothelial Growth Media-2)

Compose of endothelial basal medium (EBM-2) and the growth factors

- hEGF
- Hydrocortisone
- GA-1000 (Gentamicin, Amphotericin-B)
- FBS 10 ml
- VEGF
- hFGF-B

- R³ -IGF-1
- Ascorbic Acid
- Heparin
- Final serum concentration 2% (fetal bovine serum)

Cells Cultureing

Process

1. The recommended seeding density for HUVEC is 2,500 to 5,000 cells/cm².
2. Add the appropriate amount of medium to the vessels (1 ml/5 cm²) and allow the vessels to equilibrate in a 37°C, 5% CO₂ humidified incubator for at least 30 minutes.
3. Wipe cryovial with ethanol before opening. Quickly thaw the cryovial in a 37°C water bath being careful not to submerge the entire vial.
4. Resuspend the cells in the cryovial and using a micropipette, dispense cells into the culture vessels set up earlier. Gently rock the culture vessel to evenly distribute the cells and return to the incubator.

Subculturing

The following instructions are for a 25 cm² flask. Adjust all volumes accordingly for other size flasks.

Preparation for subculturing the first flask:

1. Subculture the cells when they are 70 to 80% confluent and contain many mitotic figures throughout the flask.
2. For each 25 cm² of cells to be subcultured:
 - Thaw 2 ml of Trypsin/EDTA and allow to come to room temperature.
 - Allow 5 ml of HEPES Buffered Saline Solution (HEPES-BSS) to come to room temperature.
 - Remove growth medium from 4°C storage and allow to start warming to room temperature.
3. Prepare new culture vessels.

4. Subculture one flask at a time. All flasks following the first flask will be subcultured following an optimization of this protocol based on calculated cell count, cell viability, and seeding density.

In a sterile field:

1. Aspirate the medium from one culture vessel.
2. Rinse the cells with 5 ml of room temperature HEPES-BSS. DO NOT forget this step. The medium contains complex proteins that neutralize the trypsin.
3. Aspirate the HEPES-BSS from the flask.
4. Cover the cells with 2 ml of Trypsin/EDTA solution.
5. Examine the cell layer microscopically.
6. Allow the trypsinization to continue until approximately 90% of the cells are rounded up. This entire process takes about 2 to 6 minutes, depending on cell type.
7. At this point, rap the flask against the palm of your hand to release the majority of cells from the culture surface. If only a few cells detach, you may not have let them trypsinize long enough. Wait 30 seconds and rap again. If cells still do not detach, wait and rap every 30 seconds thereafter.
8. After cells are released, neutralize the trypsin in the flask with 4 ml of room temperature Trypsin Neutralizing Solution. If the majority of cells do not detach within seven minutes, the trypsin is either not warm enough or not active enough to release the cells. Harvest the culture vessel as described above, and either re-trypsinize with fresh, warm Trypsin/EDTA solution or rinse with Trypsin Neutralizing Solution and then add fresh, warm medium to the culture vessel and return to an incubator until fresh trypsinization reagents are available.
9. Quickly transfer the detached cells to a sterile 15 ml centrifuge tube.
10. Rinse the flask with a final 2 ml of HEPES-BSS to collect residual cells, and add this rinse to the centrifuge tube.
11. Examine the harvested flask under the microscope to make sure the harvest was successful by looking at the number of cells left behind. This should be less than 5%.
12. Centrifuge the harvested cells at 220 x g for 5 minutes to pellet the cells.

- a. Aspirate most of the supernatant, except for 100-200 μl .
 - b. Flick the cryovial with your finger to loosen the pellet.
13. Dilute the cells in 4 to 5 ml of growth medium and note the total volume of the diluted cell suspension.
 14. Count the cells with a hemacytometer or cell counter and calculate the total number of cells. Make a note of your cell yield for later use.
 15. If necessary, dilute the suspension with the HEPES Buffered Saline Solution (HEPES-BSS) to achieve the desired “cells/ml” and re-count the cells.
 16. Assess cell viability using Trypan Blue.
 17. Use the following equation to determine the total number of viable cells.

$$\text{Total \# of Viable Cells} = \frac{\text{Total cell count} \times \text{percent viability}}{100}$$

18. Determine the total number of flasks to inoculate by using the following equation. The number of flasks needed depends upon cell yield and seeding density.

$$\text{Total \# of Flasks to inoculate} = \frac{\text{Total \# of viable cells}}{\text{Growth area} \times \text{Rec. Seeding Density}}$$

19. Use the following equation to calculate the volume of cell suspension to seed into your flasks.

$$\text{Seeding Volume} = \frac{\text{Total volume of diluted cell suspension}}{\text{\# of flasks as determined in step 18}}$$

20. Prepare flasks by labeling each flask with the passage number, strain number, cell type and date.
21. Carefully transfer growth medium to new culture vessels by adding 1ml growth medium for every 5 cm^2 surface area of the flask (1 ml/5 cm^2).
22. After mixing the diluted cells with a 5 ml pipet to ensure a uniform suspension, dispense the calculated volume into the prepared subculture flasks.
23. If not using vented caps, loosen caps of flasks. Place the new culture vessels into a 37°C humidified incubator with 5% CO_2 .

Maintenance

1. Change the growth medium the day after seeding and every other day thereafter.

2. Warm an appropriate amount of medium to 37°C in a sterile container. Remove the medium and replace it with the warmed, fresh medium and return the flask to the incubator.
3. Avoid repeated warming and cooling of the medium. If the entire contents are not needed for a single procedure, transfer only the required volume to a sterile secondary container.



สถาบันวิทยบริการ
จุฬาลงกรณ์มหาวิทยาลัย



APPENDIX G

สถาบันวิทยบริการ
จุฬาลงกรณ์มหาวิทยาลัย

Protein Tyrosine Kinase Inhibitors

The design of specific inhibitors of tyrosine kinases is important both for fundamental research and for developing therapeutic strategies for the treatment of disorders such as cancer, atherosclerosis, psoriasis, and septic shock in which increased tyrosine kinase activity has been reported (Levitzki and Gazit, 1995; Weinstein et al. 1991; Ross, 1993). Two classes of protein tyrosine kinase inhibitors have been developed. One acts by binding to the ATP binding site and the other by binding to the substrate binding site of the enzyme.

Among the inhibitors that act at the ATP binding site, genistein is the most commonly used. One drawback of this class of inhibitors is that they exhibit greater cytotoxicity and cause nonspecific inhibition of serine/threonine kinases (Levitzki, 1990).

Gazit and others have developed a series of synthetic compounds, tyrphostins, (also known as AG compounds), that inhibit protein tyrosine kinases by binding to the substrate binding site (Gazit et al., 1989; Gazit et al., 1991). They structurally resemble tyrosine and erbstatin moieties and have hydrophobic characteristics which allow them to readily traverse the cell membrane. Many of the tyrphostins have selective and distinct inhibitory activities in various tyrosine kinase assay systems.

| Kinase inhibitors | Proteins |
|--------------------------|-----------------------|
| AG1478 | ErbB-1 receptor |
| AG825 | ErbB-2 receptor |
| AG1295 | PDGF receptor |
| AG1433 | PDGF β receptor |
| PD98059 | ERK |
| LY | Akt |
| Wortmanin | PKC |

AG1478

Synonym: 4-(3-Chloroanilino)-6,7-dimethoxyquinazoline

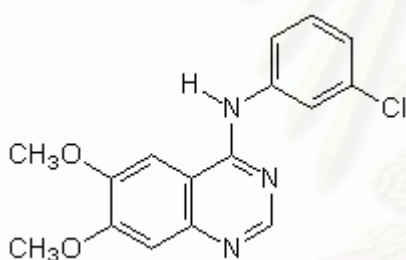
Description: A very potent and selective inhibitor of epidermal growth factor receptor kinase ($IC_{50} = 3 \text{ nM}$) versus HER2-neu ($IC_{50} >100 \text{ }\mu\text{M}$) and platelet-derived growth factor receptor kinase ($IC_{50} >100 \text{ }\mu\text{M}$). Abolishes MAP kinase (ERK) activation induced by Angiotensin II Also inhibits the activation of EGFR kinase and MAP kinase by 4-hydroxynonenal

Form: Off-white solid

Molecular Weight: 315.8

Molecular Formula: $C_{16}H_{14}ClN_3O_2$

Structure:



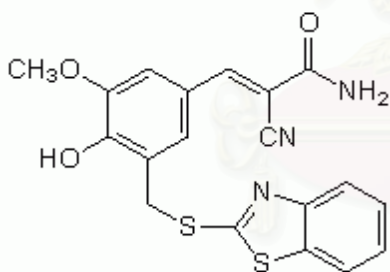
Purity: $\geq 95\%$ by HPLC

Solubility: DMSO (10 mg/ml)

Storage: Freezer (-20°C). Protect from light. Following reconstitution, aliquot and freeze (-20°C). This product is stable for 3 years as supplied. Stock solutions are stable for 2-3 months at -20°C .

AG825

- Synonym:** 4-Hydroxy-3-methoxy-5-(benzothiazolylthiomethyl)-benzylidenecyanoacetamide
- Description:** A potent and selective inhibitor of HER-2 (neu/erbB-2, IC₅₀ = 0.35 M) relative to HER-1 (IC₅₀ = 19 mM) autophosphorylation. The inhibition is competitive with respect to ATP binding. Enhances the chemosensitivity in non-small cell lung cancer (NSCLC) cell lines expressing high levels of p185^{neu}.
- Form:** Yellow solid
- Molecular Weight:** 397.5
- Molecular Formula:** C₁₉H₁₅N₃O₃S₂
- Structure:**



- Purity:** ≥95% by HPLC
- Solubility:** DMSO (10 mg/ml)
- Storage:** Freezer (-20°C). Protect from light. Following reconstitution, aliquot and freeze (-20°C). This product is stable for 3 years as supplied. Stock solutions are stable for 2-3 months at -20°C.

AG1433

Synonyms: 2-(3,4-Dihydroxyphenyl)-6,7-dimethylquinoxaline, HCl; SU 1433

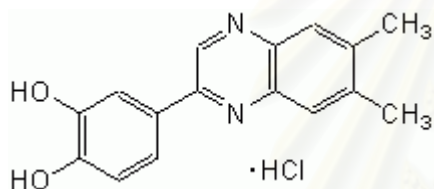
Description: A potent and specific inhibitor of the PDGF b-receptor kinase (IC₅₀ = 5.0 mM) and of KDR/Flk-1 (IC₅₀ = 9.3 mM). Also acts as an angiogenesis inhibitor.

Form: Pale yellow solid. Packaged under an inert gas.

Molecular Weight: 302.8

Molecular Formula: C₁₆H₁₄N₂O₂ HCl

Structure:



Purity: ≥95% by HPLC

Solubility: DMSO (3 mg/ml). Further dilute with aqueous buffers just before use.

Storage: Freezer (-20°C). Protect from light. Following reconstitution, aliquot and freeze (-20°C). This product is stable for 3 years as supplied. Stock solutions are stable for 1-2 weeks at -20°C.

สถาบันวิทยบริการ
จุฬาลงกรณ์มหาวิทยาลัย

AG1295

Synonym: Tyrphostin AG 1295; 6,7-Dimethyl-2-phenylquinoxaline

Description: Selectively inhibits platelet-derived growth factor (PDGF) receptor kinase (IC₅₀ = 500 nM) and the PDGF-dependent DNA synthesis (IC₅₀ = 2.5 mM) in Swiss 3T3 cells. Has no effect on epidermal growth factor (EGF) receptor autophosphorylation and shows only a weak effect on EGF- or insulin-stimulated DNA synthesis.

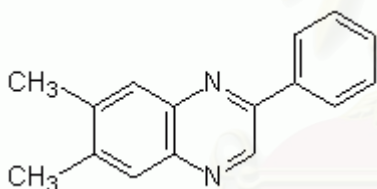
Form: Yellow solid

CAS Number: 71897-07-9

Molecular Weight: 234.3

Molecular Formula: C₁₆H₁₄N₂

Structure:



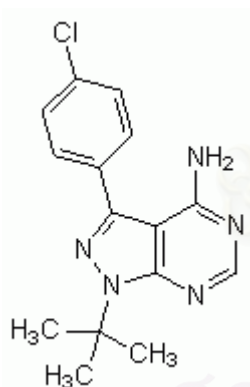
Purity: ≥95% by HPLC

Solubility: DMSO (10 mg/ml)

Storage: Freezer (-20°C). Protect from light. Following reconstitution, aliquot and freeze (-20°C). This product is stable for 3 years as supplied. Stock solutions are stable for up to 1 month at -20°C.

PP2

- Synonym:** AG 1879; 4-Amino-5-(4-chlorophenyl)-7-(*t*-butyl)pyrazolo [3,4-*d*] pyrimidine
- Description:** A potent and selective inhibitor of the src family of tyrosine kinases that is similar to PP1. Selectively inhibits p56lck (IC₅₀ = 4 nM), p59fynT (IC₅₀ = 5 nM), Hck (IC₅₀ = 5 nM), and Src (IC₅₀ = 100 nM) compared to other tyrosine kinases, such as EGF-R (IC₅₀ = 480 nM), JAK2 (IC₅₀ > 50 μM) or ZAP-70 (IC₅₀ > 100 μM). Also potently inhibits anti-CD3-stimulated tyrosine phosphorylation of human T cells (IC₅₀ = 600 nM).
- Form:** Off-white solid. Packaged under inert gas.
- Molecular Weight:** 301.8
- Molecular Formula:** C₁₅H₁₆ClN₅
- Structure:**



- Purity:** ≥95% by HPLC
- Solubility:** DMSO (20 mg/ml). Further dilute with aqueous buffers just prior to use.
- Storage:** FREEZER (-20°C). Following reconstitution, store in the refrigerator (+4°C). This product is stable for 3 years as supplied. Stock solutions are stable for up to 6 months at +4°C.

PD 98059

Synonym: 2'-Amino-3'-methoxyflavone

Description: Selective and cell-permeable inhibitor of MAP kinase kinase (MEK) that acts by inhibiting the activation of MAP kinase and subsequent phosphorylation of MAP kinase substrates. Pretreatment of PC-12 cells with PD 98059 completely blocks the 4-fold increase of MAP kinase activity produced by nerve growth factor (NGF; IC₅₀ = 2 μM); however, it has no effect on NGF-dependent tyrosine phosphorylation of the pp140trk receptor or its substrate Shc and does not block NGF-dependent activation of PI 3-kinase. Inhibits cell growth and reverses the phenotype of *ras*-transformed BALB 3T3 mouse fibroblasts and rat kidney cells.

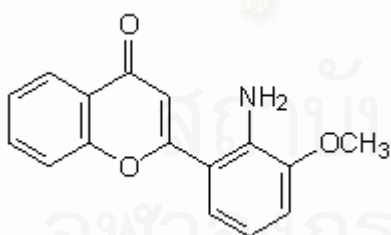
Form: Pale yellow solid

CAS Number: 167869-21-8

Molecular Weight: 267.3

Molecular Formula: C₁₆H₁₃NO₃

Structure:

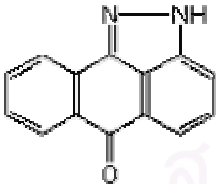


Purity: ≥98% by HPLC

Solubility: DMSO (20 mg/ml) and methanol (0.7 mg/ml)

Storage: Freezer (-20°C). Protect from light. Following reconstitution, aliquot and freeze (-20°C). This product is stable for 2 years as supplied. Stock solutions are stable for up to 3-4 months at -20°C.

SP 600125

- Synonyms:** JNK Inhibitor II, 5; anthra(1,9-*cd*)pyrazol-6(2*H*)-one; 1,9-pyrazoloanthrone
- Description:** A potent, cell-permeable, selective, and reversible inhibitor of *c*-Jun N terminal kinase (JNK) (IC₅₀ = 40 nM for JNK-1 and JNK-2 and 90 nM for JNK-3). The inhibition is competitive with respect to ATP. Exhibits over 300-fold greater selectivity for JNK as compared to ERK1 and p38-2 MAP kinases. Inhibits the phosphorylation of *c*-Jun and blocks the expression of IL-2, IFN- γ , TNF- α , and COX-2 in cells. Blocks IL-1-induced accumulation of phospho-Jun and induction of *c*-Jun transcription.
- Form:** Orangish solid. Packaged under an inert gas.
- CAS Number:** 129-56-6
- RTECS:** CB4585000
- Molecular Weight:** 220.2
- Molecular Formula:** C₁₄H₈N₂O
- Structure:**
- 
- Purity:** $\geq 98\%$ by HPLC
- Solubility:** DMSO (4 mg/ml). For every 10 μ M concentration of JNK Inhibitor II, include 0.1% DMSO in the culture medium. Pre-warming of culture medium and addition of BSA to the medium may enhance its solubility.
- Storage:** Freezer (-20°C). Protect from light. Following reconstitution, aliquot, flush with an inert gas, and store at -20°C. This product is stable for 3 years as supplied. Stock solutions are stable for 2 months at -20°C.

SB 203580

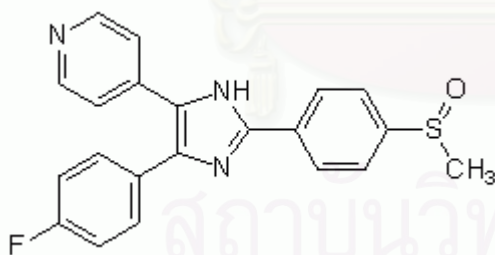
- Synonym:** 4-(4-Fluorophenyl)-2-(4-methylsulfinylphenyl)-5-(4-pyridyl) 1H-imidazole
- Description:** A highly specific, cell-permeable inhibitor of p38 kinase (IC₅₀ = 34 nM in vitro, 600 nM in cells). Also known as reactivating kinase (RK) and CSBP (cytokine synthesis anti-inflammatory drug binding protein). Does not significantly inhibit JNK or p42 MAP kinase even at 100 μM. Inhibits IL-1 and TNF-α production from LPS-stimulated human monocytes and the human monocyte cell line THP-1 (IC₅₀ = 50-100 nM). SB 203580 has also been shown to be an effective inhibitor of inflammatory cytokine production in vivo in both mice and rats.

Form: Pale yellow solid

Molecular Weight: 377.4

Molecular Formula: C₂₁H₁₆N₃OSF

Structure:



Purity: ≥98% by HPLC

Solubility: DMSO (30 mg/ml)

Storage: Freezer (-20°C). Protect from light. Following reconstitution, aliquot and freeze (-20°C). This product is stable for 5 years as supplied. Stock solutions are stable for up to 6 months at -20°C.

CURRICULUM VITAE

NAME Mrs Nopparat Nuntharatanapong
DATE OF BIRTH May 11, 1970
PLACE OF BIRTH Chiangmai, Thailand
NATIONALITY/RELIGION Thai/Buddhism
CONTACT ADDRESS 100/4-5 Moo.6 Bangkrauy-Sainoi St., Bangbuathong District,
Nonthaburi, 11110, Thailand
Tel: 66-2-9268844 Fax: 66-2-9268844
E-mail npparat@yahoo.com
WORK PLACE Department of Pharmacology and Toxicology
Faculty of Pharmacy, Silpakorn University,
Nakornpathom, 73000, Thailand

EDUCATION BACKGROUND

1988-1993 Bachelor's Degree (B. Pharm), Faculty of Pharmacy, Silpakorn University, Thailand.
1993-1996 Master Degree of Science (Pharmacology), Faculty of Pharmacy, Mahidol University, Bangkok, Thailand.
2001-2004 Ph.D in Biopharmaceutical Sciences Program, Faculty of Pharmaceutical Sciences, Chulalongkorn University, Bangkok, Thailand.

CAREER HISTORY

1995-Present Lecturer and Laboratory instructor in Department of Pharmacology and Toxicology, Faculty of Pharmacy, Silpakorn University, Nakornpathom, Thailand

SCHOLARSHIP

1993-1995 A grant from University Development Commission, (UDC), Thailand to study the Master Degree of Science (Pharmacology), Faculty of Pharmacy, Mahidol University, Bangkok, Thailand.
1998 A grant from JSPS-NRCT Cooperation Program to research at Molecular Genetics Research Center, Toyama Medical and Pharmaceutical University, Japan.
2001-2004 A grant from Thailand Research Fund (TRF) to study the Ph.D in Biopharmaceutical Sciences Program, Faculty of Pharmaceutical Sciences, Chulalongkorn University, Bangkok, Thailand.
2002, Oct -2003, Apr Visiting Scholarship to Boston University, School of Medicine from TRF
2003, Apr – 2004, Mar Continued study in Boston University, School of Medicine (grant from Prof. John F.Keaney Jr.)